Title
Functional connections of the central auditory nervous system

Author
Andersen, Richard Alan

Publication Date
1979

Peer reviewed|Thesis/dissertation

FUNCTIONAL CONNECTIONS OF THE CENTRAL AUDITORY NERVOUS SYSTEM: THALAMOCORTICAL, CORTICOTHALAMIC AND CORTICOTECTAL CONNECTIONS OF THE AI, AII AND AAF AUDITORY CORTICAL FIELDS

by
Richard Alan Andersen
B.S., University of California, Davis, 1973

DISSERTATION

Submitted in partial satisfaction of the requirements for the degree of

DOCTOR OF PHILOSOPHY

in

PHYSIOLOGY

in

GRADUATE DIVISION

of the

UNIVERSITY OF CALIFORNIA

San Francisco

TABLE OF CONTENTS

ACKNOWLEDGEMENTS

I wish to thank the teachers, colleagues, and friends who have made my graduate education an exciting and fruitful experience. My preceptor, Dr. Michael Merzenich, has generously given me his patience, time, insights, and help and has provided me with a model for true excellence in science. Dr. Russel Snyder taught me much of the neuroanatomical techniques I know and was always available with advise, help, and encouragement as a friend and collaborator. Drs. H.J. Ralston III, and Robert Mitchell gave me their much appreciated support and interest as members of my thesis committee and as teachers throughout my graduate education. Drs. William Mehler and Lindsay Aitkin gave me isights into the structure of the brain and the physiology of the auditory system. Dr. Earl Mayeri was excellent as the chairman of my orals committee and I am thankful to him for many stimulating discussions.

For their experimental expertise and the pleasure of their company, I would like to thank my collaborators, Drs. Paul Knight, Linn Roth, Pat Patterson, and Bill Crandall. I would like to thank Mary Lu and Pat Clepper for the excellent histology. For sharing the daily joys, discoveries and frustrations of neuroscience I thank Drs. Steve Colwell, Pat Leake-Jones, John Middlebrooks, Marti Silverman, Dave Zelear, Sheila Walsh, and Mark White. For the careful attention and long hours required for the physical realization of the manuscript I am indebted to Anne-Christine

Guerin, Joe Molinari, and Harriet Yarowski. I wish to thank Tom Imig and Rick Reale for sharing with me their exciting new findings and for making the Neuroscience Meetings a memorable experience.

I wish to particularily thank my dear friends Chris, Happy, Barbara, Diana, Lee, Shelby, Sandy, Sally, Jacci, Harriet, Billy, and Steve for being special people. Most especially I am indebted to my dear parents and brother for a life of love and support. And last, but most important, I wish to thank Carol for the glory of love.

ABSTRACT

The connections of the three auditory fields AI, AII and the anterior auditory field (AAF) and the inferior colliculus (IC) were studied using anterograde and retrograde tracing techniques. Microinjections of tracers were placed at physiologically identified loci after these fields had been functionally mapped with the microelectrode recording technique. This ensured that the injections were well within the borders of each cortical field that was studied and enabled the elucidation of the topographies of connections of AAF and AI re their cochleotopic organizations.

The thalamocortical and corticothalamic projections of single loci in AI were from and to single columns passing rostrocaudally through the deep dorsal nucleus (Dd) and medial division (M) of the medial geniculate body (MGB) and from and to single sheets passing rostrocaudally through pars lateralis (Vl) and pars ovoidea (Vo) of the ventral division. The connections with Vl and Vo were very strong. There were also thalamocortical and corticothalamic connections between the lateral division of the posterior group of thalamus (POl) and single loci in AI. The connectional areas in POl were continuous caudally with the connectional areas in Dd. There were strong thalamocortical and corticothalamic connections between loci in AAF and columns passing rostrocaudally through Dd and M. There were weak connections of loci in AAF with Vl and Vo with the thalamocortically projecting neurons discontinuously arrayed and often forming single columns in Vl oriented rostrocaudally. The autoradiographic label pattern in Vl

and Vo after AAF injections was similar to that seen after AI injections but was much weaker. There were also thalamocortical and corticothalamic connections between AAF and POl that were continuous caudally with the connections of Dd. AII loci were thalamocortically and corticothalamically connected with the caudal dorsal nucleus (Dc), the ventral lateral nucleus (VL) and M.

The topography of connections of AAF and AI with Vo, Vl, Dd and M varied systematically and was consistent with a cochleotopic order of connections between these subdivisions of the MGB and the two cortical fields.

The reciprocal nature of connections of these three fields allowed a direct comparison of their connections by introducing anterograde tracer in one field and retrograde tracer in another. AI and AAF were connected to the same subdivisions of the MGB and had the same systematic topography of connections whereas the connections of AII and AI were largely segregated with the only overlap occurring in M. Injections introduced into other fields and a review of the connectional literature showed that there appear to be two largely segregated connectional systems between cortex and the thalamus: the "cochleotopic system" that includes AI and AAF and the "diffuse system" that includes AII . This segregation also appeared to be present in the projection of the IC onto the MGB (Andersen et al. '78, '79).

Small injections of anterograde tracers at high frequency representational

sites in AI or AAF or retrograde tracer in AI produced a periodic pattern of dense and light labelling in V1. Reconstructions showed that these discontinuities in label, in three dimensions, formed parallel columns oriented rostrocaudally. These columns in V1 probably represent a segregation in binaural response properties in V1 that is reflected in AI through a segregation of connections between the MGB and cortex.

The projection of loci in AI onto the caudal aspect of the IC was in the form of sheets of terminals in the dorsomedial division of the central nucleus (ICC-dm) bilaterally and the pericentral nucleus (ICP) ipsilaterally. The topography of projection re the cochleotopic organization of AI appeared to be in register with the cochleotopic organizations of the central nucleus and ICP. The orientation of the sheets of terminals and systematic topography of the projection from AI onto ICC-dm were consistent with these sheets being continuous with the morphological laminations and isofrequency contours of the ventrolateral division of the ICC.

Single injections placed in AAF produced autoradiographic label in the IC that was of a similar pattern to the labelling seen with AI injections; however, it was much weaker. The projection from AII was to the lateral and medial aspects of ICP and there did not appear to be a projection from AII to the ICC.

LIST OF ABBREVIATIONS

AI	first auditory field
AII	second auditory field
AAF	anterior auditory field
AES	anterior ectosylvian sulcus
ARG	autoradiography
BIC	brachium of the inferior colliculus
CC	collicular commissure
CP	cerebral peduncle
D	dorsal division of MGB
Dc	caudal dorsal nucleus of the MGB
Dd	deep dorsal nucleus of the MGB
Ds	superficial dorsal nucleus of the MGB
DNLL	dorsal nucleus of the lateral lemniscus
EE	ipsilateral and contralateral ear stimulation, both excitatory
EI	ipsilateral ear excites, contralateral inhibits
Ep	posterior ectosylvian auditory field
HRP	horseradish peroxidase
IC	inferior colliculus
ICC	central nucleus of the IC
ICC-dm	dorsomedial division of the ICC
ICC-vl	ventrolateral division of the ICC
ICP	pericentral nucleus of IC
ICP-l	lateral aspect of the ICP

ICP-m	medial aspect of the ICP
I-T	insular-temporal cortical region
ICX	external nucleus of the IC
LGN	lateral geniculate nucleus
LL	lateral lemniscus
LSO	lateral superior olive
M	medial division of the MGB
MGB	medial geniculate body
MGm	pars magnocellularis or magnocellular division of the MGB
MGp	pars principalis or principle division of the MGB
MSO	medial superior olive
OT	optic tract
PAF	posterior auditory field
PES	posterior ectosylvian sulcus
PO	posterior group of thalamus
POi	intermediate division of PO
POl	lateral division of PO
POm	medial division of PO
R	reticular nucleus of the thalamus
SC	superior colliculus
SS	suprasylvian sulcus
T	temporal cortical region
TAA	tritiated amino acids
Vl	pars lateralis of the ventral division of the MGB
VL	ventral lateral nucleus of the ventral division of the MGB

Vo	pars ovoidea of the ventral division of the MGB
VPAF	ventral posterior auditory field
Vt	transitional zone of the ventral division of the MGB
Zm	marginal zone of ventral division of the MGB

INTRODUCTION

Introduction

The auditory neuroaxis is remarkable in its structural complexity. At each of its many levels there are multiple, morphologically distinct subdivisions. Many of these subdivisions contain functional representations of the cochlear epithelum. The divergent and convergent patterns of connection between each level of the neuroaxis, and the multiple subdivisions that each level entails, are also elaborate. However, at present, little is known about the three dimensional details of the patterns of connections of the various subdivisions at each level of the system. Even less is known of the organization of connections with respect to the functionally and anatomically defined architecture within these subdivisions. It is important to have knowledge of the structural details of these connections to understand how processing is being accomplished spatially by the auditory nervous system.

With this in mind, this study was directed at elaborating the three-dimensional details of the connections to and from several subdivisions of one level in the system, the auditory cortex. The thalamocortical, cortico-thalamic and corticotectal projections of AI, AII and the anterior auditory field (AAF) were studied. The following specific questions were addressed: 1) What are the forms (in three dimensions) of the arrays of neurons from the several subdivisions of the auditory thalamus that project to each of these fields, and what are the forms of the terminal fields in the subdivisions of the thalamus and inferior colliculus that arise from the projections of these three cortical fields? 2) What are the topographic

organizations of the connections of these cortical fields with the subdivisions of the auditory thalamus and inferior colliculus, with respect to the functional organization of these cortical fields and target nuclei? 3) How are the connections of these three cortical fields similar and how are they different?

These questions were addressed by using anterograde (tritiated amino acids) and retrograde (HRP) tracing techniques, which allow a precise reconstruction of the three dimensional structure of the terminations and the sources of the projections. An investigation of the topographic order of the connections of the cortical fields with respect to their internal functional architecture was made possible by deriving maps of these fields using microelectrode recording techniques. Thus, the sites of injections of tracers were typified in terms of the functional topography of the cortical fields. By systematically varying the positions of tracer injections within the fields, the topographic organization of the connections of these fields with the IC and thalamus were demonstrated. Additionally, a two-injection paridigm was employed, by which the connections of the three auditory fields with the medial geniculate body (MGB) could be directly compared within the MGB's of individual cats.

The understanding of the significance of the three dimensional structure and topographic organization of the connections between cortex, IC and thalamus can only be appreciated within the context of the anatomy

and physiology of the cortical, collicular and thalamic regions that give and receive these projections. Thus, in the following sections, the literature pertinent to these auditory structures and this study are reviewed in detail.

The Auditory Cortical Fields

Auditory cortical neurons are often referred to as being tuned, meaning they are preferentially more sensitive to certain frequencies of tonal stimulation. A sharply tuned cortical neuron will respond to low level stimulation over a frequency range that is quite restricted. A broadly tuned neuron will respond to low level stimulation over a much wider range of frequencies.

The best frequency of a neuron is that frequency at which a neuron will respond to the lowest level of sound, i.e., the frequency at which the unit has the lowest threshold. This type of response behavior is typical of neuron populations all along the auditory neuroaxis, as well as eighth nerve fibers (and hair cells) and will be referred to frequently is this study. The orderly arrangement of this response parameter is the basis for the designation of a cochleotopic (tonotopic) organization in cortical fields and other neural structures.

The AI Auditory Cortical Field

AI is the so called "primary" auditory field. (However, it was designated as "AI" by Woolsey and Fairman '46 because it was the first discovered auditory cortical field). It is located in the middle

ectosylvian cortex between the dorsal aspects of the anterior and posterior ectosylvian sulci (see Fig. 1). The neurons of this field are sharply tuned (Hind et al., '60, Oonishi and Katsuki '65, Evans et al., '65, Goldstein et al., '70, Merzenich et al., '75). This field contains a complete functional representation of the cochlear sensory epithelium (in cat: Woolsey and Walzl '42, Hind '53, Merzenich et al., '75; in dog: Tunturi '50, 52). The basal regions of the cochlea (high frequencies) are represented rostrally, and the apical regions (low frequencies) caudally. Limited sectors of the cochlea are represented along bands which are oriented approximately dorsoventrally within the field (Woosley and Walzl '42, Tunturi '50, Merzenich et al., '75). Approximately the same best frequencies are encountered in any vertical penetration through AI (Hind et al., '60, Oonishi and Katsuki '65, Abeles and Goldstein '70, Merzenich et al., '75). This radial organization of similar best frequencies suggests that the isofrequency contours which subtend AI are, in three dimensions, in the form of slabs. When penetrations were made tangentially thorugh cortex and normal to the isofrequency slabs, steps in best frequencies of a "significant part of an octave" were noted every 100 to 400 microns (Merzenich et al., '75), Tangential penetrations parallel to the isofrequency slabs were not made to determine if the best frequencies remained the same across cortex or changed in a stepwise or gradiential fashion. A disproportionate area of AI cortex was dedicated to the representation of the basal cochlea.

Figure 1

This figure is taken from Merzenich et al., '77 as modified from Knight '77. A is a surface view of the left lateral side of a cat brain. In this figure, the relative positions of the three cortical fields examined in this study are represented with respect to the sulcal patterns. The position of these cortical fields with respect to the sulci are not to be taken literally but only as an average or typical example. Merzenich et al., ('75) have indicated that the positions of the auditory cortical fields vary somewhat with respect to the sulcal patterns and that the sulcal patterns themselves will vary from animal to animal. AAF is indicated in the shaded region, rostral to AI. The subscripts A and B indicate apical (A) and basal (B) positions in the cochlear representations within AI and AAF. AII is indicated ventral to AI. In B, the isofrequency contours are indicated along the lines within AAF and AI. In this figure, the frequencies have been converted to cochlear place in mm from the apex (Greenwood '61). Note that the isofrequency contours assume more horizontal positions at more ventral regions along the anterior ectosylvian gyrus. Also note the reversal in cochleotopic position at the AI, AAF border. SS: suprasylvian sulcus; AES: anterior ectosylvian sulcus; PES: posterior ectosylvian sulcus.

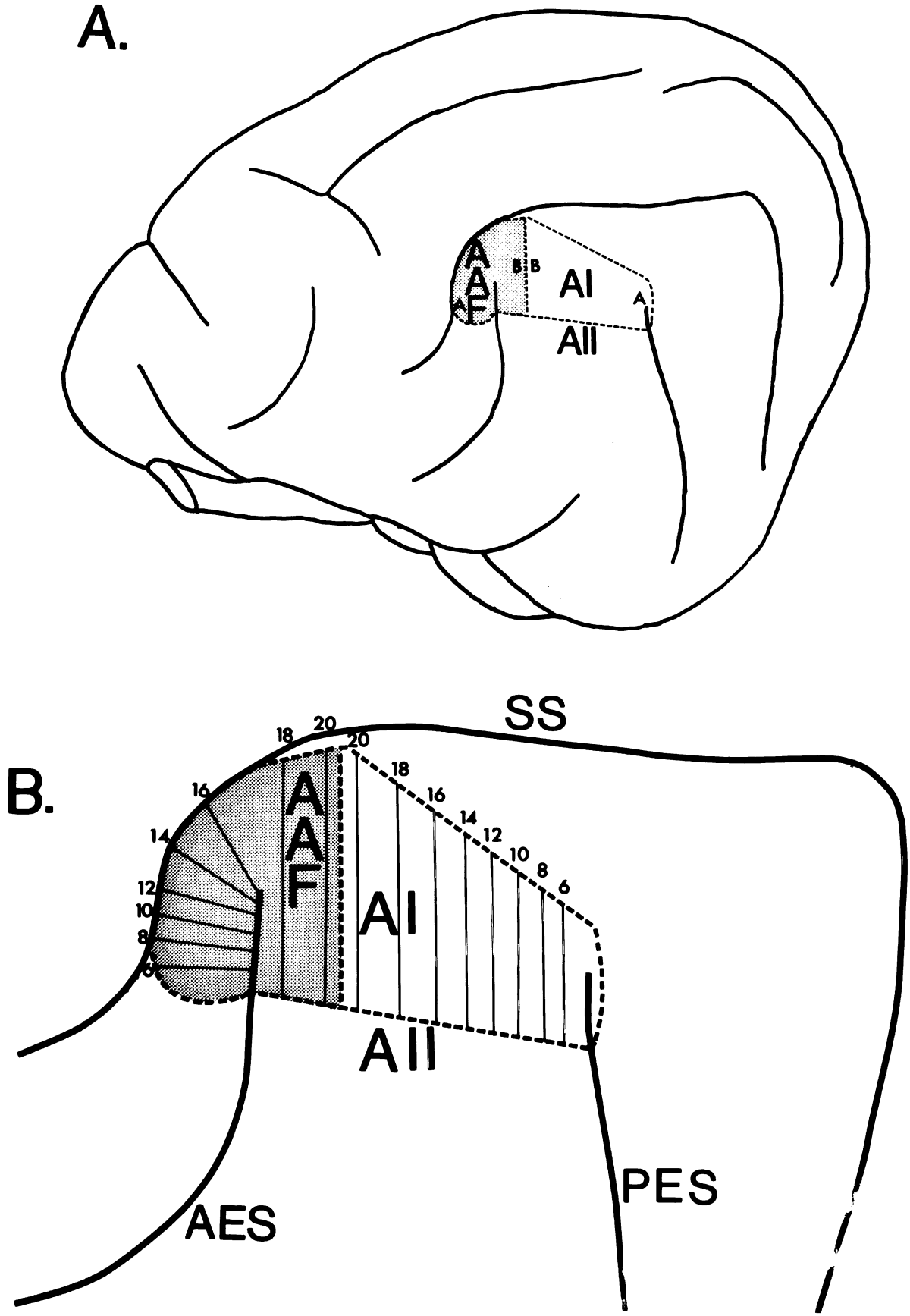
A.
A
AA
AF
B B
AI
A
AII
B.
SS
18
20
20
18
16
16
14
14
12
12
10
10
8
8
6
6
A
AA
F
AI
AII
AES
PES

A tonotopically organized AI has also been mapped in several primates (Merzenich & Brugge '73, Imig et al., '77), and in the grey squirrel (Merzenich et al., '76). Other auditory cortical fields were noted surrounding AI in all of these studies, and some of these fields are cochleotopically organized. Merzenich et al., '76 compared recording data in AI of squirrel, cat and rhesus monkey. They found the cochleotopic order, perpendicular to the isofrequency contours, to be proportional in the three species with an expansion at higher frequencies. This and other evidence of similarities between the fields led them to suggest that the "AI's" of the three species were homologous.

Brugge et al., '69 and Hall and Goldstein '68 have studied the binaural response properties of neurons in the cat AI. Brugge and colleagues examined neurons which were sensitive to interauraral intensity differences and interauaral delays. Neurons sensitive to interaural intensity disparities were generally excited by contralateral stimulation and inhibited by ipsilateral stimulation of the same frequency. For these disparity sensitive neurons ipsilateral stimulation alone generally did not produce a response. At high frequencies, the head casts a sound shadow, producing a binaural disparity. The interaural intensity differences response is a common feature of neurons at many levels of the auditory system and is believed to encode the location of sound in space for higher frequencies. Other neurons were found that were excited by stimulation of either ear. Binaural stimulation often produced a greater response than monaural stimulation; however, the binaural response was

generally less than the sum of the spike counts of each ear stimulated separately. Interaural phase sensitive neurons were found in the lower frequency range (the highest best frequency being 2400 Hz). These delay sensitive neurons behaved similarly to ones found in the inferior colliculus in that they had "characteristic" delays. A neuron exhibiting a characteristic delay is one which is most sensitive at a particular delay, regardless of the frequency or intensity of the stimulation (Rose et al., '66). Interaural phase sensitive neurons are believed to encode the location of sound in space for the lower frequencies. At low frequencies, the wavelength of the sound is too large to cast a shadow with the head. Thus, an important clue to localization is the difference in time of arrival and resulting phase shift of the sound at the two ears. Since this difference is in the order of microseconds, it is believed that the phase comparison and neural encoding is made at lower levels of the neuroaxis (probably the MSO, Goldberg and Brown '69) where the synaptic security is still great. The timing information is possibly converted to a place code and fed up the neuroaxis to the cortex.

Brugge and Merzenich '73 studied the binaural characteristics of single units in the auditory cortex of awake monkeys. They found neurons sensitive to interaual intensity differences and interaural delays. Interaural delay sensitive neurons had low best frequencies (200-1800 Hz). All neurons isolated from a given penetration had a similar delay to which they were maximally responsive, suggesting a columnar organization of absolute delays. Although not extensively studied, the delay sensitivity appeared to be "characteristic" for each neuron since the delay was usually

independent of frequency and intensity parameters.

Imig and Adrian '78 mapped the spatial distribution of binaural response properties of neurons in the high frequency sector (4-25KHz) of the cat AI. They divided the binaural response properties into two broad categories. The "summation" type had a greater response to binaural stimulation than monaural stimulation of either ear and is similar to the type described by Brugge et al., '69 which was excited by either ear. With the "suppression" type, stimulation of one ear had a greater response than binaural stimulation. This class was similar to the binaural intensity difference neurons of Brugge et al., '69 but included units in which a strong ipsilateral response was supressed by contralateral stimulation. The binaural interaction type was found to be segregated along the radial dimension of cortex (i.e., they are columnarly organized.) Along the planar dimension they were also segregated and some of the binaural columns in this study were found to occur as strips oriented normal to the isofrequency slabs. Middlebrooks et al., '78 have made extensive physiological maps of AI and have shown that the binaurally segregated regions generally form bands normal the orientation of the isofrequency contours.

Imig and Brugge '78 studied the callosal connections of AI with the contralateral AI using anterograde and retrograde tracing techniques. They found that the callosal sources and terminals were organized into "columnar" regions of periodic high and low concentrations. Combining

electrophysiological recording with the tracer studies, they were able to show that the regions of high concentration of either sources (projecting cells) or terminals were the "summation columns".

AI is cytoarchitectonically distinct and can be recognized by a split layer V (Rose '49, Sousa-Pinto '73). The outer part of layer V appears to join layer IV. The inner part of the layer is small celled and sparsely populated and thus appears as a light band in Nissl material. There is also a fusion of layers II-IV (Rose '49, Sousa-Pinto '73). Golgi observations in AI indicated upside down pyramidal cells in layer VI, pyramidal cells of small size, and stellate cells in layers III and IV (Sousa-Pinto '73). A vertical organization of neurons is apparent in Nissl material of AI (Lorente de No '33, Sousa-Pinto '73).

The AII Auditory Cortical Field

AII is an auditory field that is located on the middle ectosylvian gyrus ventral to AI (Woolsey '60). This field is typified by having neurons with broad tuning characteristics (in cat: Hind '53, Merzenich et al., '75; in dog: Tunturi '50a). Downman et al., '60 used direct electrical stimulation of eighth nerve fibers at different locations along exposed osseous spiral laminae of cats and recorded the resulting evoked potentials in AII. They reported what they believed to be a complete representation of the cochlea in AII with the basal cochlea represented caudally and the apical cochlea rostrally. Merzenich et al.,

'75 reported that AII neurons occasionally had the same best frequencies as neurons in AI just dorsal to the recording site. However, they reported that the tuning of neurons of AII was usually so broad that it was impossible to assign best frequencies to these cells. Thus, the organization of AII in terms of a cochleotopic order appears to be an unresolved question.

Early investigators believed AII was a cortical "association" field which did not receive direct input from the thalamus and relied on input from AI for activation (Ades '43, Bremer, '53). Later studies (Kiang '55, Downman et al., '60) demonstrated that AII does not depend on AI for activation. Acute or chronic bilateral removal of AI (Downman et al., '60) or isolation of cortex by removing surrounding tissue (Kiang '55) did not disrupt activation of AII. Thus AII appears to be activated directly by ascending thalamic fibers. The studies of Downman et al., '60 also indicated that AII could be activated from AI (and vise versa) demonstrating corticocortical connections between the areas.

AII is cytoarchitectonically distinct from AI (Rose '49). Whereas AI contains a split layer V, AII does not. Also, layers II-IV are distinguishable in AII whereas they are not in AI. The cytoarchitectonic transition between AI and AII type cortex is gradual.

The Anterior Auditory Field (AAF)

A low frequency representation was noted anterior to AI on the anterior ectosylvian gyrus in the evoked potential studies of Woolsey and Walzl '42 and Hind '53. Later microelectrode mapping studies indicated that there was a complete representation of the cochlea in a field anterior to AI (Merzenich et al., '75, Knight '77). The anterior auditory field shares a common high frequency border with AI. Within AAF, successively lower frequencies are represented successively more anteriorly on the anterior ectosylvian gyrus (see Fig. 1).

(Knight '77) made extensive microelectrode maps of AAF and found it to be very similar to AI. Similar best frequency regions in AAF took the form of slabs which, posteriorly, were oriented dorso-ventrally. Anteriorly, as the field bends ventrally along the anterior ectosylvian sulcus, these slabs acquired a nearly horizontal orientation. The two cortical fields (AI and the AAF) were of approximately the same area and the spatial representation of the cochlea in the two fields was approximately the same with the basal (high frequency) representation being expanded.

AAF neurons exhibited sharp turning curves (which were qualitatively indistinguishable from AI units) and responded to tonal stimuli with about the same latencies as AI neurons. Brugge et al., '69 studied the binaural response properties of neurons in the cat AAF as well as AI.

(Although they claimed that many of the AAF neurons studied were located in "AII", this was based on one older parcellation of cortex, which included a large part of AAF in "AII". Their description of the location and response properties of the cells indicate they were actually in AAF). The binaural response properties of AAF neurons were similar to those studied in AI.

Other Auditory Cortical Fields

In evoked potential studies, a high frequency region was recorded in the ventral region of the posterior ectosylvian sulcus (Woolsey and Walzl '42, Hind '53). Ades '43 found that strychninization of AI produced auditory evoked activity in this region which had previously been silent in his recordings. This was the only region of cortex which Ades found that behaved in this manner. Rose '49 recognized this region and other areas of the posterior ectosylvian gyrus to be cytoarchitectonically distinct and designated this region the posterior ectosylvian area (EP).

Reale and Imig '77 mapped another cortical field posterior to AI (posterior auditory field; PAF). The regions in this field had similar response properties to those of AI. This field contained a complete representation of the cochlea, was about the same size as AI, and also was functionally organized as a series of isofrequency contours. The low frequency representation bordered the low frequency representation of AI. Much of this field was usually located in the

posterior ectosylvian sulcus. High frequencies were located more caudoventrally on the posterior bank of the sulcus and they often extended onto the surface of the posterior ectosylvian sulcus. The high frequency region of this field may correspond to the high frequency region recorded with the evoked potential method in the dorsal EP by Woolsey and Walzl '42 and Hind '53. This field also exhibited short latencies for auditory activation.

Sindberg and Thompson '62 found ventral regions of the posterior ectosylvian gyrus which responded to clicks and stimulation of the apical cochlea. This suggested a second, more ventral representation of the cochlea in Ep. (see also Woolsey '60, Merzenich et al., '77).

An insular auditory area has also been described (Leoffler '58, Desmedt and Michelse '59, Woolsey '60). Tunturi '45 described an AIII auditory area in dog that was situated far anterior to AI and AII and overlying what is probably the face region of SII (Woosley '60). No convincing evidence for this area in cat has been found (Hind '53, Woolsey '60). Short latency responses have been noted in the precentral motor and sensory motor regions (Thompson & Sindberg '60) and long latency responses in visual area II (Bremer '53, Thompson and Sindberg '60).

Anatomy of the MGB

The medial geniculate body (MGB) has been partitioned by several authors based on observations of Nissl or Golgi preparations. Two significantly different schema have emerged: one obtained from the observations of Nissl material and one obtained from the use of the Golgi technique. It is difficult to crosscorrelate these two views in detail, although authors have claimed they could recognize the major subdivisions established by the Golgi technique using Nissl stained material on the basis of cell packing densities (Cajal '55, Morest '64, Pontes et al., '75) and cell body size (Cajal '55). In this section, the two basic schema of parcellation will be reviewed.

Parcellation of the MGB using the Golgi Technique

The medial geniculate body has been divided, on the basis of dendritic morphology, into three major nuclei. These have been called (by Morest '64) the dorsal division (also superior lobe, Cajal '55), ventral division (inferior lobe, Cajal '55), and medial division (deep nucleus, Cajal '55). In general, the dorsal and ventral divisions contain somata of medium size whereas the medial division contains the largest cells of the MGB (see Fig. 1 and 2). The dorsal division extends throughout the MGB and occupies all but the medial edge of the nucleus at its posterior pole. More anteriorly, it occupies dorso-lateral and dorsomedial regions of the geniculate. The cells are typically stellate with many radiating dendrites. Anteriorly, the dorsal

division is divided (by Morest '64) into the superficial dorsal nucleus (Ds) and the deep dorsal nucleus (Dd). Ds lies adjacent to the dorsolateral edge of the MGB nucleus; Dd is situated ventromedial to Ds. The caudal region of the dorsal division was described by Morest '64 as a separate nucleus (his "dorsal nucleus"). It will be referred to herein as the caudal dorsal nucleus (Dc) of the MGB. The neurons of Dd, Ds and Dc are similar in appearance; however, the soma and dendrite fields of Ds are larger and more widely spaced than Dc and the dendritic fields of Dd are smaller and less branched than Dc.

The ventral division begins in the rostral aspect of the posterior third of the MGB and extends rostrally through the nucleus (see Figs. 1 and 2). Caudally, the ventral division is situated in the ventrolateral region of the MGB, and is bounded medially by the medial division. More rostrally it occupies the lateral aspect of the MGB, and is bordered medially by the superior acoustic pathway and deep dorsal nucleus. The nucleus contains several morphologically definable subdivisions. Of particular interest is the laminated pars lateralis (Vl) of Morest '64 (which corresponds to the external region of Cajal '55). This region contains neurons whose dendrites are tufted. The dendritic fields are discoid with the long axes oriented dorsoventral and anteroposterior (Morest '64). They are arranged to form parallel laminar sheets roughly parallelling the lateral surface of the MGB (Morest '64, '65). These cell bodies are slightly smaller than those of the dorsal division (Morest '64).

In the ventromedial region of the ventral nucleus is pars ovoidea (Vo) of Morest '64 (or "subnucleus ovoideus" of Cajal; see Figs. 1 and 2). The morphological laminations assume different orientations in this region. In the ventral region of pars ovoidea, Morest '65 described a "sprial zone" that he believed contained dendritic laminations which formed one dense coil rostrally and two dense coils caudally. Dorsal to this region and interposed between pars lateralis and the "spiral zone" Morest '65 described a region of horizontally placed laminae, which he called the "transitional zone" (Vt). The more vertical columns of dendrites in pars lateralis were continuous medially, with the horizontal columns in the transitional zone which were in turn continuous with the "leaves" of the coils in the spiral zone (Morest '65). The cells within the pars ovoidea assume varied appearances and include neurons whose dendrites have long ascending and descending bouquets (Cajal '55). Cajal also noted that cells in pars ovoidea clustered into dense linear groups.

Ventral to Vo and, more rostrally ventral to Vl, is the ventral lateral nucleus (VL) of the ventral division. The dendritic fields of neurons in this region are less tufted (Morest '64) and there is no apparent morphological lamination of this nucleus (Morest '65). A thin marginal zone (Zm) on the lateral edge of the ventral division has also been described. The dendrites of these neurons are less tufted than Vl, are arranged parallel to the surface, and send their

axons into the external capsule of the MGB (Cajal '55, Morest '64).

The medial division is bordered dorsally by the dorsal division and laterally by the ventral division (Morest '64). Fascicles of the brachium of the inferior colliculus (BIC) pass through the division caudally. Within this division, two cell types have been described (Morest '64). Caudally, in the region of penetration of the BIC into the division, there are many relatively small neurons with radiating dendrites. More anteriorly, large neurons with tufted dendrites predominate.

Parcellation of the MGB using Nissl Cytoarchitecture

The MGB has been partitioned, on the basis of cytoarchitecture using Nissl stains, into a pars principalis and a pars magnocellularis in dog (Rioch '29) and cat (Rose '49, Rioch '29, Moore & Goldberg '63). The pars principalis (or "principle division"), contains medium sized cells that are closely packed. The pars magnocellularis, or "magnocellular division", contains large cells that are loosely packed and intensely stained.

Several investigators included what later authors described as a division of the posterior thalamic group (Rose '49, Rose & Woolsey '58, Poggio and Mountcastle '60, Moore & Goldberg '63 and Jones & Powell '71) within the MGB (see Rioch '29). The more recent terminology will be used in this study.

Anteriorly, the principle division (MGp) begins lateral to the magnocellular division (MGm). It extends ventrolaterally with MGm occupying a dorsomedial position. Caudally, MGp extends dorsomedially as well. The nucleus acquires a broad "C" shaped appearance, roughly parallel to the lateral surface. The MGm occupies the ventromedial quadrant at this level. The posterior pole of the MGB is composed entirely of the cells of MGp.

MGm extends from the rostral pole of the MGB into the most anterior region of the posterior third of the nucleus. Anteriorly, it abuts POl; a line of transition between the two regions is not sharp. Caudally, it extends ventrolaterally and becomes more extensive in area, comprising most of the medial region of the nucleus.

MGp is bounded dorsally by the intermediate division of the posterior thalamic group (POi), caudomedially by the BIC and cells of the interstitial nucleus, and rostromedially by the superior acoustic pathway and MGm. MGm is bounded dorsally by POi, caudally by the BIC and interstitial nucleus, caudomedially by the midbrain tegmentum and rostrally by POl.

Within this broad scheme of classification, some variations were noted. The cells of MGp increase in size and decrease in packing density more medially (Rose '49, Rioch '29). Rose '49, examining horizontal sections, noted that dorsally there was little difference

between MGp and MGm. He concluded that this was a consequence of the fact that the cells of the dorsal aspect of the MGp were larger and more loosely packed than the cells in the other regions of MGp.

Basis of the Parcellation of the MGB used in this Study

In order to define the structure of the thalamocortical and corticothalamic projections, the morphology of the MGB has been examined with the use of two methods. The Nissl cytoarchitecture structure was revealed in the autoradiographic and HRP material by counterstaining with cresyl violet (or neutral red.) However, boundaries between MGB subdivisions were usually difficult to define in this material. To obtain a limited view of the dendritic morphology of the neurons multiple and large injections of HRP were made in the cortex, and the tissue was reacted according to Hanker et al, '77. The tissue was sectioned, unfrozen, on a vibratome in 100μ sections. This method of sectioning best preserved the morphology of the cells close to the cutting surface.

The HRP method has the disadvantage of staining only about 50μ of the dendritic arborizations out from the perikaryon. However, it has two advantages over the Golgi method: 1) large numbers of neurons and their dendrites are stained within each section, and 2) all thalamocortically projecting cells are stained, and no intrinsic neurons (Golgi type II's) are labelled.

The portions of the MGB which were recognizable in this HRP material and which will be discussed in this study are the pars lateralis (Vl), pars ovoidea (Vo), and ventral lateral nucleus (VL) of the ventral division; the deep dorsal nucleus (Dd), superficial dorsal nucleus (Ds) and caudal dorsal nucleus (Dc) of the dorsal division; and the medial division (see Fig. 2 and Fig. 3). The positions of these nuclei and the morphology of the neurons within these nuclei, recorded from this material, concurred in most respects with the observations of Cajal '55 and Morest '64, '65. Only a few details of the morphology and structure of the MGB, derived from examination of this material, will be mentioned here.

Pars lateralis contained medium sized neurons with generally ovoidal or fusiform perikaryon and dendritic profiles that were polarized along the long axes of the cell bodies. These neurons were oriented with respect to one another, and the orientation of this arrangement was consistent with the laminar structure of pars lateralis as described by Morest '65. The neurons of pars ovoidea were of mixed morphology (as described by Cajal '55) and some were of relatively large size. There was some indication of a consistent orientation of the neurons in this region; however, it was not as apparent as in Vl and may require more distal segments of the dendrites to be labelled to be better demonstrated.

Figure 2

Nissl stained frontal sections through the MGB. The sections in all the figures are in the transverse (frontal) plane. The top section is taken through the rostral third of the MGB and the bottom section through the middle third. Dd: deep dorsal nucleus; Vl: pars lateralis; Vo: pars ovoidea; M: medial division; Dc: caudal dorsal nucleus; VL: ventral lateral nucleus.

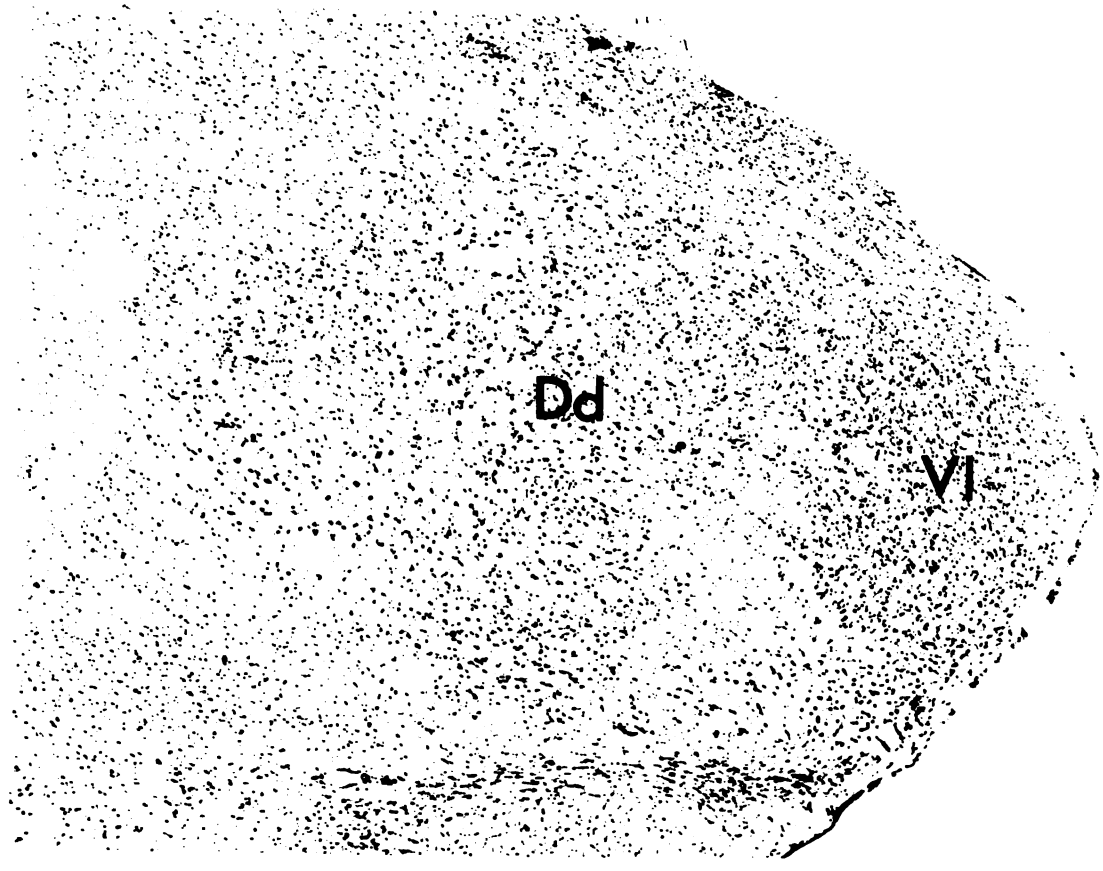
Dd
Vl

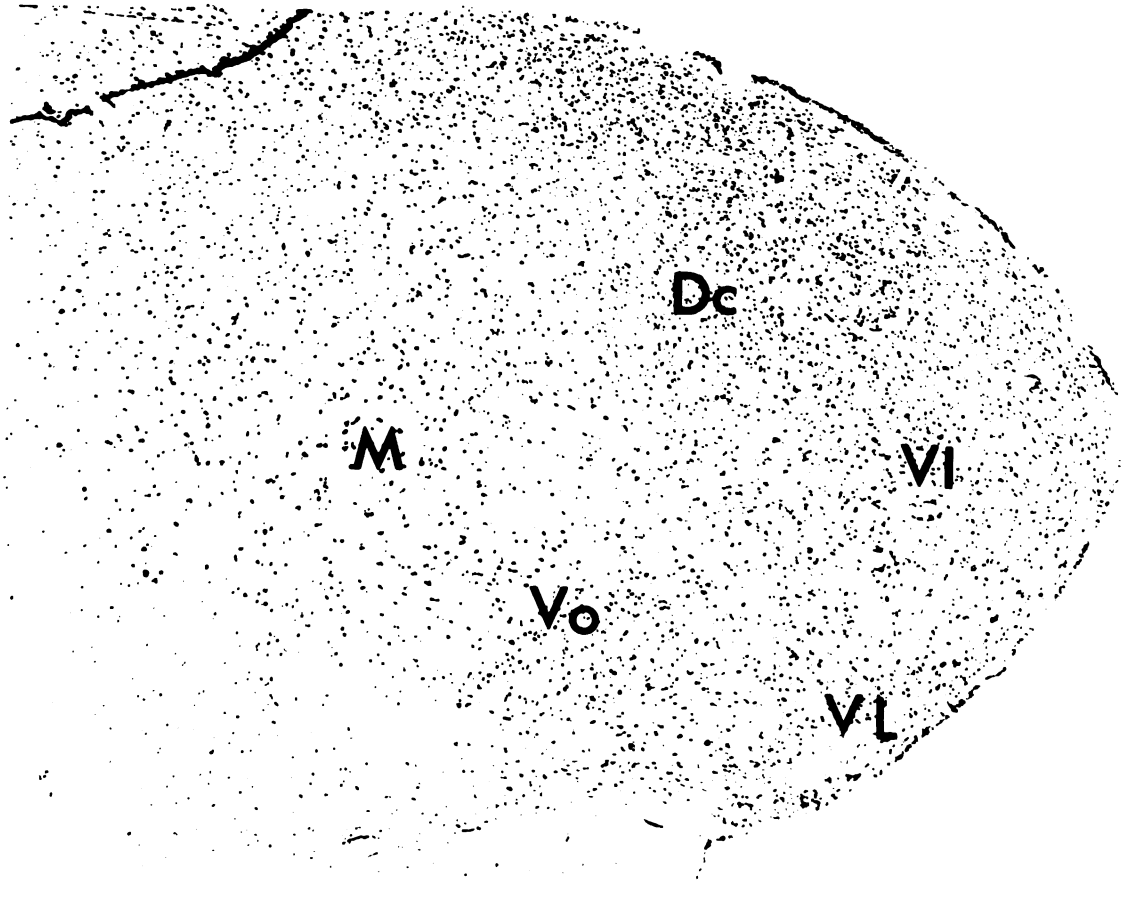
Dc
M
Vl
Vo
VL

Figure 3

An example of HRP labelled neurons in MGB after a large injection of HRP in AI. The top bright field photomicrograph shows labelled cells in the rostral third of the MGB and the bottom photograph labelled neurons in the middle third of the MGB. The line drawings of the frontal sections from which these photographs were made indicate the nuclei in the MGB that are labelled. The label in Vl in the bottom photograph sometimes appears as dark, large patches due to the close packing through the depths of these rather thick (100 μ) sections, of sets of small labelled cells.

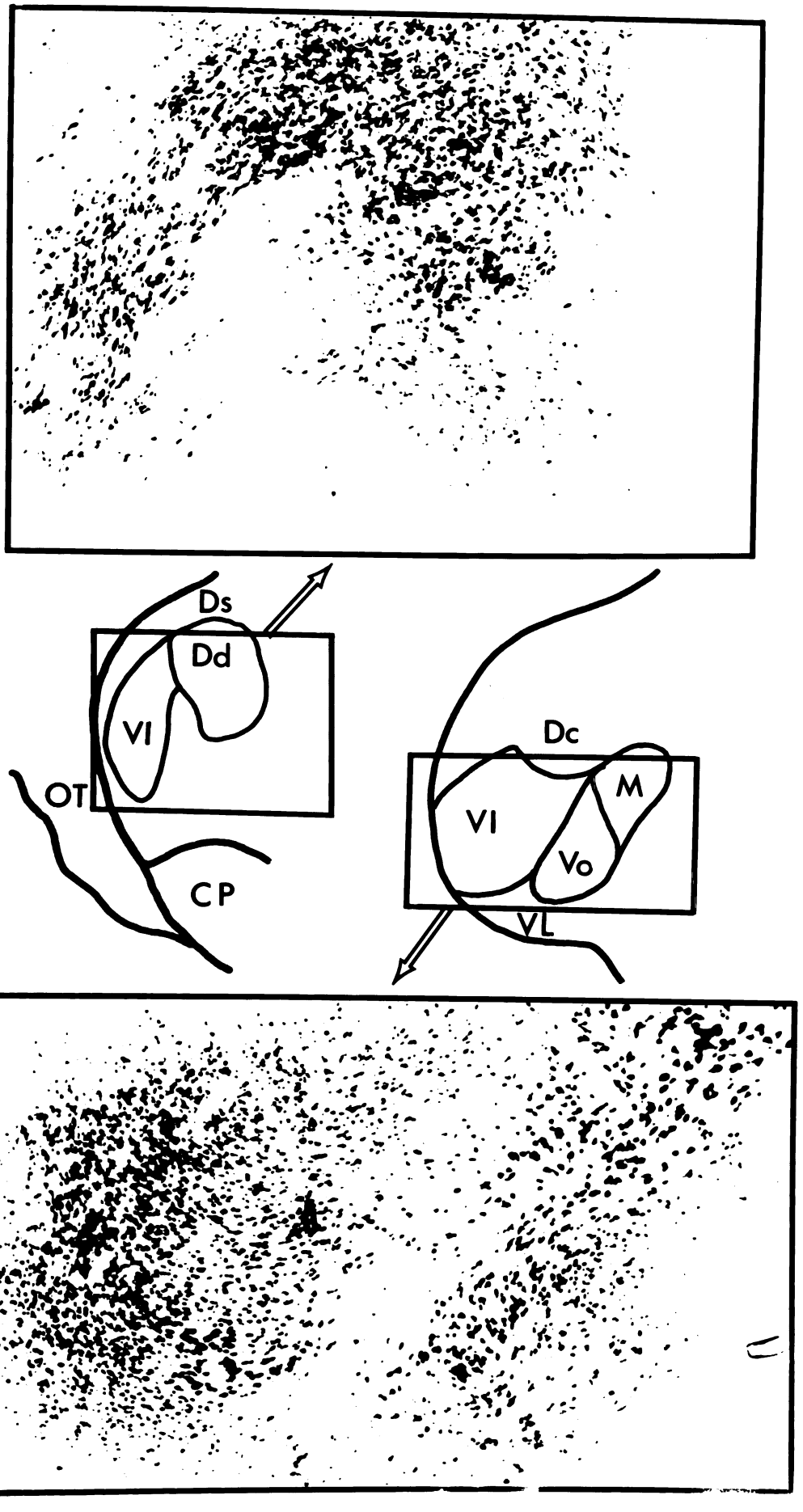
Ds
Dd
VI
OT
CP
Dc
VI
M
Vo
VL

The deep dorsal nucleus was located medial and slightly dorsal Vl in the rostral half of the MGB. Vl and Dd were joined dorsally. Ventrally, the two nuclei were separated by the superior acoustic pathway. The cells of Dd were slightly larger than those in Vl and slightly less packed. The perikaryon were generally star shaped and the dendrites radiated from all surfaces of the cell bodies. In the middle third of the MGB, the Dd nucleus was joined at its caudal aspect by the medial division. The large, multipolar cells of M first appeared ventromedial and adjacent to Dd. The two divisions coexisted for several hundred microns at which point the medial cell field predominated. The packing density was very low within M.

Comparison of HRP material with counterstained Nissl material enabled us to directly compare subdivisions made on cytoarchitectural bases with those made on the basis of dendritic morphology (Fig. 2,3). The pars principalis includes all subdivisions of the ventral division of MGB, as well as the caudal dorsal nucleus and the dorsolateral aspect of the deep dorsal nucleus. The pars magnocellularis includes the medial division and the ventromedial aspect of Dd. These correlations are in general agreement with those made by Morest '64.

Rose '49 noted, in horizontal sections, that dorsally cells in both MGp and MGm appeared similar and were larger and more loosely

packed than those in more ventral regions of MGp. This is probably because his sections were transecting the dorsal division (and particularly Dd), a region that has been typically divided between MGp and MGm. He also noted that the medial cells of MGp were larger and more loosely packed. This region probably corresponds to the "transitional zone" of pars ovoidea.

Once the divisions are recognized on the basis of cell morphology, it is easy to identify the various divisions in Nissl-stained material, on the basis of cell size and packing densities (Fig. 2). The packing densities of the various subdivisions are in general agreement with those of Morest '64 with Vl > D > VL > M. We would add that pars ovoidea is less densely packed than pars lateralis. Also, in the tracing experiments to be described in the results, HRP injections provided dendritic profiles. Since the projections from all the cortical fields studied were reciprocal (with reservations described later), this also aided in assigning the autoradiographic (corticothalamic) labelling to various subdivisions of the MGB. Finally, the identification of the nuclear origins of projections from the MGB to AAF and AII was aided by directly referencing the complex thalamocortical projections of AAF and AII to the well understood corticothalamic terminations of AI (Colwell and Merzenich '79, Colwell '77) in the MGB. This was made possible by injecting anterograde tracer into AI and retrograde tracer into AAF or AII of the same hemispheres of single cats and processing the single

MGB's for both tracers.

MGB Physiology

Early microelectrode recordings in the MGB showed neural responses to clicks only in MGp and not MGm (Rose and Galambos '52). It was found that excitatory responses could be generated in the vicinity of the microelectrode with clicks delivered to either ear (Galambos et al., '52). Using pure tone stimuli, no clear spatial pattern of frequency location was discerned (Galambos '52).

Rose and Woolsey '58 presented data which suggested a cochleotopic organization in MGp. In these experiments, the cochlea was exposed and the apical and basal turns were electrically stimulated. Evoked potentials were recorded with needle electrodes which were advanced through the contralateral MGB. Penetrations were made dorsoventrally through the pars principalis. It was found that apical stimulation was more effective in producing excitation in the lateral regions of MGp and basal stimulation was more effective in more medial regions. This same sequence was found for penetrations in the rostral MGp and more caudal regions of MGp. Along the course of each dorsoventral penetration, best responses were generally obtained only from either the apical or basal region of the cochlear partition. This data is consistent with an interpretation of a cochleotopic organization in the portion of the MGp which corresponds to pars lateralis, such that

sectors of the cochlear partition are represented as slabs whose long dimensions are situated rostrocaudally and dorsoventrally in the nucleus.

More extensive microelectrode recording experiments with tonal stimulation have been performed in cat in the ventral division (Aitkin and Webster '72) and in regions of the MGB medial to the ventral division (Aitkin '73) and in the auditory thalamus of squirrel monkey (Gross et al., '74). In the experiments of Aitkin and Webster '72, neurons were sampled from both the lateral and ovoidal nuclei of the ventral division. No apparent differences in pattern of discharge (i.e., onset, offset, sustained), sharpness of tuning, or binaural response properties were noted between these two populations of neurons. The lateral nucleus of the ventral division was found to be tonotopically organized, with high frequencies represented medially and low frequencies laterally. Best frequencies recorded along vertical penetrations remained relatively constant. These investigators noted that the organization of best frequencies in Vl was in accord with the laminar structure of the nucleus (Morest '65) and they implied that each lamina would have a common best frequency (Aitkin and Webster '72). The sequence of best frequencies recorded in the ovoidal nucleus was irregular, with only a tendency for high frequencies to be located medially and low frequencies laterally. A tonotopic organization in auditory regions medial to the ventral division was not observed by

Aitkin '73; however, units of similar best frequencies often occurred in groups. * In squirrel monkey (Gross et al., '74), the laterally placed small celled region of the auditory thalamus was found to be organized similar to pars lateralis of the cat with low best frequencies represented laterally and high best frequencies medially. At the junction between the small celled group and the more medially placed large celled group, there was a reversal in recorded best frequencies with progressively lower best frequencies being encountered as the microelectrodes passed more medially in the large celled region. (The large celled region of the squirrel monkey probably corresponds to the magnocellular division of the cat.)

Aitkin and Webster '72 reported that the frequency tuning curves of the neurons of the ventral division were sharp, but not as sharp as those recorded from cochlear nerve fibers or neurons of the central nucleus of the inferior colliculus. This was in discord with the assertation of Kutsuki et al., '59 that MGB neurons are the most sharply tuned neurons of the auditory system. Neurons in the MGB located medial to the ventral division had much broader tuning curves than the neurons of the ventral division and responded more irregularly to repetitive tone pips (Aitkin '73).

* Recordings made in regions of MGB medial to the ventral division by Aitkin '73 were stated to have been made within the medial division. However, as is apparent from Figure 1 of that paper, at least some of the recordings were in the deep dorsal nucleus as designated by the present study.

Binaural responses of the EE type (both ears excite) and EI type (contralateral ear excites and the ipsilateral ear inhibits) were reported (Aitkin and Webster '72) for neurons of the ventral division. EI responses had high best frequencies and EE responses that were delay sensitive had low best frequencies. Neurons located medial to the ventral division also exhibited binaural response properties of the EE and EI types, and some of the EE neurons of low best frequencies were delay sensitive (Aitkin '73). For neurons of the ventral division, sustained responses to tonal stimuli were rare (4%); most neurons responded to the onset (78%) or the offset (18%) of the stimulus (Aitkin and Webster '72).

The MGm also appears to have bimodal, auditory-somatosensory neurons (Poggio and Mountcastle '60, Rowe and Sessle '69, Curry '72, Berkley '73). However, these neurons are generally located on the medial most border of MGm (Curry '72). This region has been shown to receive a projection from a component of the spinothalamic tract (see Mehler et al., '60, Goldberg and Moore '66). It appears to lie medial to the projection of the inferior colliculus onto MGm (see Goldberg and Moore '66) and medial to the thalalmocortical and corticothalamic projections onto MGm reported in this study.

Summary for MGB

The MGB can be divided into three major subdivisions on the basis of Golgi material; the ventral division, medial division and dorsal

division (see Figs. 1 and 2). The ventral division has been further divided into a lateral nucleus, ovoidal nucleus and ventral lateral nucleus. The lateral nucleus contains cells whose dendrites are discoid and arranged into laminae that roughly parallel the free surface of the MGB. Recording experiments indicate that there is a tonotopic organization within this nucleus and the isofrequency contours are of the same orientation as the cell laminae. The dorsal division can be further divided into deep dorsal, superficial dorsal and caudal dorsal nuclei. The rostral aspect of the medial division contains the largest cells in the nucleus. There is some evidence that suggests that Dd and M are also tonotopically organized with high frequencies represented more laterally (Gross et al., '74, Aitkin '73).

A second scheme of parcellation, based on Nissl stained material, divides the MGB into a principle division and a magnocellular division. The principle division contains smaller, more densely packed cells than the magnocellular division. The principle division includes the entire ventral division, the caudal dorsal nucleus and a lateral portion of the deep dorsal nucleus. The magnocellular division contains the medial division and the remainder of the deep dorsal nucleus.

The cells of the ventral division, and cells medial to the ventral division, have binaural response properties. These include units with high best frequencies that are sensitive to interaural intensities and

units with low best frequencies which are sensitive to interaural delays. Units in the ventral division are more sharply tuned than those in more medial nuclei of the MGB. Most neurons of the ventral division respond to the onset or offset of a tonal stimulus.

Posterior Group of the Thalamus

The thalamic posterior group is a complex aggregate of cells intercalated between the MGB, lateral geniculate body and ventrobasal complex of the thalamus (Rose '49, Rose & Woolsey '58, Poggio & Mountcastle '60, Moore & Goldberg '63, Jones & Powell '71). This group has clear boundaries with the midbrain tegmentum and pretectal region caudomedially, the ventrobasal complex rostromedially, the auditory radiations rostrolaterally, and MGp caudolaterally. It has less clear boundaries dorsally with the pulvinar and lateral posterior nucleus and ventrally with MGm (Moore & Goldberg '63).

The posterior thalamic group (PO) has been divided into lateral (POl) and medial (POm) divisions on the basis of IC projections which end in POl but not POm (Moore & Goldberg '63). POl occupies a region just anterior to the MGB, ventral to the LGN, medial to the reticularis thalami and lateral to the ventrobasal complex.

The POm has been further divided, on the basis of connections, into intermediate (POi) and medial (POm) divisions. POm receives ascending somatosensory input and is reciprocally connected with SI and SII (Jones & Powell '71). POi receives input from the superior colliculus (Altman

& Carpenter '61) and is connected with regions of cortex that give and receive reciprocal projections with the pulvinar and lateral posterior nuclei of the thalamus (Jones & Powell '71). The intermediate division lies dorsal to MGp. The medial division lies dorsomedial to the ventral posterior nucleus of the thalamus anteriorly and dorsomedial MGm posteriorly.

PO Physiology

Poggio & Mountcastle '60, in microelectrode recording experiments, found the posterior group of thalamus of cat to contain populations of neurons with large somatosensory receptive fields with no apparent somatotopic organization. Many of these cells were polyvalent with respect to somatosensory stimulation and could be activated by light touch in one region of the body and noxious stimulation in another. Other cells were polymodal and could be activated by light mechanical stimuli and sounds. Cells were found in PO which were purely auditory. The auditory units which were studied were generally intermingled with purely somatic cells and cells which were responsive to both auditory and somatosensory stimulation. A majority of the PO cells studied responded to noxious stimuli. Some evidence also suggested that the activity of many of the PO neurons was influenced by the temperature of the skin. It was suggested, in the discussion of these experiments, that PO is a major thalamic target for the spinothalamic tract.

Similar results were recorded by Perl and Whitlock '61 in cat and monkey after the dorsal columns (and one ventrolateral column) were lesioned. (These lesions enabled them to study the spinothalamic input to the thalamus uncontaminated by dorsal column derived input). However, these investigators (and also Curry '72) were not able to confirm a major noxious activation of PO neurons, possibly due to differences in the level of anesthesia. Bimodal sound-touch neurons were also noted in PO in this study.

Bimodal, sound-touch neurons have been recorded by several other investigators (Berkley '73, Hotta and Kameda '63, Curry '72). Curry '72 reported that these bimodal neurons were found along the medial to lateral transition zone between the magnocellular division of the MGB and ventral POm, and in POi. Purely auditory neurons were located in MGm and purely somatosensory in POm. On the other hand, Jones and Powell '71 stated that the bimodal neurons studied by Poggio and Mountcastle '60 "were situated at what is almost certainly the junction of the somatic (medial) and auditory (lateral) parts of the posterior group".

Phillips and Irvine ('76, and personal communication) studied the response of PO neurons to tonal stimuli. 70% of the auditory neurons they sampled in POl were sharply tuned. 80% of the auditory neurons recorded from in MGm and POi were broadly tuned. No cells were found

in POm which responded to auditory stimuli. The mean response latencies of POl (16.2 msec) and MGm (15.2 msec) were short whereas the mean latency of POi neurons (37.1 msec) was long. Most of the cells in MGm, POl and POi exhibited binaural response properties where both ears excite the cell or the contralateral ear excites the cell and is inhibited by simultaneous ipsilateral stimulation. There was no apparent segregation of the binaural response properties noted with respect to the POi, POl and MGm subdivisions.

Inferior Colliculus

The inferior colliculus (IC) has been divided, on the basis of cell morphology and connections, into three nuclei (Cajal '55, Morest '64a, '66, '66a, Geniec and Morest '71, Rockel and Jones '73, '73a). The largest nucleus is the central nucleus (ICC) that is encircled by the other nuclei. The names internuclear rind or roof nucleus (Cajal '55), cortex (Genic and Morest '71) and pericentral nucleus (Berman '68, Rockel and Jones '73, '73a) have been used to describe a sheetlike structure that overlies much of the dorsal, lateral and dorsomedial surfaces of the ICC. The external nucleus (Cajal '55, Berman '68, Rockel and Jones '73, 73a) or pericollicular tegmentum (Geniec and Morest '71) covers the anterior and lateral surfaces of the ICC. Regions of the midbrain tegmentum ventral and medial to the ICC have been included within this division by some investigators (Geniec and Morest '71). The partition of the inferior colliculus into a central nucleus (ICC), pericentral nucleus (ICP) and external nucleus (ICX), according to the descriptions of Rockel and Jones '73, '73a will be used here, since this subdivision is consistent with the patterns of the projections examined in this study. Fig. 4 demonstrates these divisions in the frontal plane through the middle of the IC.

The Central Nucleus (ICC)

The central nucleus occupies the core of the inferior colliculus (Cajal '55). It is an ovoidal structure, flattened rostrocaudally, with its long axis directed ventral, anterior and lateral (Rockel & Jones '73).

Figure 4

This schematized frontal section through a middle level of the IC shows the relative positions of the subdivisions of the IC (modified from Rockel and Jones '73).

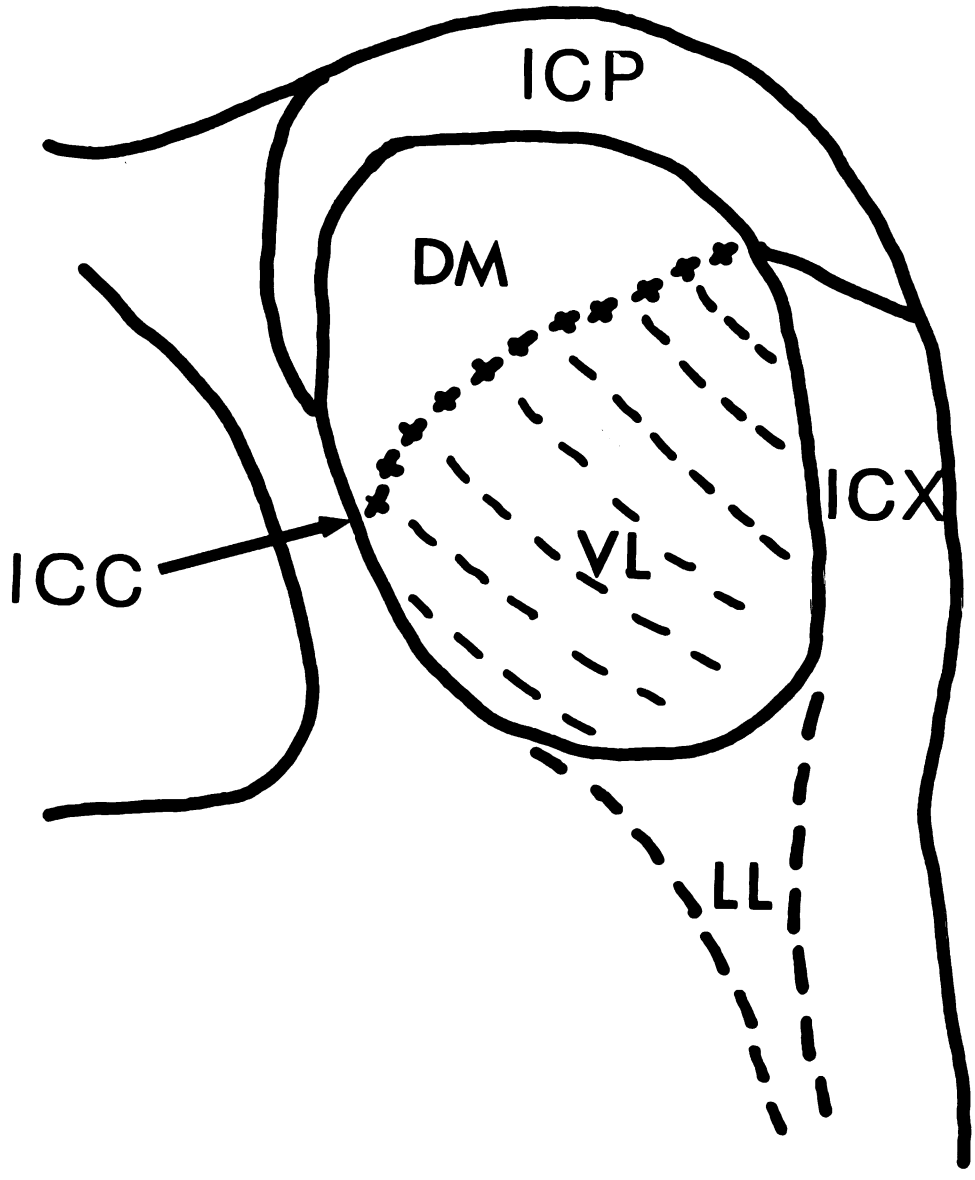
ICP
DM
ICX
ICC
VL
LL

The ICC occupies about two thirds of the total mass of the IC (Rockel & Jones '73). The nucleus contains large, medium and small cell bodies apparent in Nissl and Golgi preparations (Cajal '55, Rockel and Jones '73, Geniec and Morest '71), that are separated by an abundant nerve plexus (Cajal '55).

The rostral aspect of the nucleus is bounded ventromedially by the pericequaductal gray, dorsomedially by the collicular commisure (CC) and the pericentral nucleus, dorsally by the pericentral nucleus and laterally and rostrally by the external nucleus. Caudally, the nucleus is bounded by the fourth ventricle ventromedially, the lateral lemnicus (LL) ventrolaterally, and the ICP dorsomedially, dorsally, laterally, and posteriorly.

ICC Laminations

The central nucleus is a morphologically laminated structure. It derives this structure from the orientations of the dendrites and axons within the nucleus (Morest '64a, Geniec and Morest '71, Rockel and Jones '73, FitzPatrick '75) and the long axes of the perikaryon of certain cell classes (Rockel & Jones '73).

Cells whose dendrites conform to the laminated pattern are of small and medium size (Rockel & Jones '73) and have discoid dendritic fields (Morest '64a, Geniec and Morest '71, Rockel & Jones '73). The disk-shaped dendritic fields overlap to form continuous laminae. The dendritic fields also overlap with the dendrites of the adjacent laminae.

Thus individual laminations are usually not discrete from their neighbors (Jones & Rockel '73, Geniec & Morest '71). The afferent and efferent axons of the ICC run parallel to the laminations and thus they are a part of the laminar structure (Morest '64a, Rockel & Jones '73, Geniec & Morest '71).

Some cell classes within the ICC have dendritic processes which do not conform to the laminar structure of the nucleus. Cells which send their dendrites across several laminae are usually multipolar (stellate) and large (Morest '64b, Geniec & Morest '71, Rockel & Jones '73).

The laminations, in cat, exist as a series of parallel and (in the center of the nucleus) nearly flat planes. At the edges of the ICC, the laminae curve dorsally. The planes in the central region of the nucleus are oriented posterior lateral to anterior medial. The planes are also inclined, with the dorsal edge positioned more medially (Rockel & Jones '73).

Subdivisions of the ICC

The ICC of cat has been subdivided into a dorsomedial region and a ventrolateral region on the basis of morphology and connections (Rockel & Jones '73, Van Noort '69). The Golgi method indicates that the dorsomedial region contains large cells with long, radiating dendritic fields. The structure in this region does not appear laminated, although oriented

dendrites from perikaryon located in the ventrolateral division do extend a short distance into the ventral region of the dorsomedial division. The ventrolateral division is the laminated region of the ICC (Rockel & Jones '73) (see Fig. 4).

The Pericentral Nucleus

The pericentral nucleus of cat is .5 to .75mm thick and covers the dorsal and posterior aspects of the central nucleus (Rockel & Jones '73a, Berman '68). This is a region of large, medium and small cell bodies which are densely packed (Rockel & Jones '73). The smallest cells are located externally and the largest cells internally (Rockel & Jones '73a, Cajal '55, Morest '66, Geniec & Morest '71). On the basis of Golgi impregnations, some investigators have divided the pericentral nucleus into layers (Cajal '55, Morest '66, Geniec & Morest '71) whereas others have not (Rockel & Jones '73).

The External Nucleus

The external nucleus (ICX) covers the ICC anteriorly and laterally, and is bordered dorsally by the ICP (Rockel & Jones '73, Berman '68, Morest '64a). The ICX is approximately 1 to 1.5mm thick (Rockel & Jones '73). It contains cells of various sizes (Rockel & Jones '73); however, some of the largest cells in the inferior colliculus are found in its ventral region (Van Noort '69). Although the ICX and ICP merge, they can be clearly distinguished on the basis of Golgi material since, in these preparations, the ICX cells appear larger and more loosely packed.

The separation of the two nuclei, using Nissl material, is not sharp (Rockel & Jones '73a). The ICX contains fibers of the brachium of the inferior colliculus along the lateral margin (Cajal '55, Van Noort '69, Geniec & Morest '71).

Fiber Paths Within the Inferior Colliculus Central Nucleus

The lateral lemniscus enters the inferior colliculus at its posterior, ventrolateral pole (Rockel & Jones '73, Geniec & Morest '71). The ascending lemniscal axons parallel the laminations of the ICC, and thus contribute to the laminated structure (Morest '64a, Rockel & Jones '73). The lemniscal afferents form strong pericellular connections with the principal cells of the ICC (Rockel & Jones '73, Morest '64a). Leminiscal fibers have also been observed in the dorsomedial division of the ICC; however, they are much sparser in number in that region.

The corticotectal axons are thin, occur only in the dorsomedial division, and enter the dorsomedial division from the ICP. They run parallel to the bits of lamination that protrude into the dorsomedial division and parallel and opposite to the direction of the lemniscal axons. They make contacts with the distal segments of the dendrites of the neurons in the dorsomedial division (Rockel & Jones '73).

Fiber Paths Within the Pericentral Nucleus

The ICP contains a transverse system of corticotectal fibers of medium size (Rockel & Jones '73). These fibers are derived from the

ipsilateral BIC and distribute to all depths of the ICP, but are most common in the deeper layers. Some of these fibers enter the collicular commisure. Other corticofugals incline ventrolaterally to enter the dorsomedial division of the ICC. As the pericentral nucleus is followed caudally in frontal sections, it expands medially and covers the medial aspect of the ICC. Corticofugal fibers in this region become almost vertically disposed. On the posterior aspect of the ICP the corticotectal fibers fan out and descend from dorsolateral to ventromedial.

The efferents to the ICP are axons of large diameter that are vertically oriented and enter the ICP in the vicinity of the lateral lemniscus (Rockel & Jones '73a). They ascend ventrolaterally to dorsomedially in the posterior aspect of the ICP giving off collaterals and end predominantly in the dorsal aspect of the ICP. They exist at all depths throughout the dorsal and posterior aspects of the ICP. These ascending fibers cross the corticotectal fibers, on the dorsal aspect of the ICP, at right angles. On the posterior surface the two systems also form a grid but they are more obliquely oriented due to the fanning out of the corticotectal fibers on the posterior face.

The origin of the efferent fiber system is unknown. However, Rockel & Jones '73a speculated that the fibers arose from the dorsal nucleus of the lateral lemniscus (DNLL) since undercuting the lateral lemniscus ventral to the DNLL, or lesioning the midbrain tegmentum and trapezoid body did not produce degeneration in ICP. However, other investigators have lesioned the DNLL as well and not produced degen-

eration in the ICP (Goldberg & Moore '67, Van Noort '69). Since lesions of the central nucleus do not produce degeneration in the ICP (Rockel & Jones '73), this creates an unusual problem in assigning an origin to these fibers and in determining the ascending input to ICP.

Tonotopic Organization of the Inferior Colliculus

Rose et al., '63, using the microelectrode recording technique, found thata representation of the cochlea was contained within the central nucleus, with the best frequencies progressing from low to high moving dorsolaterally to ventromedially within the nucleus. Similar results have been noted in the central nucleus of cat (Aitkin et al., '70, Merzenich & Reid '74), rat (Clopton & Winfield '73) rabbit (Aitkin et al., '72) and chinchilla (Adams & Teas '73).

With the description of the laminar structure of the central nucleus (Morest '64a),Morest '64b proposed that the elongation of the dendritic fields and the restricted and strong contacts made by afferents traveling parallel the elongation, provided an optimal structure for the maintenance of a cochleotopic organization. Rockel & Jones '73 also proposed that the laminations of the central nucleus represented some form of the tonotopic organization.

Merzenich & Reid '74 (in cat) and Fitzpartick '75 (in squirrel monkey) established that the laminations are the morphological substrates

for the tonotopic order of the central nucleus. Reconstructing, in three dimensions, data obtained from multiple microelectrode penetrations into the central nucleus, Merzenich & Reid '74 showed that regions of similar best frequencies formed discs which had approximately the same orientation as the morphological laminations reported in cat (Rockel & Jones '73). Fitzpatrick '75, using Golgi methods and the microelectrode recording technique, showed that the morphological laminations and isofrequency contours of the central nucleus of the squirrel monkey have the same orientations.

Sharp tuning curves and an orderly sequence of best frequencies are also characteristic of the non-laminated dorsomedial division of the central nucleus of the cat (Roth '77). The orderly arrangement of best frequencies within the dorsomedial division appears to be contiguous with that in the ventrolateral division and thus results in a single representation of the cochlear sensory epithelium within the entire central nucleus. Fitzpatrick '75, also noted a single representation of the cochlea in squirrel monkey that spanned both the central nucleus and a region dorsal the ICC which is probably homologous to the dorsomedial division. This dorsal region contained the lower frequencies and the laminated central nucleus contained the higher frequencies. Electrode penetrations through the two regions resulted in an uninterupted progression of best frequencies.

Rose et al., '63 observed a tonotopic representation in the lateral aspect of the ICP. The sequential best frequencies proceded from high to low moving externally to internally and spanned about 1mm. At least some of the tuning curves of these neurons were broad (e.g., see their Fig. 5, p. 301). Merzenich & Reid '74 and Aitkin et al., '75 recorded this same sequence of best frequencies from the lateral aspect of the ICP. The tuning curves were reported to be very broad. Merzenich & Reid also made penetrations in the medial regions of ICP and found the neurons of this region to have low best frequencies and no apparent tonotopic organization. Overall, they reported that the neurons of ICP of the barbituate anesthetized cats had higher thresholds and were driven only sporadically at the onset of tonal stimuli, if at all.

ICX

The external nucleus of cat receives auditory projections from the ICC (Van Noort '69) but apparently not directly from the lateral lemniscus (Van Noort '69, Rockel & Jones '73, Osen '72, Goldberg & Moore '67). This region also receives somatosensory system projections from the dorsal column nuclei of cat, hedgehog and opossum (Hind & Liu '66, Hand & Van Winkle '77, Morest, Jane & Schroeder '71, Robards et al., '76) and the spinal cord and somatosensory cortex of opossum (Robards et al., '76).

The external nucleus contains cells which respond to auditory, somatosensory and both auditory and somatosensory stimuli. No apparent segregation of these response classes have been noted (Aitkin et al., '78).

A large majority of the cells of ICX respond to auditory stimuli (Aitkin et al., '78). The tuning curves of these cells are broad. A majority receive binaural input and are about equally divided between units which are excited by both ears and units which are excited by the contralateral ear and inhibited by the ipsilateral ear (Aitkin et al., '75, '78). The broad tuning of ICX neurons makes it difficult to discern a tonotopic organization, although a tendancy for low best frequency responses to be located rostrally and high best frequency responses to be located ventrocaudally has been reported (Aitkin et al., '78).

Response Properties of ICC Neurons

Although a majority of the cells of the ICC are binaural (Erulkar '59, Aitkin et al., '75) there are many cells in this nucleus which respond only to stimulation of one (generally the contralateral) ear (Roth '77, Aitkin et al., '75, Erulkar '59). These cells are generally located in the posterior aspect of the ICC and presumably receive a direct projection from the contralateral (monaural) cochlear nuclear complex (Roth '77).

Many binaural neurons are sensitive to interaural delays or interaural intensity differences. Many delay sensitive neurons of the ICC are said to have "characteristic" delays since they respond maximally at a particular delay regardless of the frequency or magnitude of stimulation (Rose et al., '66). Most, but not all, ICC delay sensitive neurons exhibit

this property (Geisler et al., '69). Delay sensitive neurons have low best frequencies (Rose et al., '66, Geisler et al., '69, Roth '77) and are located in only a limited portion of the apical representation of the cochlea in the dorsal ICC (Roth '77). A majority of the delay sensitive neurons responded maximally with the contralateral ear leading (i.e., represented the contralateral sound field) and neurons with similar delays appeared to be grouped together (Roth '77). Most intensity difference sensitive neurons are stimulated by the contralateral ear and inhibited by the ipsilateral ear (Rose et al., '66, Geisler et al., '69, Roth '77). These neurons usually have higher best frequencies and occupy restricted areas in the more ventral regions of the ICC (Roth '77). Binaural neurons also exist in the ICC which are not sensitive to interaural intensities or delays (Roth '77). These neurons generally responded to binaural stimulation by summing or facilitating the responses obtained from monaural stimulation of the two ears. These neurons were evenly distributed with respect to best frequency but were also segregated to restricted regions within the nucleus (Roth '77).

A majority (2/3) of the neurons in the ICC of cat exhibit sustained activity to tonal stimuli (Roth '77). This is in sharp contrast to the cortex (Brugge et al., '69) and MGB (Aitkin & Webster '72) of cat where sustained activity is very rare. Units which are time or intensity difference sensitive tend to be sustained whereas the other binaural units are equally divided between onset and sustained behavior (Roth '77).

Summary - Inferior Colliculus

The inferior colliculus has been divided into three nuclei on the basis of cell morphology; the central nucleus (ICC), pericentral nucleus (ICP), and external nucleus (ICX). The central nucleus is a roughly ovoidal structure that occupies the core of the inferior colliculus and accounts for about two thirds of its mass. The ICC is covered dorsally and posteriorly by the sheetlike ICP and laterally and anteriorly by the ICX. The central nucleus can itself be divided into two morphologically delineable regions; a dorsomedial division and a ventrolateral division. In the ventrolateral division many cell dendrites and the incoming and projecting axons are oriented to produce parallel laminations.

The inferior colliculus contains at least two representations of the cochlea; one in ICC and one in ICP. The representation in ICC is in the form of stacks of isofrequency contours whose orientations coincide with those of the morphological laminations. The cochlear representation is continuous across both the dorsomedial and ventrolateral divisions of ICC.

The tuning curves of ICP neurons are much broader than ICC neurons. The ICC contains monaural and binaural neurons. The monaural neurons generally respond to contralateral stimulation and are usually encountered in the posterior and far medial aspects of the ICC. The binaural neurons include intensity difference sensitive neurons (of high best frequencies and dorsally located) and delay sensitive neurons (of low best frequencies

and ventrally located). Two thirds of the neurons give a sustained response to tonal stimulation. All classes of response properties are segregated within the ICC although the exact architecture of this segregation is at present unknown.

METHODS

METHODS

Animal Preparation

Successful cortical recording-injection experiments were performed in 39 hemispheres of 28 cats. The protocol for animal preparation was similar to that described by Merzenich and colleagues, ('75) and Knight, ('77). The recording and injection phase of experiments in which a partial map was made in only one cortical field lasted 4 to 8 hours. Experiments in which 2 or 3 or 4 fields were mapped and injections introduced typically lasted 10 to 20 hours.

In most experiments, the animals were sacrificed 2 days after the acute recording-injection experiments. In these experiments, clean surgical conditions were used. In some experiments, animals recovered and were maintained 8 to 18 days after the surgery. In these studies, the surgery was performed under sterile conditions.

Animals were initially anethetized with an intramuscular injection of ketamine hydrochloride (25 mg/kg.) 6 mg doses were subsequently administered to maintain a surgical level of anesthesia. Prior to the initial phase of surgery, the cat was administered a single injection of sodium pentabarbital (12 mg, I.P.).

A craniotomy was performed over the cortical field or fields of interest in each experiment. The dura was carefully resected. The cortical surface was kept moist by regular application of warm (38°)sterile saline and by placement of saline soaked cotton over regions of the cortical surface when recording was not in progress.

After exposure of the cortex, a photograph was made of the cortical surface vasculature. A 10X working print with an overlying .5mm grid was made. It was used to record the sites of vertical microelectrode penetrations, and of tracer injections.

Recordings were made with glass-coated, platinum-iriduim microelectrodes with impedances of 2.5 to 3.5 megohms (at 1.0 kHz). Penetrations were introduced normal to the cortical surface with a hydraulic microdirve controlled by a stepping motor placed outside the sound room. The microdrive was mounted on the H bar of a stereotaxic apparatus. All penetrations were parallel to one another. Each penetration or injection was placed under visual control with the use of a Zeiss dissecting microscope, and the location was marked on the working photograph.

After recording and injection, the surface of the cortex was washed with sterile saline. The incision was closed. The animal was transferred to an incubator and returned to it's cage the following day.

Stimulation and Recording

All experiments were conducted in an IAC sound room. Stimuli were delivered to the animals via a hollow flexible tube sealed into the contralateral external auditory meatus with low melting point beeswax. The outer end of the tube was sealed into a chamber in which an audiometric driver (Telex model 61476) was sealed. The stimuli were tone pips, generated by shaping the output of a General Radio Corporation oscillator (type 1309A) with an artifact-free electronic switch (Ludwig, '70). Tone pips had trapeziodal envelopes, with rise and fall times of 5 msec. The signals were fed through an attenuator (Hewlett Packard 350D) that enabled manual

control of the stimulus intensities in 1 or 10 dB steps. Programmable timers controlled the stimulus duration and repitition rates. A stimulus duration of .2 seconds and a repetition rate of .8 or 1.0 seconds were used in these experiments.

The drivers were calibrated with a probe microphone (Bruhl and Kjaer, 0.50 inch) and a waveform analyzer (General Radio Model 1900). The frequency response of these speakers was relatively flat to about 13 kHz but was attenuated at higher frequencies. The dynamic range of the driver allowed for definition of best frequencies up to 30 to 35 kHz. The "best frequency" of a unit (or unit cluster) was determined by finding that frequency at which the unit responded at the lowest sound pressure level. This was determined by viewing unit discharges on the stimulus-synchronized sweep of an oscilloscope (Tektronix Type 565) and by listening to the amplifier output fed to a loudspeaker. Best frequency determinations were made at three or more positions within the responsive zone of cortex in each vertical penetration.

Injection of Tracers

Injections of anterograde and retrograde tracers were introduced at locations in auditory cortex that had been physiologically typified with a brief map derived with the microelectrode recording techniques outlined above. In the physiological phase of the study, the location of the cortical field to be injected was defined; the approximate boundaries of the field were determined (in the region of the injection); and the approximate axis of "isofrequency lines" was defined. These partial maps generally required

10 to 20 penetrations in each cortical field. They insured that injections were always made well within given field boundaries. The effective spread of tracers at the injection sites was usually difficult to access on the basis of examination of the injection site alone. With .2 microliter injections and 2 day survivals, a core of heavily, autoradiographically labelled cell bodies with intervening more lightly labelled neuropil was observed that was at most 1mm in diameter. Some investigators believe this type of labelled profile defines the area that has incorporated the amino acids for protien production and transport (Cowan et al., '72). The entire spread of ARG label at the injection site was generally about 2 to 3mm in diameter. As has been observed by others (Hedreen and McGrath, '77), the size of the HRP labelled injection site varied with time, being largest at one day and progressively smaller at two and three days.

Although it was not possible to judge the effective spread of HRP at the injection site, and although there was some uncertainty of the true effective spread of the 3H-l-leucine at the injection site, it was possible to estimate it for both tracers, by defining the limits of the labelling in the target structure. Small injections (e.g., .1 to .2 microliters) of either tracer into AI or AAF produced label in pars lateralis that never occupied more than one fourth to one third of the nucleus. AI and AAF occupy about the same cortical surface area (Knight, '77, Merzenich, et al., '77) and they are about 6mm long normal to their cochleotopic representations and 4 to 5mm along their isofrequency axes in the center of the field. Pars lateralis contains one representation of the cochlear epithelium which is not grossly dissimilar in proportional dimensions to the cochlear representation in AI or AAF (Aitkin and Webster, '72). Thus, a rough estimate of 1.5

to 2.0mm as the upper limit to the diameter of the effective injection site can be made for V1. (It was, on the average, 1mm in diameter.) That this is a reasonable estimate of a limit for spread of tracer at AAF injection sites was further confirmed in several cases in which two injections were made into different, widely separated cochleotopic representational sites in the AAF. This produced two distinct and completely separated bands of label in V1, even when the injections were placed only 2mm apart on the cortical surface (e.g., see Fig. 12).

The effective injection site could be similarly estimated by examining the projection arrays from AI injection loci to the dorsomedial division of the central nucleus. As will be shown in the results, the topography of this projection, with respect to the cochleotopic organization of AI, conformed to the cochleotopic organization of the central nucleus. The width of each projection lamina in the ICC was measured and converted into the best frequency range it spanned using the "recording depth vs. best frequency" data of Merzenich and Reid '74. Each frequency range was then compared with the "best frequency vs. distance on the cortical surface" graphs of Merzenich et al., '75. These data were consistent with an effective spread of tracer at the injection site of .5 to 1.5mm diameter for small (.1 to .2µl) injections. (It was usually .5mm in diameter). These measurements were again, further confirmed in those cases where two injections were made at different positions in the cochleotopic representation in AI (e.g., see Fig. 25). (That the effective injection site was smaller for the AI projection onto the ICC than the projection onto V1 may be in some way a result of the larger transport distance, or it may suggest that the divergence of the projection from AI loci to the ICC is not as great as the projection to V1.)

For anterograde tracing .1 ml of 4,5 3H-leucine (61 C/mM, .5 mC/ml) was desiccated and redissolved in 5 microliters of sterile saline. The final label concentration was 10 microcuries/microliter. (In one case 3H-l-proline was used). For retrograde tracing, saturated solutions of HRP (Sigma type VI) were prepared in 5 microliters of sterile saline. For injections of both tracers together, the HRP was dissolved in the leucine solution (Colwell, '75, Trojanowski and Jacobson, '75).

Pressure injections were made with 1 or 5µl Hamilton microsyringes with 27 or 31 gauge needles. A glass micropipette was often affixed to the tip of the metal needle with sticky wax. The syringe was attached to the microdirve, which was mounted on a micromanipulator attached to the stereotaxic apparatus. The micropipette needle was advanced carefully into the cortex while being visualized through the Zeiss dissecting microscope.

Injections were made in the middle layers of cortex (500-1000µdepth). Injections were made manually, over several minutes, or by attaching the plunger to the hydraulic microdrive and initiating a continuous rate of advancement that completed the injection in 20 or 30 minutes. Injection volumes ranged between .05 and .5µl liters with .15 and .2µl the most common volume of injection. After an injection was completed, the micropipette or needle was left in place for 15 to 30 minutes.

In two experiments where long survival times were used for anterograde tracing, the cortex was re-exposed one or three days prior to sacrifice and the same loci that received 3H-l-leucine were injected with HRP. The previous injection sites had been marked with carbon black. This method of combined tracing was used in long survival experiments, since the HRP must be processed

after no longer than a four day survival period to ensure maximum activity of the enzyme.

Anatomical Proceedures

Postoperative survival periods were either short (2 days) or long (8 to 18 days). Longer survival times increased autoradiographic labelling of fiber tracts (Cowan, et al., '72, Hendrickson '72) and increased the level of labelling of terminal fields.

Following the postoperative period, animals were anesthetized with sodium pentobarbital and perfused intracardially with cold (4°c) heparinized saline followed by cold .2M phosphate buffered (pH 7.6) 2.5% paraformaldehyde solution. The brains were removed from the skull and placed in cold fixative overnight. The brains were then passed through a graded series (5, 15, 30%) of cold .1M phosphate buffered (pH 7.6) sucrose solutions over a 24 hour period.

Brains were blocked anterior to the injection sites and posterior to the IC's and were sectioned serially in the frontal plane on a freezing microtome. Sections were collected on a 90μ, 30μ and 30μ rotating schedule or on a 100μ , 50μ and 50μ schedule. The 90 or 100μ sections were incubated for 10 to 20 minutes in a .07% solution of 3,3' diaminobenzidine in Trisma buffer (pH 7.6) with hydrogen peroxide (Graham and Karnovsky '66, LaVail and LaVail, '72, Ralston and Sharpe '73, LaVail, et al., '73). The sections were washed in 3 changes of Trisma buffer, mounted on gelatinized slides, dried, dehydrated, cleared and coverslipped. One serial set of 30 or 50μ sections were also processed for HRP. After being dried, defatted, rehydrated and dried, these sections were subsequently processed for autoradiography (Cowan, et al., '72). This allowed the simultaneous demonstration of HRP and autoradiographic labelling in single

sections (Colwell '75; Colwell and Merzenich, '79) The third set of sections was processed for autoradiography alone (Cowan, et al., '72). Slides were dipped in 40°c Kodak NTB-2 nuclear track emulsion diluted 1:1 with distilled water. The slides were dried for 2 hours and then stored in light tight boxes containing drierite capsules. The autoradiograms were placed in a refrigerator at 4°c for 3 to 4.5 months before being developed. The autoradiograms were developed in Kodak D-19 developer at 16°c for 2 minutes, rinsed in distilled water containing a few drops of glacial acetic acid, fixed for 2 minutes with Kodak Rapid Fix (diluted 1:4 with distilled water) and washed for 2 hours in running distilled water. Slides processed for HRP and autoradiography were dehydrated and coverslipped after drying; slides processed for autoradiography alone were counterstained with cresyl violet or neutral red. Relevant slides from the HRP and HRP - ARG series were also counterstained after HRP containing neurons were identified and plotted.

Data Analysis

Sections were examined under brightfield and darkfield illumination with a Zeiss Photomicroscope III or a low power Olympus Photomicroscope. Low power dark field photomicrographs were made of autoradiograms using a Nikon Ultraphot mounted over a Sage (model 281) stereo light box. Photomicrographs were made with Kodak High Contrast Ortho Process 4x5 sheet film or with Kodak Panatonic X (ASA 32) 35mm film. HRP labelled cells were plotted only if the cell bodies or proximal dendrites contained the darkly-stained HRP reaction granules seen under high power bright or dark field illumination. This avoided false identification of labelling in cells with endogenous peroxidase activity (Wong-Riley '76). Labelled cells were located on darkfield photo-

micrographs. The micrographs were printed underdeveloped on high contrast paper to bring out as many "landmarks" in the sections as possible on the prints to facilitate plotting cells located with the microscope. Often, the HRP cells could be directly visualized on the darkfield photomicrographs and under the microscope (i.e., see Fig. 21) enabling the precise location of the cells on plots of the sections.

RESULTS

AI Connectivity with Auditory Thalamus

The principle aim of this study was to investigate the thalamocortical and corticothalamic connections of AAF and AII. It was advantageous to relate the connections of these two fields to those of AI. This added a second reference that together with the cytoarchitecture of the MGB enabled a more complete understanding of the spatial organization of the complex ascending and descending connections of AAF and AII. It also enabled a direct, detailed comparison of the organization of connections of these two fields with those of AI and, through the comparison with AI, with each other. Thus, regions of common and uncommon projections from the thalamus to the three fields could be defined. In the course of this study, then, the connections of AI and the auditory thalamus were reexamined. The basic patterns of AI-MGB connections recorded in these studies confirmed and extended descriptions of earlier studies using similar techniques (Merzenich and Colwell, '75, Colwell and Merzenich, '75, Colwell, '77, Colwell and Merzenich '79, Merzenich et al., '79).

The corticothalamic projection of AI was investigated by placing single (or occasionally multiple) microinjections of 3H-l-leucine at physiologically defined loci within AI. Successful experiments were performed in the AI auditory fields of 16 hemispheres. The physiologically typified loci of injections had best frequencies ranging from 1.5 to 25 KHz. Injections were introduced (in different experiments)

across the entire five-octave range.

The thalamocortical projection of AI was studied in a similar way, using the retrograde tracer HRP. Restricted injections of HRP were made at physiologically defined loci in the AIs of 3 hemispheres. In another two hemispheres, large and multiple injections of HRP were made into AI. The patterns of HRP labelling of neurons in the MGB and PO1 were similar to autoradiographic labelling patterns resulting from 3H-l-leucine injections (e.g., see Fig. 13, Secs. B and C).

The coincidence of the origin of the thalamocortical projection and the termination of corticothalamic projection of AI has been studied in great detail by investigators in this laboratory (Colwell and Merzenich, '75; Merzenich and Colwell, '75; Colwell, '77; Colwell and Merzenich, '79). They found that after injections of both orthograde and retrograde tracers into single loci in AI, the resulting distribution of both labels in the MGB and PO1 were superimposable. Every region of auditory thalamus that contained HRP labelled cell bodies was overlain with above background autoradiographic labelling. Conversely, foci of autoradiographic label in the MGB or PO1 only existed in regions that also contained HRP labelled cells. This reciprocity of thalamocortical and corticothalamic connections was seen regardless of the site of the injection of the combined tracers in AI. Injections of HRP and leucine into AI produced only autoradiographic label in the reticular nucleus,

i.e., this projection is not reciprocal.

Most of the illustrated projections in this section summarize labelled terminal arrays resulting from injections of 3H-l-leucine into AI. However, in view of the reciprocity of connectivity, the patterns of autoradiographic label seen in the MGB and POl identify the basic outline of the array of neurons projecting to the injection-site locations of AI.

Corticothalamic Projection of AI

After AI injections of 3H-l-leucine and short survival times (i.e., 2 days), fibers were followed from the cortical injection site to the thalamus. Fibers left the injection site as a tight bundle arching ventrolaterally. Corticothalamic fibers descended from this bundle in a broader, anastomosing group in the internal capsule. The remaining fibers continued medially in the frontal plane, arched dorsally, and entered the corpus callosum (destined for contralateral cortical areas). The corticothalamic tract coursed ventral and lateral to the rostral pole of the lateral geniculate nucleus. Fibers entered the reticular nucleus of the thalamus lateral to the lateral posterior group of the dorsal thalamus. Dense pericellular clustering of autoradiographic grains around cells in the reticular nucleus indicated terminal fields in this region (see Fig. 5).

Corticothalamic fibers continued medially through the reticular

Figure 5

An example of the path of cortical efferent fibers leaving a 3H-l-leucine injection site in AI. The injection site is the bright white area in the upper left hand corner labelled I.S. The transcallosal corticocortical fibers arch dorsomedially from the injection site. In this figure they are labelled C.C. and the path of the labelled fibers is indicated by the white arrows. In the upper right hand corner of the darkfield photomicrograph these fibers enter the corpus callosum. The labelled corticothalamic fibers (which are probably intermingled with labelled corticotectal, corticopontine and corticostriatal fibers) course ventrally in a broader, anastomosing pattern. The corticothalamic tract is labelled C.T. in this figure. The course of the labelled fibers, portions of which dropped out in this reproduction but which were visible under the microscope, is indicated by the white arrows. Heavy ARG terminal labelling from this projection is present in the reticular nucleus of the thalamus (R), ventrolateral to the lateral geniculate nucleus (LGN).

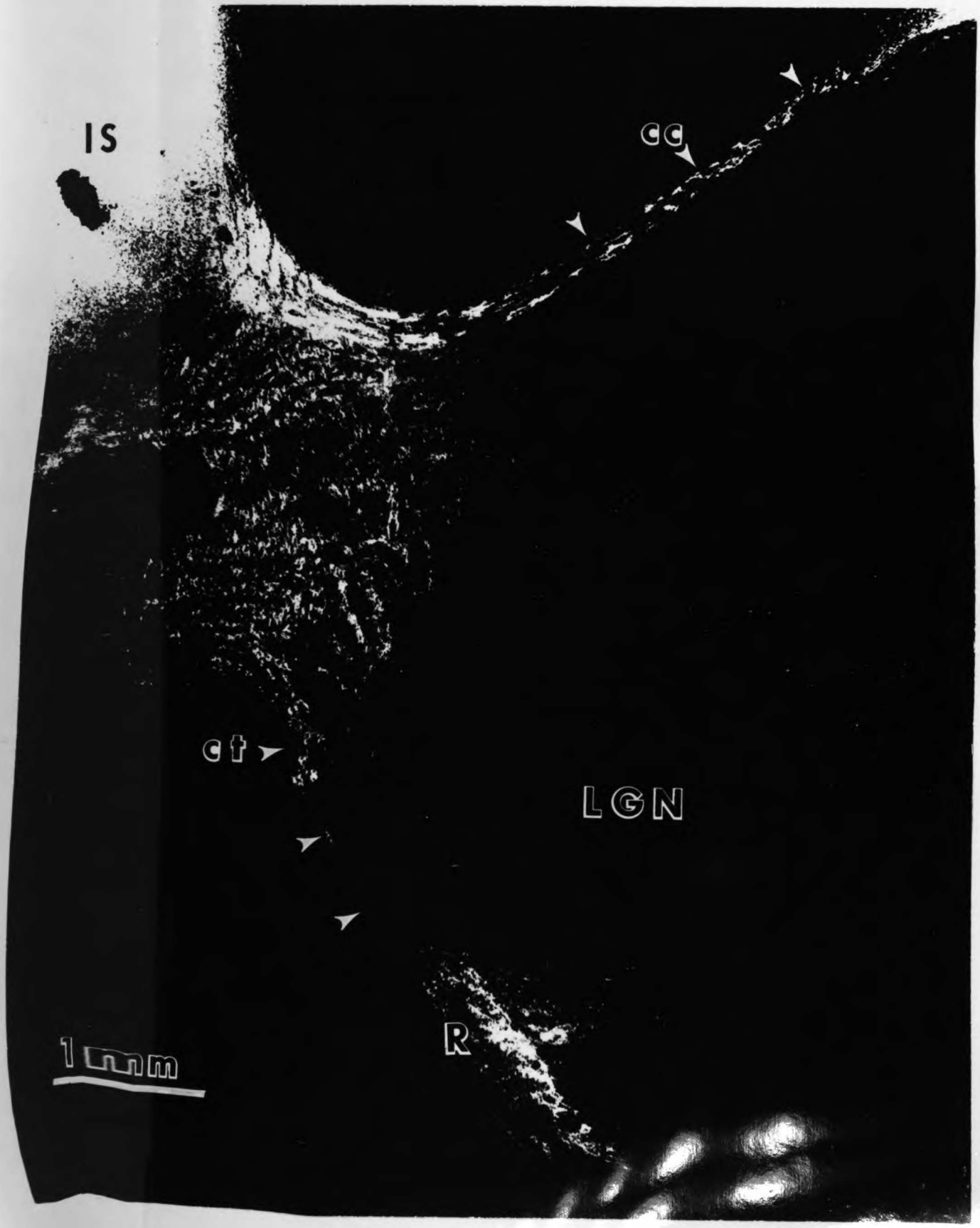
IS
cc
ct
LGN
R
1 mm

nucleus ventral to the LGN and entered the lateral division of the posterior group of the thalamus. Autoradiographic labelling within this region indicated that the projection to POl was complex. At least two and often as many as four or five foci of autoradiographic (ARG) labelling were seen after single injections (i.e., see Sec. 18 of Fig. 14).

Caudal to the posterior group, two descending profiles of continuous ARG labelling coursed from the rostral pole of the MGB into its posterior third. One component was located laterally and the other medially. The label in the medial component was continuous rostrally with the label in POl.

The medial column of ARG labelled neurons passed along the rostrocaudal axis for 2 to 3mm from the rostral pole of the MGB into the rostral aspect of the caudal third of the geniculate before attenuating (see Figs. 6 and 14). Examination of these sections counterstained with Nissl stains, or examination of the morphology of the HRP-containing neurons of this cell array after injections of HRP into AI, revealed that this column extended through the deep dorsal nucleus rostrally, and through the medial division caudally (Figs. 6, 7, 13, 14, 15). In the terms of the other major scheme of parcellation, this projection extended through the rostrocaudal extent of the magnocellular division. *

Figure 6

This figure represents the corticothalamic projection of AI onto the MGB. An injection of 2μ Curies of 3H-l-leucine in a volume of .1μ liters sterile saline was made at an 11 kHz locus in AI (see Figure 15 for the microelectrode maps of the cortical surface and the position of the injection site). Each section number represents a sequential 200μ step. The darkfield photomicrographs are of sections taken in the frontal plane. Unless otherwise indicated, all sections are cut in the frontal plane. Section 10 is taken from the anterior portion of the rostral third of the MGB; Section 13 the posterior portion of the rostral third of the nucleus; Section 16, the anterior portion of the middle third of the MGB. (The nucleus is 3.6mm in the rostrocaudal dimension in this cat; beginning with Section 9 rostrally and ending with Section 27 caudally.)

The projection can be seen in Section 10 to comprise a lamina in the pars lateralis (Vl) of the ventral division of the MGB and a more medial and dorsal column in the deep dorsal nucleus (Dd) of the dorsal division of MGB. Section 13 indicates that the lamina in the pars lateralis divides to form dorsally pars lateralis and ventrally pars ovoidea (Vo) of the ventral division. The orientation of the lamina within the ventral division has changed from a dorsoventral orientation to a dorsolateral to ventromedial orientation for Vl and a ventrolateral to dorsomedial orientation for Vo. Both laminae point medially to the transitional zone (Vt) of the ventral division; a column of label oriented in the rostrocaudal dimension. At this level, the medially located label is also

Figure 6 Cont'd.

undergoing a transition from the deep dorsal nucleus dorsolaterally to the medial division (M) ventromedially. Section 16 is a common example of periodicities of label density in the projection array of the ventral division. In three dimensions, these discontinuities of label form parallel columns with their long axes oriented rostrocaudally. Pars lateralis comprises the three rostral columns, the most medial column corresponds to Vt and the most ventral label, Vo. Medially is the lightly labelled medial division. Labelling continues in this pattern until Section 19 where the ovoidal division is the last remaining focus of autoradiographic grains within the MGB. The posterior third of the MGB is unlabelled, as is the case with all AI injections.

77-12, AI, 11 KHZ

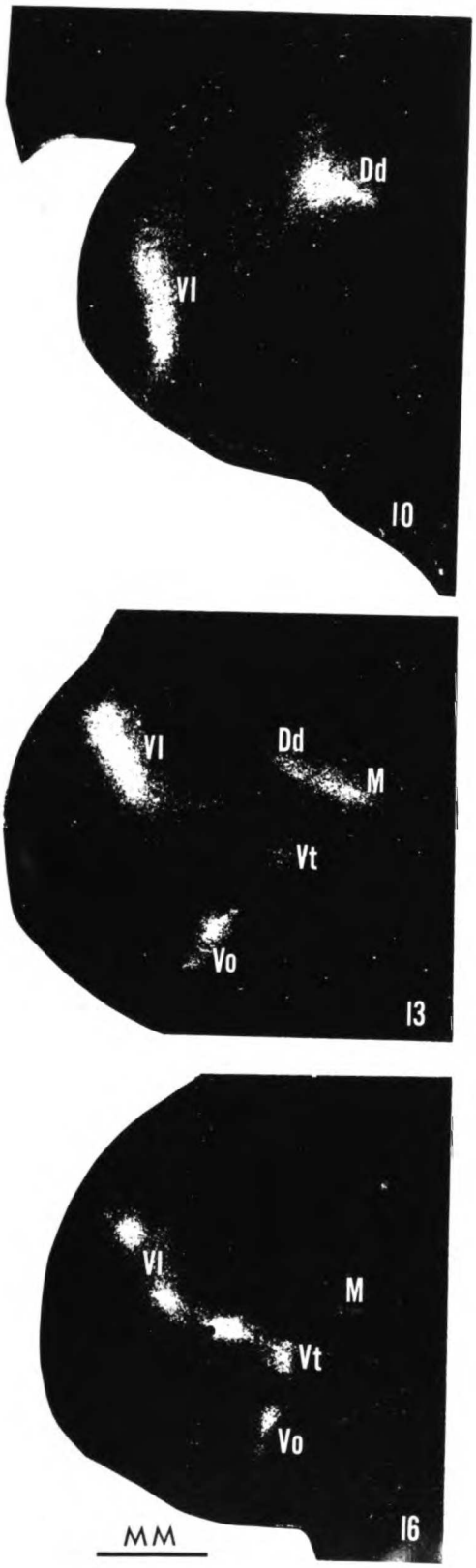

Figure 6a

An example of banding in Vl of the corticothalamic projection. Adjacent sections have been aligned with the most caudal on the left and the most rostral on the right. The discontinuities of label in Vl (the top three groups of patches), Vt (the most medial patches), and Vo (the bottom patches), in three dimensions, are in the form of parallel columns oriented rostrocaudally. This banding is restricted to the caudal half of Vl, just caudal to the partition of Vl into Vl and Vo. This banding was noted only after small volume injections at higher frequency representational loci in AI (and AAF).

1mm
M
V

* An exception to this was when injections were made at very high best frequency representations in AI. In those cases the rostral aspect of the column which lies in the deep dorsal nucleus was situated along the medial aspect of the "principle division". The caudal aspect of the projection in the medial division remained in MGm. The shift in divisions of the rostral aspect of the projection was a result of the topography of the projection to Dd (see the section on "Topography of Projection") and the fact that Dd is divided between MGp and MGm.

The lateral ARG-defined corticothalamic projection began at the rostral pole of the MGB and ended caudally in the rostral aspect of the posterior third of the MGB at about the same level as the end of the ARG-labelled medial column. The rostral label first appeared, in the transverse plane, as a band along the dorsolateral margin of the MGB, parallel to the surface of the nucleus. This grain field was situated in the rostral aspect of the pars lateralis of the ventral division (see Fig. 15, Sec. 15). As the sheetlike projection proceeded caudally in pars lateralis, it acquired a more vertical and medial orientation (see Fig. 6, Sec. 10; Fig. 7. Sec. 16: Fig. 14, Sec. 26; Fig. 20, Sec. 17).

In the middle third of the MGB, the sheetlike projection divided to form a larger lamina in pars lateralis and a smaller lamina in pars ovoidea (see Fig. 7). This continuous transition occurred at about the same rostrocaudal level at which the medial column passed from the deep dorsal nucleus into the medial division. Caudal to the level at which label in Vo first appeared, the ARG-labelled terminal fields in Vl and Vo were continuous, and together formed a folded terminal field array (see Fig. 6, Sec. 16; Fig. 14, Sec. 29; Fig. 22, Sec. C; Fig. 23, Sec. B).

Figure 7

Two representative examples of how pars ovoidea of the ventral division is derived from a split in pars lateralis of the ventral division. The sequential sections on the left represent 150μ steps, on the right 200μ steps. Numbering is rostral to caudal.

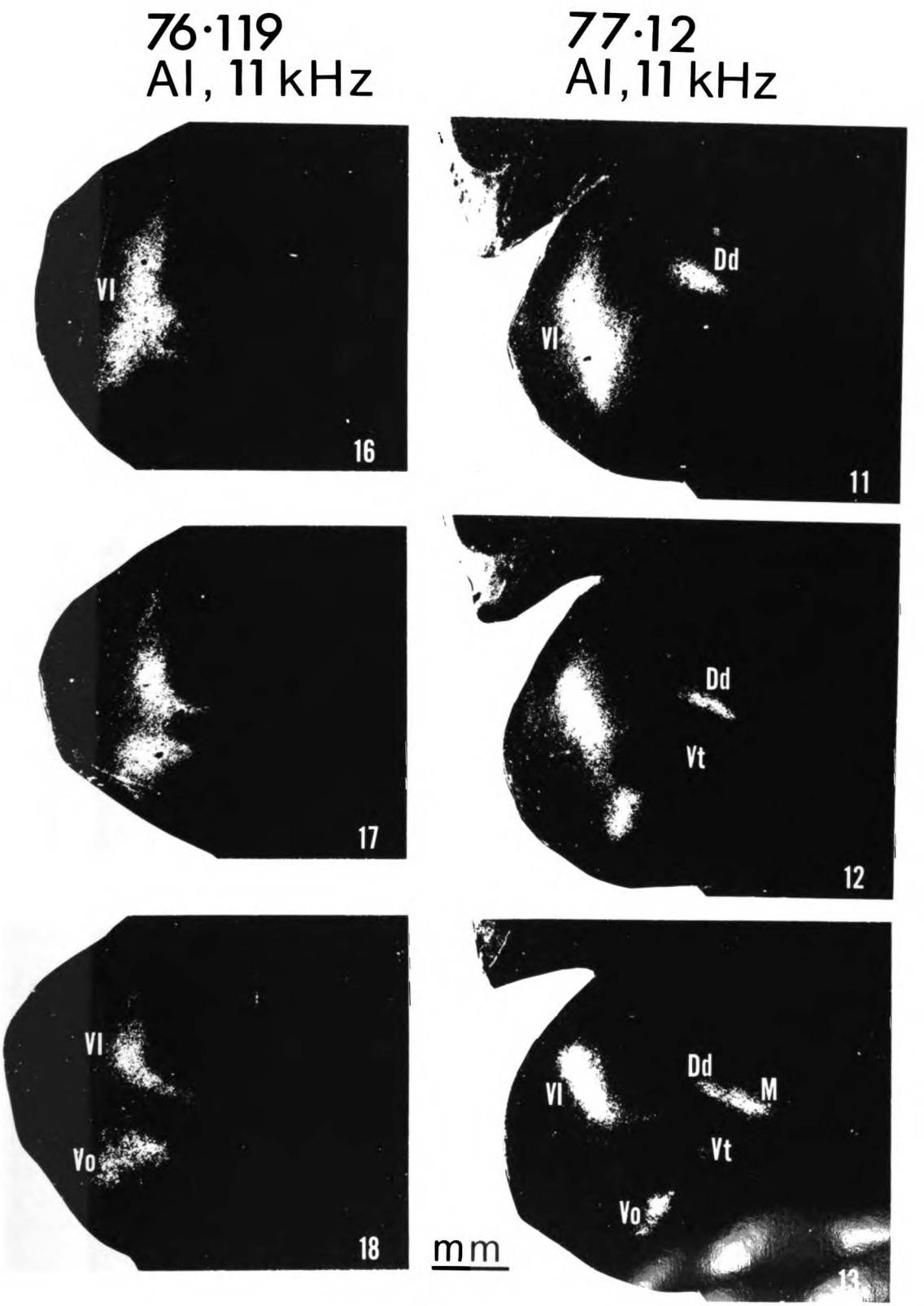
76·119
Al, 11 kHz
77·12
Al, 11 kHz
Vl
16
Dd
Vl
11
17
Dd
Vt
12
Vl
Vo
18
Vl
Dd
M
Vt
Vo
13
mm

A focus of ARG label appeared rostrally, just preceding the division of Vl into Vl and Vo, in the medial aspect of the ventral division (see Fig. 6, Sec. 13; Fig. 14, Sec. 26; Fig. 20, Sec. 17). This label became incorporated in the in-folded sheet caudally (see Fig. 6, Sec. 13 and 16; Fig. 14, Sec. 26 and 28). It constituted the most medial sector of this folded sheet. Caudally, this region had larger cells than those of Vl. These neurons were, in fact, similar to the cells of Vo. This focus of ARG label was thus believed to be in the dorsal part of the pars ovoidea and probably corresponds to the "transitional zone" (Vt) of Morest, '65. There was always a region of lighter label between the Vt and Vo components of the folded sheet (Fig. 6, Sec. 16; Fig. 14, Sec. 29; Fig. 23, Sec. B).

The entire lateral projection array was within the two laminated nuclei (Morest, '65) of the ventral division, the pars lateralis and pars ovoidea. Likewise, this projection was restricted to the principle division of the MGB.

To summarize, there is a rostral corticothalamic projection from AI to the reticular nucleus and POl. Beginning at the border between POl and MGB, two components of label extended rostrocaudally through the rostral and middle thirds of the geniculate. The medial projection array was in the form of a column that passed rostrocaudally through the

deep dorsal nucleus and the medial division. The lateral projection array was in the form of a sheet that passed through pars lateralis and pars ovoidea of the ventral division. Caudally, this sheet was folded (see Fig.31, Part B). In terms of the parcellation of MGB based on Nissl cytoarchitecture, the medial column was contained primarily within the magnocellular division, and the lateral folded sheet was within the principle division. Most of the posterior third of the geniculate was free of label.

Topographic Organization of the AI Projection onto MGB

Injections at different physiologically determined locations in AI revealed that all nuclei of the MGB which received projections from (and project to) AI were topographically interconnected with it. The corticothalamic projections to pars lateralis and pars ovoidea of the ventral division were highly ordered, and consistent with a cochleotopic organization. The projections to the Dd and M divisions also had a topographic organization. However, this organization was less precise.

With injections of anterograde tracer into the sites of representation of successively higher frequencies within AI, the sheetlike labelled arrays shifted medially within the rostral aspect of pars lateralis (compare Fig. 6, Sec. 10 and Fig. 20, Sec. 17). More caudally, where the labelled array in V1 curved medially, successively higher-frequency site injections resulted in labelled arrays that shifted successively more dorsally, as well as medially. In pars ovoidea, injections at successively higher best frequency locations in AI resulted in ARG labelled terminal arrays that were successively more medial, dorsal, and rostral within the

nucleus (compare Fig. 6, Sec. 16 with Fig. 20, Sec. 21). In the transitional zone, labelled arrays that resulted from higher best frequency AI site injections were relatively medial, dorsal and rostral (compare Fig. 6, Sec. 13 and Fig. 20, Sec. 17). There is a reversal in the apparent topographic representation of frequency along the mutual border of Vo and Vl. That is, the region of AI representing lowest frequencies is interconnected with neurons along this border. Away from the Vo-Vl border, successively higher frequency AI site injections resulted in labelling in successively more medial locations within Vo and in successively more dorsal and medial locations in Vl . Thus, the folded sheetlike projection, which in the caudal region of the ventral division comprises Vl, Vo and Vt, is interleaved, in three dimensions, such that progressively higher best frequency place injections in AI produce folded sheets which are located relatively more dorsally, medially and rostrally. (see Fig. 23, Sec. B).

With injections into the sites of representation of relatively higher frequencies in AI, labelled terminals of neurons were recorded at more dorsal and lateral locations within Dd. There was an apparent reversal in the topographic interconnections of AI along the Dd-Vl border, with the rostral margin of AI (representing highest frequencies) interconnected along this boundary. Injections of anterograde tracer at the higher best frequency representations in AI produced ARG label in relatively more dorsal and rostral positions in the medial division (compare Fig. 6, Sec. 16 and Fig. 14, Sec. 28).

Two or more injections placed along an isofrequency contour in AI produced the same basic pattern of ARG label in the MGB as a single injection. Thus, positions along an isofrequency lamina in AI all appear to project into the same lateral "isofrequency" sheet and medial column in the MGB.

Larger areas of Vo were labelled with injections at higher best frequency positions in AI. With injections made at sites of representation of very low frequencies, the sheet of label in Vo became extremely thin (of the order of 100 μ), compared to arrays resulting from equal-volume injections at higher frequencies.

Other Variations in Projection Array

In the folded region of the laminar projection within the ventral division, there were commonly variations in the intensity of ARG labelling along the lamina. There was always a region of light label between Vo and Vt (see Fig. 6, Sec. 16; Fig. 14, Sec. 29; Fig. 15, Secs. 23; Fig. 20, Sec. 20; Fig. 22, Sec. C; Fig. 23, Sec. B). Almost invariably, injections into the higher frequency part of AI resulted in either two or three foci of relatively intense ARG label in Vl (Fig. 6, Sec. 16; Fig. 6A; Fig. 23, Sec. B, left MGB). Between the intensely labelled regions, ARG grain density dropped to relatively low levels. There appeared to be an increased likelihood of distinctive banding of the label if very small injection volumes (i.e., .1 microliters) were used.

When this banding pattern of ARG labelling appeared in Vl, there was generally a region of lighter labelling between Vl and Vt as well (e.g., see Fig. 6, Sec. 16 and Fig. 6a).

The three dimensional forms of the foci of strong label in Vl were columns or bands with the long axes oriented rostrocaudally in the nucleus. When banding occurred, Vt also appeared as a column or band situated rostrocaudally in the MGB. Thus, along the sheet of ARG label passing through Vl, Vo, and Vt, there were commonly 4 or 5 distinctly delimitable bands of more intense labelling (see Fig. 6a).

HRP injections into high frequency regions of AI also produced banding of HRP labelled cells in the caudal aspect of the ventral division. These HRP labelled cell bands were identical in form to the autoradiographically labelled bands.

With low frequency injections a distinct banding pattern was not seen in pars lateralis (Fig. 20, Sec. 20; Fig. 23, Sec. B, right MGB,; Fig. 30, Sec. 29), although a suggestion of a periodic pattern was seen in two cases (e.g., see Fig. 23, Sec. B, right MGB).

The transition, in the medial column of label, from the deep dorsal nucleus into the medial division exhibited some variability in the pattern of ARG labelling. Often, the transition was smooth and the ARG label formed a single straight column passing through both divisions (i.e., Fig. 14). In other instances, the label in Dd swept medioventrally

into M (see Fig. 6, Sec. 13). In some cases, the column was broken, with label disappearing in Dd and reappearing, a few hundred microns later, in M. When there was a break between the label in Dd and M, the labelled region in Dd was in the form of a short column (1.5 to 2mm long) oriented rostrocaudally and the labelled region in M was roughly spherical. Smooth transitions were usually seen after higher best frequency AI injections. Sweeping transitions generally occurred for injections at middle frequency loci, and "broken" transitions generally resulted from injections at lower frequency loci. These differences as a function of the site of AI injection are consistent with a different orientation of the internal topography of Dd as compared with M.

Often the Dd and Vl components of the projection were joined at their dorsal aspects in the rostral third of the MGB (see Fig. 15, Sec. 15). This occurred with injections into the high best frequency representation of AI and presumably manifests a high best frequency reversal along the border between the two topographic representations in Vl and Dd.

Summary

1) The corticothalamic projections of AI are complex. The Dd, Vl, Vo, and M subdivisions of the MGB all receive input from single injection loci located anywhere within the borders of AI.

2) In spite of the complexity of the projection, it is highly ordered. Vl and Vo receive a very restricted topographic projection with reference to the cochleotopic organization in AI. The projection to Dd and M is less restricted but still topographic.

3) Within this projection, there exists interesting geometries of connectivity. Any locus in AI projects into the MGB in the form of sheets and columns of nerve terminals.

4) Along the folded, laminar projection in the caudal ventral division, periodicities of light and heavy label were often seen. This banding was most striking when small volume injections were introduced into high best frequency locations in AI.

5) The conclusions outlined above also pertain to the arrays of thalamocortically projecting neurons in the MGB onto single loci in AI. That is, there is an overlapping array of thalamocortical neurons and corticothalamic terminals that provide input to and receive projections from any given AI locus.

Connections of AAF with the Thalamus

The thalamocortical and corticothalamic connections of the anterior auditory field (AAF), a cochleotopically organized field anterior to AI (Knight, '77; see Fig. 1), were examined by placing microninjections of anterograde and retrograde tracers at physiologically defined loci in that field. In all, there were 17 successful cases in which microinjections of HRP were placed in AAF and 13 successful cases in which ^{3}H-l-leucine microinjections were made into AAF. The physiologically typified loci of injections spanned five octaves (1.5 to 25 kHz) and were evenly distributed over this range.

The cortical dimensions of the cochleotopic representation in AAF are very similar to those of AI (Knight, '77; Merzenich et al., '75). These two fields are also cytoarchitectonically similar (Rose, '49). Likewise, the response properties of individual neurons in AI and AAF appear to be similar with respect to frequency tuning, latencies, thresholds and binaural response properties (Knight, '77; Merzenich et al., '75; Brugge et al., '69). Do these two cortical representations of the cochlea have correspondingly similar connections with the thalamus? To address this question, a protocol was adopted by which the connectional pattern of these two fields could be directly compared in single medial geniculate bodies. It was found that the thalamocortical and corticothalamic connections of AI and AAF are different in several respects. At the same time, AI and AAF give and receive projections from the same nuclei of the MGB, and the topography of connections with respect to these nuclei is in many respects the same

for both fields.

The Thalamocortical Connections of AAF

Single injections of HRP into AAF produced multiple groups of labelled neurons in POl (see Fig. 8, Sec. 27). Caudal to the posterior group, two components of labelled neurons, one located medially and one laterally, extended through the rostral and middle thirds of the MGB. The medial component was rostrally continuous with the HRP labelled cells in POl. The label extended as a column, in the rostral-caudal dimension, through the deep dorsal nucleus and the medial division. The labelled cells in Dd, in three dimensions, formed a short column (approximately 1.5 to 2.0mm long) in the rostro-caudal dimension (Fig. 8 and Fig. 9). This column through Dd continued into M caudally (Fig. 12, Sec. 20; Fig. 15, Sec. 23). Labelled cells in the medial division formed a sphere in 3 dimensions. Cells labelled in Dd after AAF injections were stellate, had radiating dendrites, and were of medium size. The packing density of labelled cells and the intensity of labelling of individual cells in this region was relatively high. In M, HRP labelled cells were large and multipolar. The density of cells labelled was generally not as great as in Dd; nor was the intensity of label in individual cells as great.

The lateral component of labelled neurons extended throughout the ventral division. It first appeared rostrally at the border of Vl with POl and extended as a discontinuous array into the rostral aspect of the

Figure 8

A representative example of the thalamocortical and corticothalamic connections to and from a cortical locus in AAF. In this particular experiment, (76-62), a .5 μl mixture of HRP and 3H-l-leucine (5μ Curies) was injected at a 6 kHz, best frequency locus in AAF. A) is a surface view of the cortex. Numbers indicate the best frequency determination of vertical microelectrode penetrations. The locus of the injection is indicated by the dark spot. B) indicates the HRP labelling with each dot representing a single HRP granule containing neuron. Sections are numbered rostrally to caudally in 120 μ steps. C) are adjacent autoradiograms to the sections in B. The dark stippling indicates label at least x2 above background, the light stippling label above background.

Examination of the sections in B and C indicate that the thalamocortical and corticothalamic connections are reciprocal. In this particular experiment, ARG labelling became very weak caudal to section 40. However, other AAF experiments demonstrated that the corticothalamic projection of AAF proceeds more caudally to include M and Vo (e.g., see Figure 12). D) is a darkfield photomicrograph of one of the autoradiographically processed sections. ARG labelling can be seen in Dd. The light areas of the optic tract and cerebral peduncle are due to fiber reflections and are not labelled with silver grains. OT: optic tract; CP: cerebral peduncle; LGN: lateral geniculate nucleus.

CASE 76-62
6 kHZ, AAF
HRP & TAA INJ.

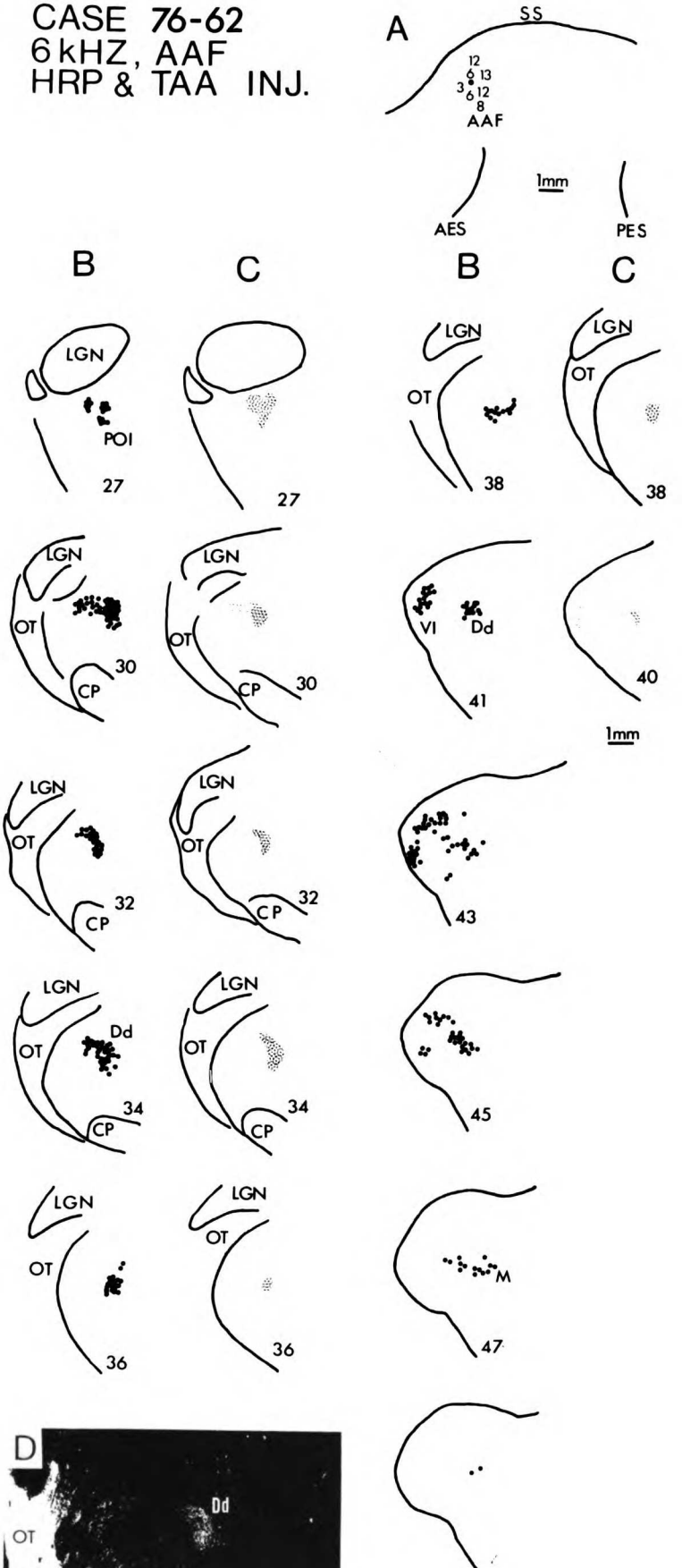

Figure 9

A representative example of the thalamocortical and corticothalamic connections of an isofrequency contour in AAF with the MGB. In this experiment (76-66), three injections (.5μl each) of a mixture of 3H-l-leucine (5μ Curies) and HRP were made along a 3 kHz isofrequency contour in AAF. A) is a surface view of cortex indicating the injection site and best frequency determinations of microelectrode penetrations. The darkfield photograph to the left is of a frontal section taken through the injection site that has been processed for HRP. The white arrows indicate the limit of the reaction product. The darkfield photograph to the right is of a frontal section through the injection site that has been processed for autoradiography. The exposure time of this injection site (and all injection sites) is the same as the exposure time for the sections through the MGB that contain the terminal labelling. B) are sections processed for HRP numbered rostral to caudal in 120μ steps. C) are drawings made from D. D) are darkfield photographs of adjacent sections to B that have been processed for autoradiography.

A comparison of columns B and C show that the thalamocortical and cortico-thalamic connections of Dd with the isofrequency contour in AAF are reciprocal. Also, a compairson of the three dimensional form of the cell and terminal arrays in the MGB after several injections along an isofrequency contour in AAF are similar to the form of cell and terminal arrays after a single injection in AAF.

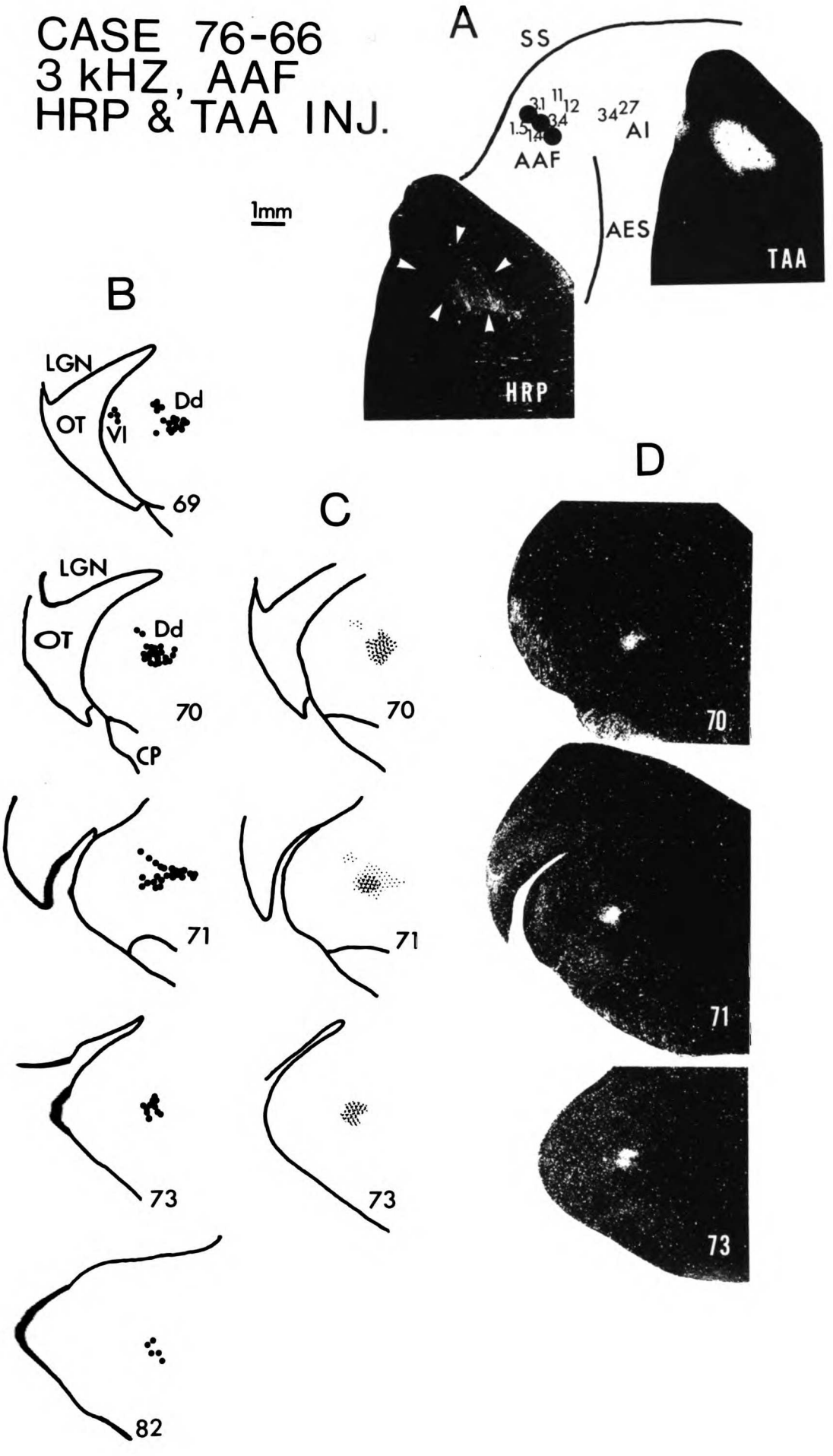
CASE 76-66
3 kHZ, AAF
HRP & TAA INJ.
A
SS
31
11
12
1.5
14
34
34
27
AI
AAF
1mm
AES
TAA
HRP
B
LGN
OT
VI
Dd
69
C
D
LGN
OT
Dd
70
CP
70
70
71
71
71
73
73
73
82

posterior 1/3 of the MGB. Labelled cells appeared in both pars lateralis and pars ovoidea. The overall pattern of labelling through this division was not as simple as the pattern seen with AI injections (Fig. 8; Fig. 14). With AAF injections cells in V1 were almost invariably clumped and occupied limited sectors of the "isofrequency planes" of V1. (Fig. 9, Sec. 69; Fig. 8, Sec. 43, 45; Fig. 10; Fig- 12, Sec. 18). Occasionally, a single clump of cells was labelled in the rostral V1 and appeared roughly as a column oriented rostrocaudally (Fig.10). More often, a single intensely labelled clump or column was present, but a few scattered neurons were also seen in other regions of V1. When this occurred, the overall distribution of cells, at least in the rostral V1, approximated a sheet oriented rostrocaudally (Fig. 12, Sec. 18). Quite often, the column of high density labelling in the rostral half of V1 appeared along its ventral aspect (Fig 10; Fig. 12, Sec. 18). Overall, the number of cells labelled in the ventral division after AAF injections of HRP was much less than resulted from equal volume AI injections. Labelled cells in V1 were of medium size and in general had ovoidal or fusiform cell bodies. They had proximal dendrites that tended to be polarized at both ends and that paralleled the long axis of the soma.

In summary, a locus in AAF received thalamocortical projections from POl and the MGB. After single injections of HRP into AAF, two components of labelled cells were seen. One was located laterally and the other medially. Both extended rostrocaudally through the rostral two thirds

Figure 10

A representative example of the columnar array of HRP labelled neurons that is often seen in V1 after injections of HRP in AAF. The column of labelled neurons in V1 in this particular case occupies a ventral and lateral region within the nucleus. Within each transverse section there are about 20 labelled neurons in the column. The long axis of the column is oriented rostrocaudally and dips ventrally as it proceeds caudally. The column is .8mm long and .2mm in diameter.

CASE 76·133

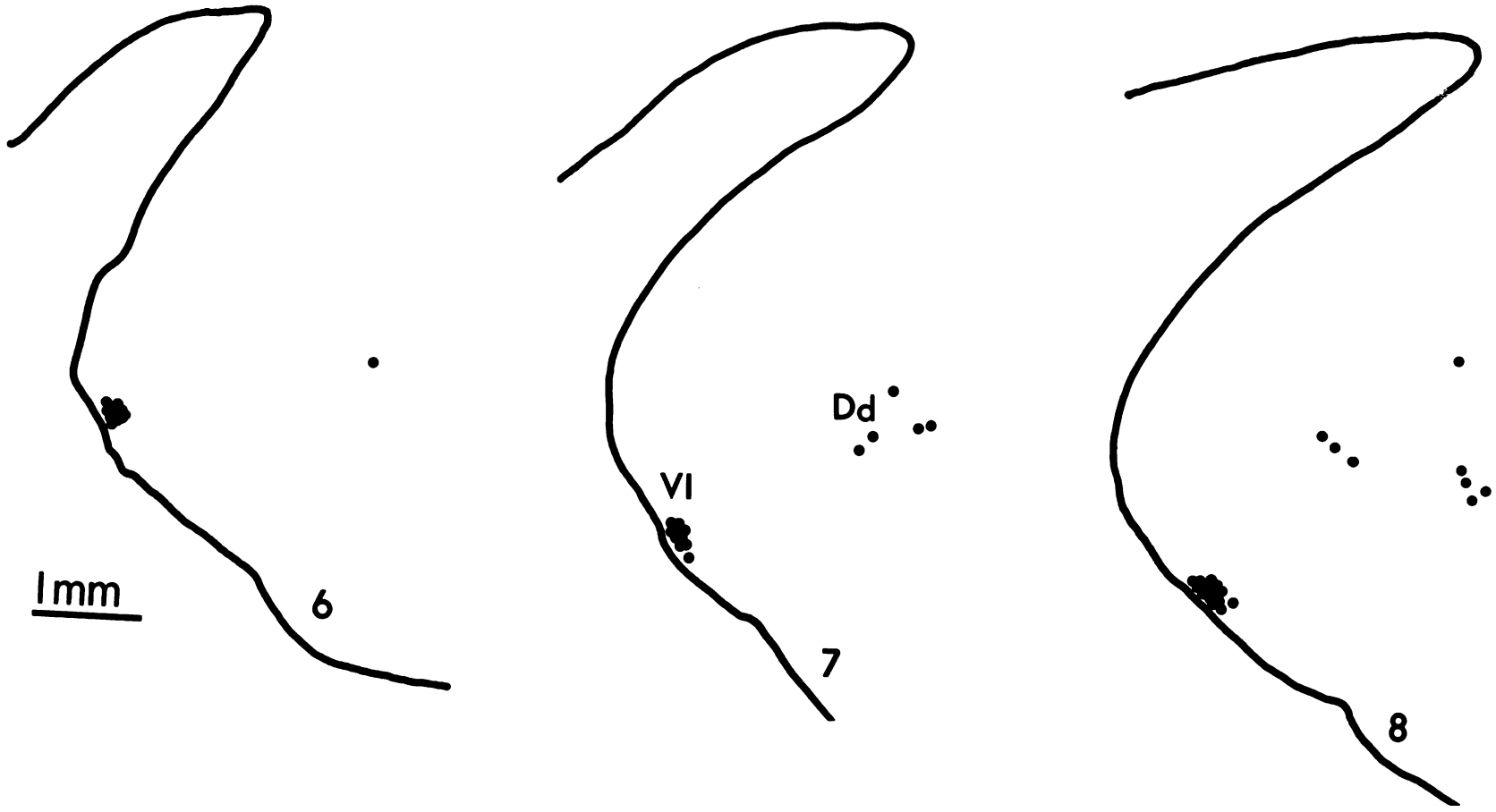

of the MGB and into the rostral aspect of the posterior third. The medial component was heavily labelled and extended through the Dd nucleus and M division of Morest, '64 (or the magnocellular division of Rioch, '29). The lateral labelled array of neurons was sparse and clumped. It was located in pars lateralis and pars ovoidea of the ventral division of Morest, '64 (or the principle division of Rioch, '29). All but the rostral most aspect of the posterior third of the MGB was free of labelled neurons.

Corticothalamic Projection of AAF

The corticogeniculate fiber path into the thalamus was similar to that taken by AI corticothalamic fibers. After single injections of ^{3}H-l-leucine into AAF, fibers were seen coursing ventral to the injection site in the white matter, and arching ventromedially in the frontal plane. The corticogeniculate fibers descended ventroposteriorly from this fiber bundle in a broad plexus that entered the internal capsule. The remaining fibers arched dorsomedially and entered the corpus callosum.

In only one case was autoradiographic label seen in the reticular nucleus of the thalamus. Whereas AI injections produced autoradiographic labelling in the reticular nucleus just lateral to the anterior third of the lateral geniculate nucleus, the labelling after the AAF injection occurred much farther rostrally, being located just lateral to the nucleus ventralis lateralis of thalamus. Since this was also the only case in which the thalamus was sectioned that far rostrally, it is assumed that the autoradiographic label in the reticular nucleus was missed in the other experiments. Thus, this scanty evidence suggests that fibers from AAF enter the thalamus more rostrally than do AI fibers.

Single injections of 3H-1-leucine produced multiple loci of autoradiographic label in PO1 (Fig.11,Secs.9L,9R). Caudal to PO1, in the rostral pole of the MBG, two components of continuous autoradiographic label descended to the rostral aspect of the posterior third of the MGB. One component was located medially; the other laterally. These two components of autoradiographic label corresponded to the medial and lateral labelled cell arrays seen after HRP injections (the spatial relationship of the two tracers is described in the next section). The medial component was continuous rostrally with the autoradiographic label in PO1. It's three dimensional form was that of a column whose long axis extended rostrocaudally through the Dd and M divisions. The label in Dd was very intense, the most intense of the entire projection; and existed as a short column (about 1.5mm to 2mm long) oriented rostrocaudally (Fig. 8, Fig. 9, Fig. 11, Fig. 12). The autoradiographic label in the medial division, although continuous with Dd, was less intense than over Dd (Fig. 12). This label assumed various appearances in the frontal plane, but in general it was roughly spherical in three dimensions.

In all cases of 3H-1-leucine injections into AAF, autoradiographic labelling was above background in the ventral division. However, this lateral component of label was usually extremely light. In all but one case, it was too faint to appear prominently in our photomicrographs

(e.g., Figs. 8, 9 and 11). In the one experiment in which the lateral component of label was dense enough to be clearly depicted photographically, it was still much less intense than the label over Dd (see Fig. 12 - In this figure the photomicrographs have been underexposed to bring out the ventral division projection). This case had the longest ARG exposure time (4.5 months) and this may have accounted for the relatively prominent labelling of the lateral projection component in this case. (Reconstructions of the physiological experiment defining the injection site revealed that the injection was, unequivocally, centered within AAF, and did not spread to AI.) The fact that the AAF corticothalamic projection to V1 was topographically organized (see Fig. 12) demonstrates that this lightly ARG labelled projection did not arise from the spread of 3H-1-leucine into AI, which borders AAF only at its high best frequency representation.

While autoradiographic label in the ventral division resulting from AAF injections was always much lighter than labelling after AI injections, the pattern of this lighter labelling was remarkably similar to the AI labelling pattern. Autoradiographic labelling began in the rostral pole of the ventral division in pars lateralis. In the frontal plane it appeared as a band, pressed against the dorsolateral aspect of the MGB (see Fig. 11, Sec. 10L; and Fig. 12, Sec. 16). This band of autoradiographic label was sheetlike in three dimensions and passed rostrocaudally through the rostral aspect of pars lateralis. The other long axis of the sheet was oriented dorsoventrally. Proceeding caudally, the sheet moved medially in the MGB as pars lateralis expanded

medially (Fig. 12, Sec. 18). In the middle third of the MGB, the sheet of label in pars lateralis was divided into a larger sheet of label in pars lateralis and a smaller sheet of label in the ventrolateral region of pars ovoidea. The sheet of label in Vl was curved and oriented dorsolaterally to ventromedially. The sheet in Vo was oriented diagonally in a ventrolateral to dorsomedial orientation. Caudal to the division of Vl, the label in Vo and Vl formed a continuous folded sheet (see Fig. 12, Sec. 20, 23). The division of Vl occurred at roughly the level at which the medial column of label passed from the deep dorsal nucleus to the medial division.

Just rostral to the division of Vl into Vl and Vo, a focus of autoradiographic label appeared in the medial aspect of the ventral division. Caudally, it became incorporated in the medial aspect of the folded sheet in the "transitional zone" in the dorsal aspect of pars ovoidea.

Again, the projection pattern was vitrually identical to that recorded with a homotypic injection of either HRP or tritiated amino acids (TAA) into AI.

Reciprocal Relationship of the Thalamocortical and Corticothalamic Connections of AAF

In 11 cases, mixtures of both 3H-l-leucine and HRP were injected at single physiologically defined loci in AAF. This always produced

spatially related (and partially superimposed) patterns of label in the POl and MGB. Results from sections processed for both tracers showed that all HRP labelled cells were overlain by the restricted autoradiographic arrays. The autoradiographic label pattern was highly reciprocal with the medial cell column (POl, Dd, M)(e.g., see Fig. 9) and was relatively continuous over the very patchy and often strikingly discontinuous lateral cell array (Vl, Vo, Vt) (e.g., see Fig. 12).

Topographic Organization of the AAF Projection to and from the MGB

The topography of projection of the thalamocortical and corticothalamic connections of AAF are similar to the topography of the AI connections with respect to the cortical cochleotopic representations. Only the topography of the AAF corticogeniculate projection will be described here.

In a sense, a description of the corticogeniculate projection topography as a function of cortical injection site (and represented cochlear position) applies to the projection arrays of thalamic neurons. While the array of the neurons within the ventral division projecting to any cortical locus in AAF is usually patchy and discontinuous, these cells are all contained within the limits of the laminar grain field of the corticothalamic projection from the same locus. The topography of the autoradiographic label in Dd and M directly reflects that of the HRP labelled neurons, as the reciprocal coincidence of the two labels is more exact.

The topographic organization of projection was apparent in the comparison of cases in which single injections were placed in

AAF at different loci in the cochleotopic representation. In four cases, two injections were made at different best frequency locations in AAF. This allowed a direct demonstration of the topographic organization in a single MGB. The projection onto the ventral division was shown to be strictly topographically ordered. Injections into higher best frequency sectors of the cochleotopic representation produced label in relatively more medial regions of pars lateralis rostrally (Fig. 12, Sec. 18) and relatively more dorsal and medial regions caudally (Fig. 12, Sec. 23). Autoradiographic label in pars ovoidea (including the "transitional zone") occurred more medial, dorsal and rostral than when injections were placed into relatively higher best frequency representational sectors of AAF (Fig. 12, Sec. 23). The folded-sheet configuration was located further rostrally with higher best frequency AAF injections than with lower best frequency injections (see Fig. 12, Sec. 20). There was a topographic reversal of autoradiographic labelling between pars ovoidea and pars lateralis that corresponded to injections in the lowest frequency places in the tonotopic map in AAF.

The medial, columnar projection through Dd and M was also topographic but not as precisely organized as was the projection onto the ventral division. This was apparent in comparisons of the restricted regions of autoradiographic labelling of Dd with labelled Vl regions. Examples are illustrated in Figures 12 and 11. In the experiment represented in Figure 12, injections placed at 2 and 14 KHz did not produce two separable ARG labelled regions in Dd; by contrast separable labelled regions in Vl were very distinct. In

Figure 11

A comparison of the pattern of the corticothalamic projections from a single locus in AAF with the pattern of projections from two cochleotopically dissimilar representational positions in AAF. In this experiment, .2μl injections of HRP and 3H-l-leucine (2μ Curies) were made at 1.5 and 25 kHz loci in the left AAF and at a 2.5 kHz locus in the right AAF. A and B are surface views of the left (A) and right (B) cortices and indicate the positions of the best frequency determinations and injections. D are darkfields of the left thalamus; 9L is taken through PO1 and 10L the rostral MGB. C are drawings made from D. The stippling indicates above background ARG labelling. E (and F) are sections taken from the same level as D (and C) of the right MGB. Note the topographic organization of the projection in section 10L with Dd_1 corresponding to the projection from the higher frequency locus in AAF and Dd_2 corresponding to the lower frequency place projection. Also, the complex topographic projection from a single locus in AAF to PO1 is to several distinct cell groups in PO1 (section 9R). This general pattern in PO1 does not change but each component appears to expand in area after two injections at dissimilar cochleotopic representational positions in AAF.

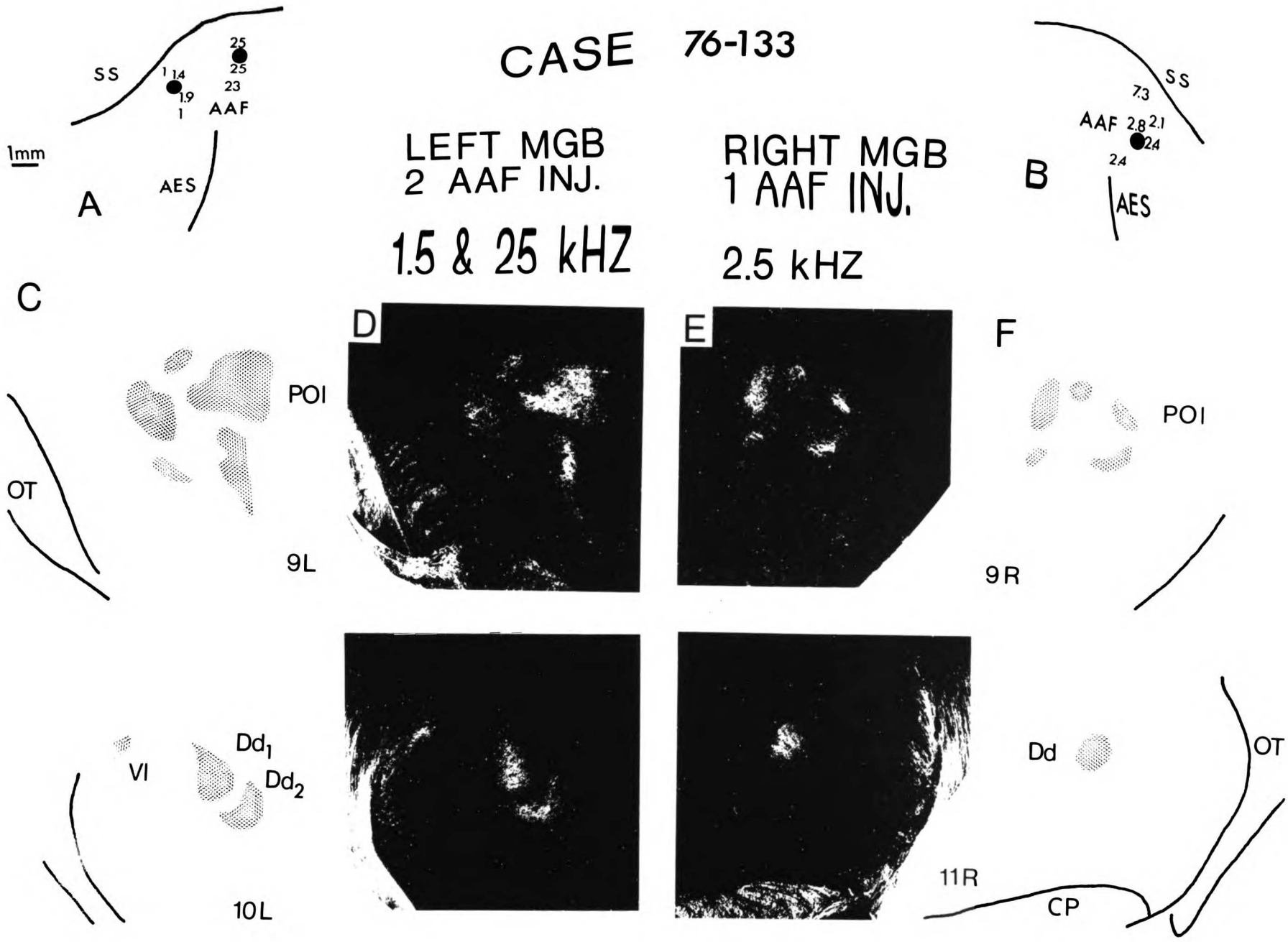
CASE 76-133
LEFT MGB
2 AAF INJ.
1.5 & 25 kHZ
RIGHT MGB
1 AAF INJ.
2.5 kHZ
A
B
C
D
E
F
SS
AAF
AES
1mm
25
25
23
1.14
1.9
1
7.3
2.8
2.1
2.4
2.4
POl
OT
9L
9R
VI
Dd1
Dd2
10L
Dd
11R
CP

Figure 12

An example of the topographic order of the corticothalamic and thalamocortical connections with respect to the cochleotopic organization of AAF. In this experiment (77-14), the left AAF was injected at 2 and 14 kHz loci with .1µl of HRP and 3H-1-leucine. The surface view of the cortex indicates the injection loci and recording data. The darkfield photographs on the left are of sections that have been processed for both HRP and autoradiography. These sections have been redrawn on the right. Each dot represents an HRP granule containing cell and the stippling indicates autoradiographic labelling that is x2 above background. The projections are topographically organized and denoted by a subscript; 1 corresponding to the label resulting from the 14 kHz place injection and 2 from the 2 kHz place injection. The sections are numbered rostral to caudal in 200µ steps. The exposure time for autoradiography was unusually long (4.5 months). The fact that all HRP labelled cell arrays are overlain by x2 above background autoradiographic labelling indicates a degree of reciprocal connectivity.

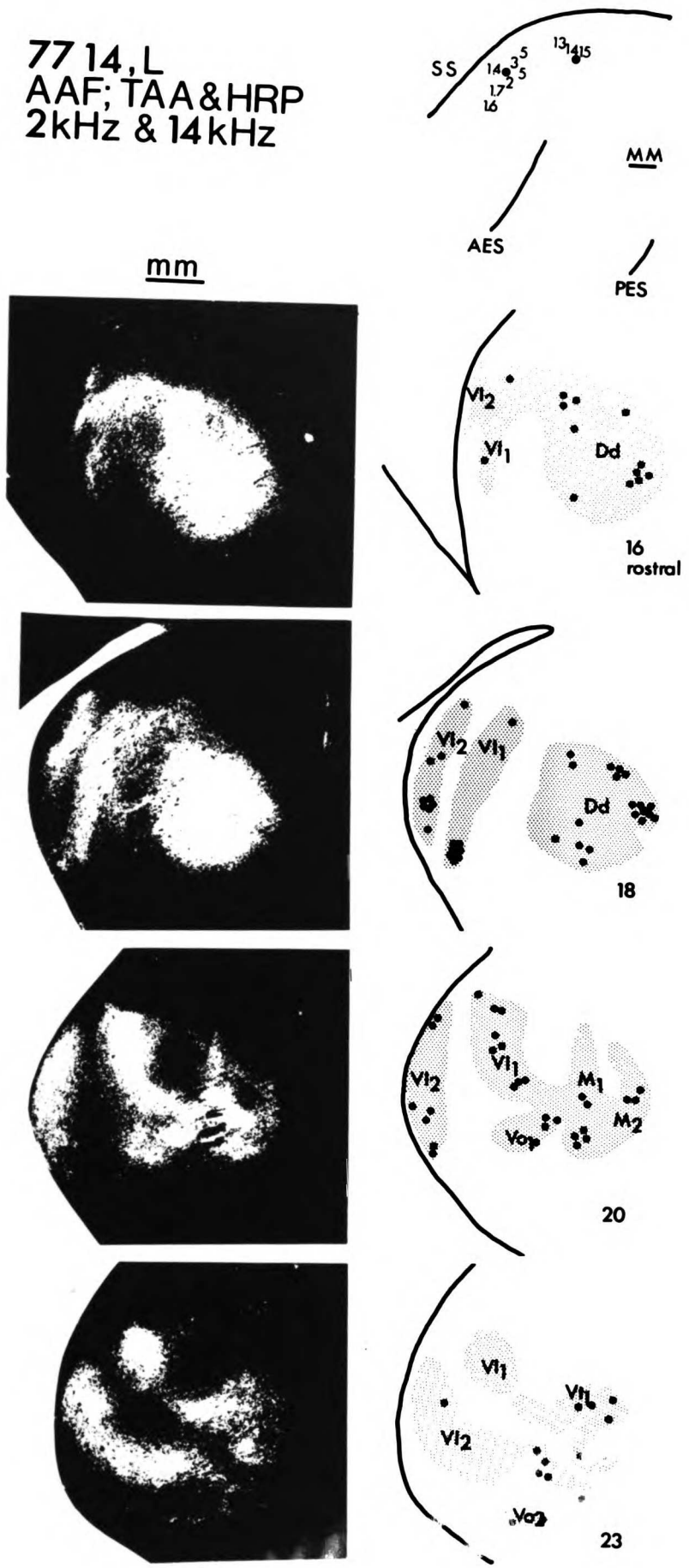
77 14, L
AAF; TAA&HRP
2kHz & 14kHz
mm
SS
MM
AES
PES
VI2
VI1
Dd
16
rostral
18
M1
M2
Vop
20
23

the experiment represented in Figure 11, the injections were placed further apart in the tonotopic map in AAF (1.5 and 25 KHz locations). In this double injection case, two separable columns of label were evident in Dd. In this experiment, and the other two injection experiments, the injection that was placed at the higher best frequency location in the AAF cochleotopic representation produced a column of ARG label that was located relatively more dorsal and lateral in Dd (see Fig. 11, Sec. 10L, Dd_1). Conversely, the injection at the lower best frequency site in AAF produced a column of label that was relatively more ventral and medial to the column of label resulting from the higher best frequency site injection (see Fig.11, Sec. 10L, Dd_2). There was a topographic reversal of autoradiographic labelling between Dd and Vl that corresponded with injections in the highest best frequency places in the cochleotopic representation in AAF.

Relatively more dorsal and rostral regions of the medial division were labelled with injections placed at relatively higher best frequency locations in the tonotopic map in AAF.

As with AI, there is a disproportionate representation of the volume of projection from the higher best frequency locations of AAF in pars ovoidea. With injections within AAF at best frequency locations of usually less than 2 KHz, the sheet of label passing through Vo becomes relatively thin when compared with labelling resulting from equal volume injections at higher best frequency locations (i.e., compare Vo_1 in section 20 with Vo_2 in section 23 of Figure 12).

Other Variations in Projection Arrays

When injections were made at higher best frequency represented

loci in AAF, often a banding pattern in the folded sheet of autoradiographic label in the caudal region of the ventral division resulted. This pattern appeared to be identical to the banded pattern seen after injections into the higher best frequency representation of AI. It consisted of 4 or 5 foci of more dense label; one in Vo, usually one in Vt and two or three in Vl (Fig. 12, Sec. 23). Perhaps due to the sparse distribution of HRP labelled neurons seen with AAF injections, a banded pattern of light and heavy HRP labelling, corresponding to the banded pattern seen with the corticothalamic projection array, could not be clearly defined.

With high best frequency place injections, the autoradiographic labelling in Dd and Vl often joined at their dorsal borders in the rostral third of the MGB. This apposition of labelled regions apparently reflected a topographic reversal between Dd and Vl that occurs in the projection from the high frequency representation in AAF. A similar pattern in the corticothalamic projection array was observed after injections in the high best frequency representation of AI.

Direct Comparison of the AI and AAF Connections

The results of the preceding sections have demonstrated that AAF and AI have connections with the thalamus that are quite similar in both structure and topography of organization. Four experiments were

performed to obtain a direct comparison of the connectional structure and organization of the two fields. In these experiments, partial maps of both fields in single hemispheres were made, and single injections of anterograde tracer in AI and retrograde tracer in AAF were made at cochleotopically homotypic locations. As stated earlier, the corticothalamic autoradiographic projection array, seen with AI injections, was of the same basic form as the array of projecting (HRP-labelled) neurons. Thus, these experiments directly compared the spatial architecture of the AAF thalamocortical projection with the architecture of both the AI corticothalamic and thalamocortical projections. Since the AAF corticothalamic terminal projection array to Dd and M was of the same basic form as the thalamocortical projecting neuronal array from Dd and M to AAF, these experiments also allowed for a direct comparison of the reciprocal Dd and M connections of AI and AAF. Although the thalamocortical neurons projecting onto a locus in AAF from the ventral division were in the form of a sparse and discontinuous array, they were contained within the limits of the spatial pattern of the AAF corticothalamic projection. Thus, in a rough way, these experiments also allowed for a comparison of the spatial pattern of the projection from AAF to the ventral division with the spatial form of the reciprocal connections of AI with the ventral division.

3H-l-leucine injections into AI produced the usual, restricted column of label passing rostrocaudally through Dd and M. HRP

injections into homotypic loci in AAF's produced a column of HRP labelled cells in Dd and M which always appeared within the restricted regions of Dd and M defined by the autoradiographically labelled AI corticothalamic projection field (see Fig. 13, Sec. A and C; Fig. 14, Sec. 23, 28; Fig. 15). Likewise, HRP cells appeared only within the regions of autoradiographic label in the ventral division. This overlap encompassed all components of the sheetlike, lateral projection and included Vl (Fig. 14, Sec. 25-26; Fig. 15, Secs.on left), Vo (Fig. 14 and Fig. 15) and Vt (Fig. 15). The connections of both auditory fields also overlapped in POl (Fig. 14, Sec. 18 and 20).

The results of experiments in which alternate sections were processed for one label and then the other, showed that the overall pattern of connections for the two fields are very similar (Fig. 13 and 14). In cases where each section was processed for both tracers, the degree of overlap was shown to be very exact for Dd and M (i.e., Fig. 15). The thalamocortical projection to AAF was contained within the region of the ventral division demarcated by the corticothalamic projection of AI (see Fig. 15). However, this projection was typically sparse and discontinuous, and did not conform in pattern detail to the more dense and more continuous autoradiographic labelling that defined the AI corticothalamic projection array.

These experiments demonstrated that the thalamocortical and corticothalamic connections of Dd and M with AI and AAF are of the same form

Figure 13

An example in which the connections of AI and AAF with the MGB are compared directly in a single cat. In this experiment, the left AI cortical field was injected with .25μ 1 (2.5μC) of 3H-1-leucine at an 11 kHz locus, the left AAF was injected with .25μl of HRP at an 11 kHz locus, and the right AI was injected with .25μl of HRP at an 11 kHz locus. Section A represents the AAF thalamocortical projection; Section B represents the AI thalamocortical projection; and Section C represents the AI corticothalamic projection. All sections are taken from the same level of the MGB. A comparison of Sections B and C indicate that the AI projection is reciprocal. Comparison of Sections A and C indicates that AI and AAF give and receive projections from the same region of the Dd nucleus. Sections A and B indicate that the thalamocortical projection from Vl to AAF is sparser than the projection from Vl to AI.

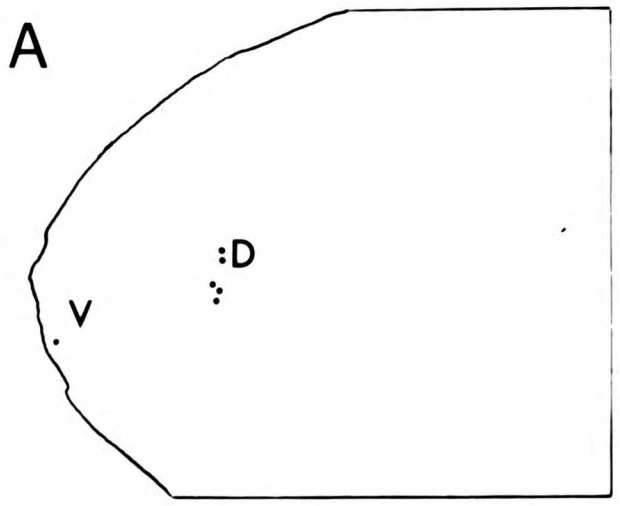

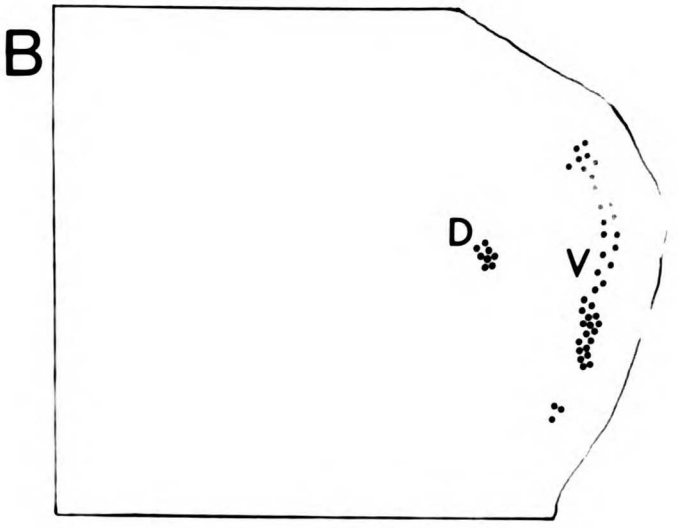

1mm 76-119

A: left AAF, 11kHz, 0.25μl HRP

B: right Al, 11kHz, 0.25μl HRP

C: left Al, 11kHz, 2.50μC ^{3}H-leucine

CASE 76-119

Figure 14

An example of the direct comparison of the patterns of connections of cochleotopically homotypic loci in AAF and AI,of a single hemisphere, with the MGB. In this experiment, .25µl of HRP was injected into an 8 kHz locus in AI. The upper right hand corner of the figure shows the surface view of the cortex with the injection sites and recording data. The darkfield insets are frontal sections through the two injection sites, the arrows on the frontal section through AAF indicate the extent of the HRP spread. The sections on the left have been processed for HRP and each dot represents an HRP granule containing cell. The sections to the right are adjacent sections that have been processed for autoradiography. Numbering is rostral to caudal in 200µ steps. There is a reasonable spatial coincidence of the thalamocortical connections of AAF with the corticothalamic connections in AI, considering that the comparison is made between adjacent sections.

CASE 77-7
AI; ARG; 8 kHZ
AAF; HRP; 8kHZ

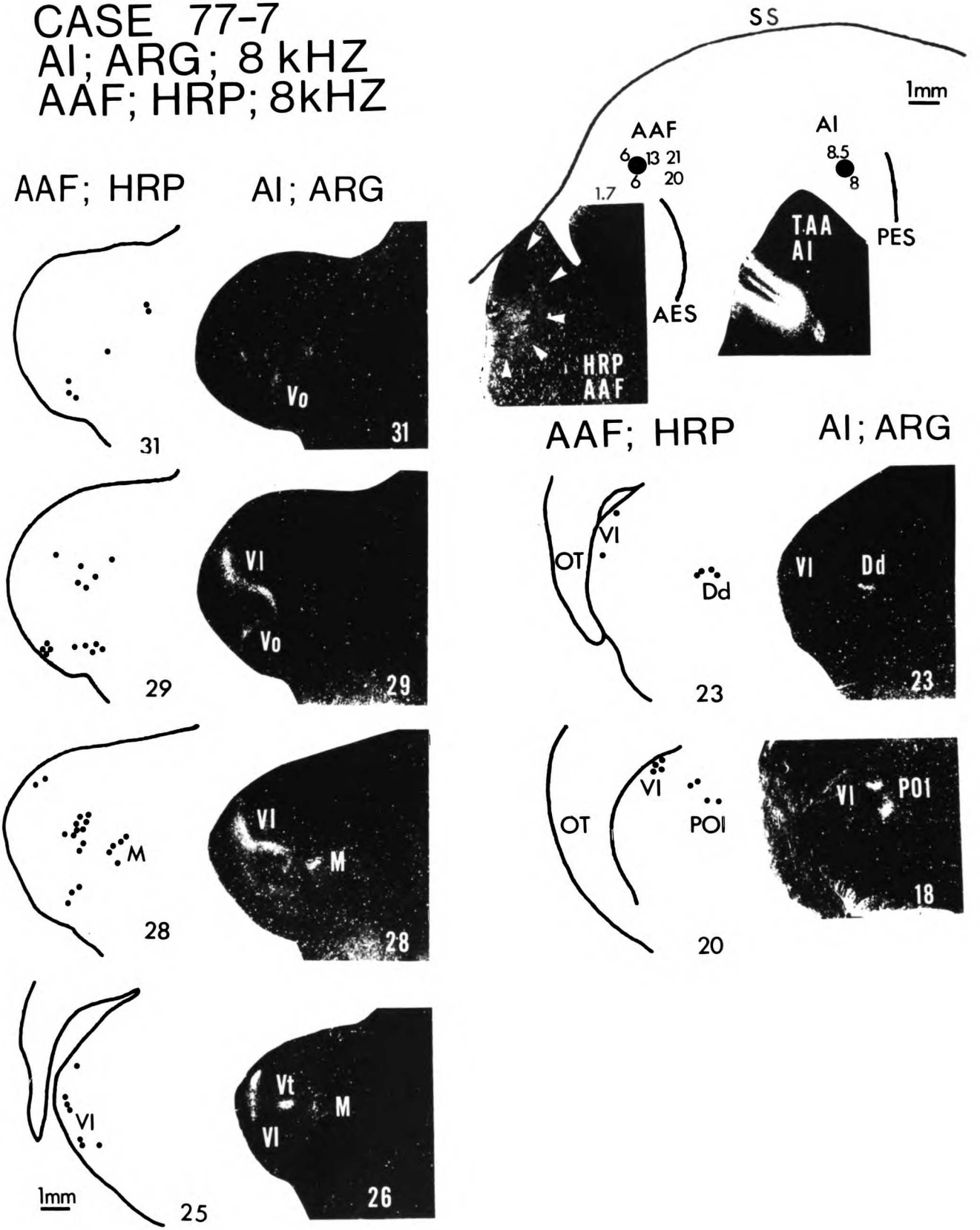

Figure 15

Another two examples of a direct comparison in single hemispheres of the connections of cochleotopically homotypic loci in AI and AAF with the MGB. In the experiment of the left of this figure .15µl of HRP was injected into AAF at a 13 kHz locus and .15µl of 3H-l-leucine was injected into AI at a 13 kHz locus. The sections on the left have been processed for both HRP and autoradiography and are photographed with darkfield illumination. These sections have been redrawn on the right. Each dot represents an HRP granule containing cell and the stippling indicates regions of autoradiographic labelling; dark stippling indicates x2 above background labelling and light stippling indicates above background labelling. This experiment demonstrates the similarity of the AI and AAF connections to the MGB. In the experiment on the right, .2µl of HRP was injected at an 11 kHz locus in AAF and .1µl (2µC) of 3H-l-leucine was injected at an 11 kHz locus in AI. Again, the sections have been processed for both autoradiography and HRP and are redrawn on the right. The similarity of the AI and AAF connections to MGB are apparent. Sections in these two experiments are numbered rostral to caudal in 200µ steps.

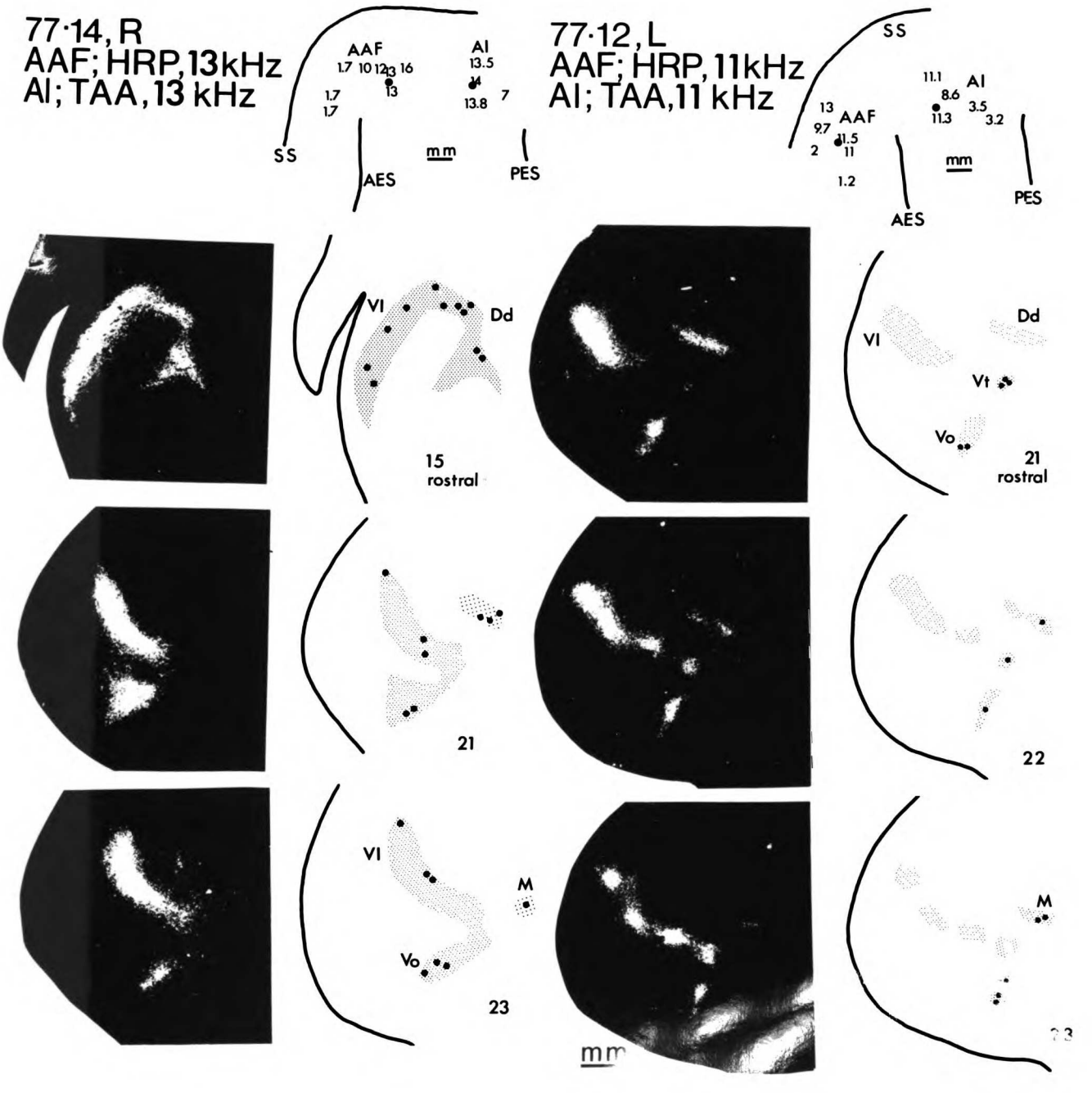
77·14, R
AAF; HRP, 13kHz
AI; TAA, 13 kHz
AAF
AI
SS
AES
PES
mm
VI
Dd
15
rostral
21
23
M
Vo
77·12, L
AAF; HRP, 11kHz
AI; TAA, 11 kHz
Vt
21
rostral
22
mm

and topographic order (with respect to the cortical cochleotopic representations). The corticothalamic connections of AI and AAF with the ventral division also appear similar, with the exception that the AI projection is much more dense. The thalamocortical projections to AI and AAF from the ventral division are similar, in that they are derived from the same regions of the nucleus, as defined by the corticothalamic projection of AI. However, within this region, the neurons of the AAF thalamocortical projection array are much more sparse (and discontinuously distributed) than are the arrays of AI projecting neurons.

Summary

1) AAF gives and receives projections from the POl and MGB. The reciprocal connections with MGB subdivisions are limited to the Dd, Vl, Vo and M. The thalamocortical and corticothalamic connections with Dd are relatively stronger than the connections with the other MGB nuclei. They are in the form of a column which extends rostrocaudally through Dd (and into M). The corticothalamic projection into Vo and Vl is relatively weak. This projection takes the form of a sheet passing rostrocaudally through the ventral division. The sheet is folded caudally. The populations of neurons in Vl and Vo which project into single loci in AAF are sparsely distributed across this sheet. Most thalamocortically projecting neurons within Vl are usually concentrated in a single, restricted column of neurons.

2) The thalamacortical and corticothalamic projections are topographic with respect to the tonotopic organization in AAF. The topographic

connections of AAF with Vo and Vl are highly ordered and restricted. The topographic relationship with Dd and M is less precise.

3) Along the folded region of the corticothalamic projection in the caudal ventral division, bands of relatively light and heavy autoradiographic labelling are often seen after injections in high best frequency loci of AAF. This banding pattern is similar to the one seen after injections into the high best frequency region of AI (described earlier).

4) Two tracer (HRP and 3H-l-leucine) two field (AAF and AI) experiments demonstrated that in terms of structured geometry and topographic organization, AAF and AI connections with the MGB are very similar. The reciprocal connections of Dd and M with AI and AAF appear to be identical (within the limits of the techniques used) in form and topographic organization. While the topography and form of the AI and AAF corticothalamic projection arrays onto the ventral division are virtually indistinguishable, AAF gives a relatively weaker projection than AI. Similarily, the thalamocortical projection from the ventral division to AAF is weaker than the projection to AI. Most neurons in Vl projecting to a locus in AAF arise from a single clump or column of cells that included only a limited portion of the area encompassed by the sheetlike array of neurons in Vl projecting into a homotypic locus in AI. A sparse population of labelled neurons in Vt, and Vo also project to AAF and fall within the same basic topographic figure defining the limits of the arrays of neurons within these nuclei projecting to homotypic locations within AI.

Thalamo-cortical, cortico-thalamic projection of a cochleotopic field posterior and ventral to AI

Figure 16 (A) shows a microelectrode recording map of auditory cortex. In this case, a partial cochleotopic map of AI is indicated dorsally. The "b"s indicate regions of neurons with broad tuning characteristics indicative of AII cells. This figure shows that a portion of a field ventral to AI and AII was mapped that contained neurons with sharp tuning curves. The best frequencies of neurons in this field varied spatially in a systematic fashion with respect to the cortical surface; i.e., this field appears to be cochleotopically organized. Whether this field is the cochleotopically organized posterior auditory field (PAF, Reale & Imig '77) or another cochleotopic field ventral to PAF is not known. A more complete map would have been required to determine its complete relation to the other auditory cortical fields. However, PAF has a low frequency reversal with the posterior border of AI and high frequencies are represented posterioventrally. Much of PAF is often contained in the posterior ectosylvian sulcus. The cochleotopic sequence of the field posterior and ventral to AI in Figure 16 indicates that the low frequencies are located ventrally. This would suggest that this is a different field from PAF (the ventral posterior auditory field, VPAF) and shares a high frequency reversal with PAF at PAF's ventral border. Reale & Imig have noted a tonotopic field ventral to PAF in this region (personal communication). However, what exact field this recording corresponds to is inconsequential to the point to be made here. The essential fact is that this is a cochleotopic field that contains neurons with sharp tuning curves that is not AI or AAF.

Figure 16

This figure indicates the thalamocortical connectivity of a cochleotopically organized field ventral and posterior to AI (probably the ventral posterior field - VPAF). It also shows a large extent of the AII auditory field on the cortical surface that is ventral to AI.

A) is a reconstruction of microelectrode penetration positions taken from a photograph of the surface of the auditory cortex. Dorsally, a partial map of AI was made and best frequency determinations are indicated in kHz by the numbers. An extent of AII was mapped. "b"s indicate vertical microelectrode penetrations where only broadly tuned units and clusters were observed. Units responding over a wide range of frequencies with similar thresholds are indicative of the AII field. The numbers in the ventral region of the drawing of the cortical surface indicate best frequency determinations of a cochleotopically organized field ventral and posterior to AI. Neurons in this region had relatively sharp tuning curves. The dark spot indicates the locus of injection of .15µl of HRP and 3H-l-leucine (1.5µC).

B) indicates the pattern of thalamocortical projection from cells in the MGB to the field ventral and posterior to AI. Each dot represents an HRP containing cell. The autoradiographic results indicated that this thalamocortical projection is reciprocal with respect to the corticothalamic projection. Notice that the general pattern of projection to and from the MGB is quite similar to the general pattern seen after an AI or AAF injection. Section numbers indicate 200µ steps.

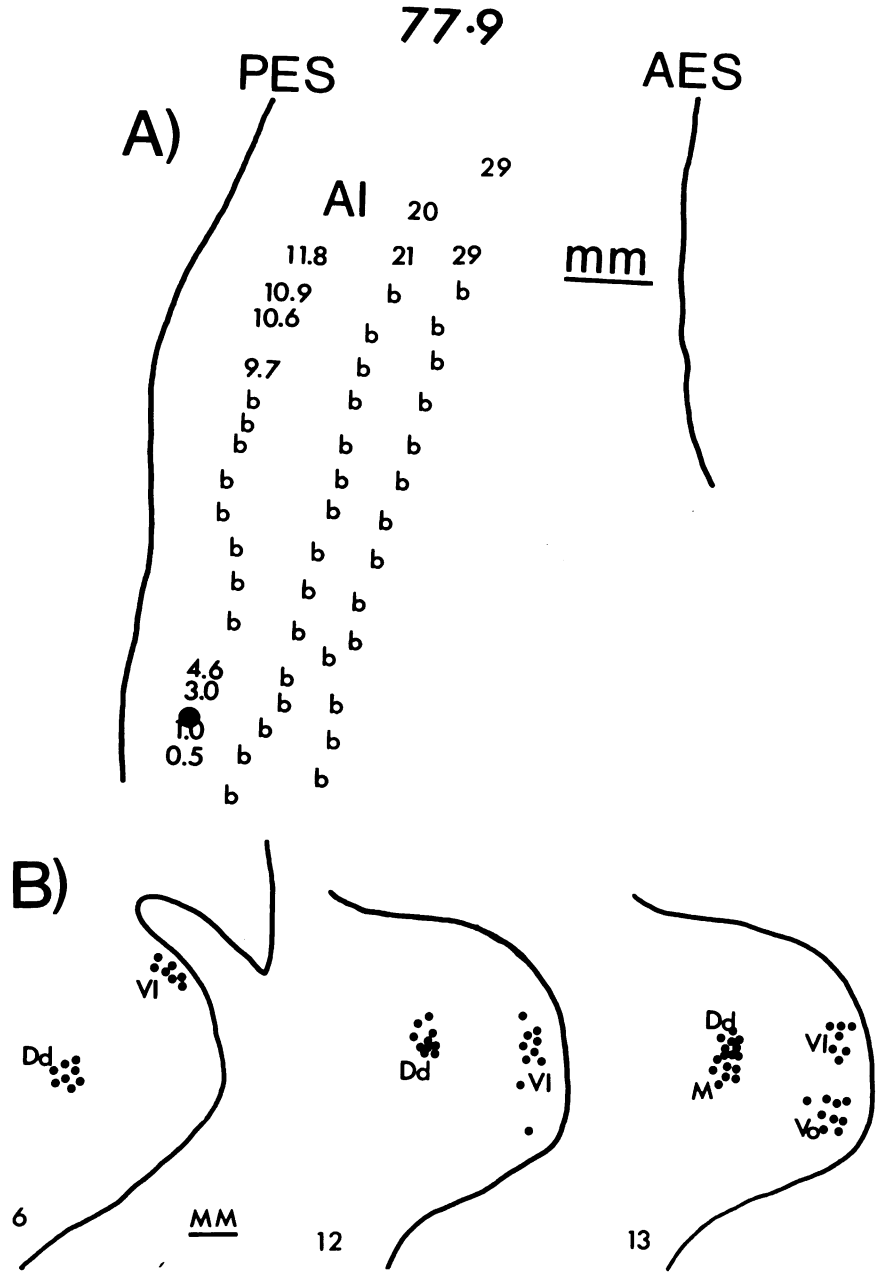
77·9
PES
AES
A)
AI
29
20
11.8
21
29
mm
10.9
10.6
9.7
4.6
3.0
1.0
0.5
B)
VI
Dd
6
MM
Dd
VI
12
Dd
VI
M
Vo
13

An injection of combined tracers was made into this field ventral and posterior to AI. Part B of Figure 16 indicates HRP labelling after an injection into this field. It was noted that the pattern of labelling is similar to that seen after injections into AAF. An examination of the autoradiographic labelling indicated that this field is also reciprocally connected to MGB. Also, the position of the labelling within the subdivisions of the MGB is similar to the positions of labelling seen after similar, low frequency place injections in AAF or AI.

The Thalamocortical and Corticothalamic Connections of AII

A series of experiments conducted to delineate the thalamocortical and corticothalamic connections of the AII auditory field are outlined in this section. The AII field borders AI ventrally (see Fig. 1). AII boundaries (of at least the dorsal border) were identified electrophysiologically. As described by Merzenich et al., '75 and Hind '53, neurons in this field have relatively broad frequency tuning characteristics. In other words, the thresholds of a typical AII neuron are almost equally as sensitive for a broad range of frequencies (sometimes several octaves).

The functionally defined border between AI and AII, was sharp. In penetrations made near the border (especially those that were oblique from the vertical axis) neurons in both fields were sometimes encountered. In these instances, successive neurons of one type were recorded; followed by an abrupt change to neurons whose responses were typical of the other field. The AI-AII border was generally oriented ventroposterior to dorsoanterior (Fig. 16A).

Extensive maps of AII were made in 2 hemispheres in an attempt to define its ventral borders. Posteriorly, in the region of the posterior ectosylvian sulcus, AII is bordered by cochleotopically organized regions of cortex (Fig. 16A). The ventral border of AII was difficult to determine. The broad tuning region below AI can extend for at least

6mm ventrally (Fig. 16A). However, from the recording data the impression was acquired that this large "AII" region may contain more than one cortical field with neurons of broad tuning characteristics. For instance, there was generally a strip of AII that borders AI ventrally, roughly 1mm in width, in which neurons were more responsive to auditory stimuli. Neurons in this region had lower thresholds and a greater number of spikes was evoked by equivalent suprathreshold stimuli. Injections were centered within this strip and below it. No differences in the thalamocortical connectivity of this AI-bordering strip with respect to more ventral AII cortex was found.

Because of the uncertainty of the homogeneity of the broad tuning region ventral to AI, all injections of tracer were made only 1 to 2.5mm from the AI-AII border. Partial maps of the cochlear representation of AI near the AII border were made prior to injections. This enabled the AII injection sites to be referenced to best frequency locations in the adjacent AI field.

The referencing of the AII injection sites to the functional architecture of nearby AI may prove to be a useful index for relating this work to future experiments. AI and AAF are always found to be in functional register with respect to one another. There is, in every cat, a high frequency reversal in best frequencies at their common border. This consistency of positions of these two fields with

respect to one another is in marked contrast to their position with respect to the cortical sulcal patterns, which vary from animal to animal. A consistency of cortical field positions may also apply with respect to AI and AII. If this is true, the functional organization that exists within AII would be consistently related to the organization of AI.

Thalamocortical Connections of AII

In 14 cases, HRP microinjections were placed at physiologically identified loci in AII. These experiments demonstrated that AII receives projections from the caudal and middle thirds of the MGB. The projecting nuclei were the caudal dorsal nucleus (Dc) of the dorsal division, the ventral lateral nucleus (VL) of the ventral division and the medial division (M). The Dc projection was the heaviest of the three projections in terms of the numbers and packing densities of the labelled cells (see Fig. 21A). The VL projection was the next heaviest, followed by M (see Fig. 18, Sec. 50).

After injections of HRP into AII, a continuous array of labelled cells could be followed caudorostrally. The caudal pole of the MGB was extensively labelled (Fig. 18, Sec. 46 and 48; Fig. 19, Sec. 7; Fig. 20, Sec. 23, 24 and 26). These neurons were located in Dc. They were of medium size, were closely packed and had dendrites which radiated from stellate soma. The projection pattern from Dc was complex, with labelled cells often occurring in groups (Fig. 18, Sec. 48).

Figure 17

An example of the corticothalamic and thalamocortical connections of a locus in AII with the MGB. In this experiment, an injection of .25µl of 3H-l-leucine and an injection of .3 µl HRP (7 days later) were made at the same locus in AII. The surface view of the cortex at the right shows the position of the injection site in AII with respect to the functional organization of AI. The numbers indicate the best frequency determinations of penetrations into AI. "AII's" indicate the position of penetrations where broad frequency responses of units and clusters indicative of the AII field were noted. The dark field photographs on the left are of sections processed for autoradiography. Section 57 is taken from the rostral pole of the MGB, section 55 from the rostral third of the nucleus and section 53 from the middle third of the MGB. The sections drawn on the right are of adjacent sections processed for HRP. Each dot represents an HRP containing cell. The ARG labelling in the MGB in sections 57 and 55 appears to be of fiber passing to more caudal regions of the MGB. "CP" in section 57 indicates labelled, probably corticopontine, fibers in the dorsal aspect of the cerebral peduncle.

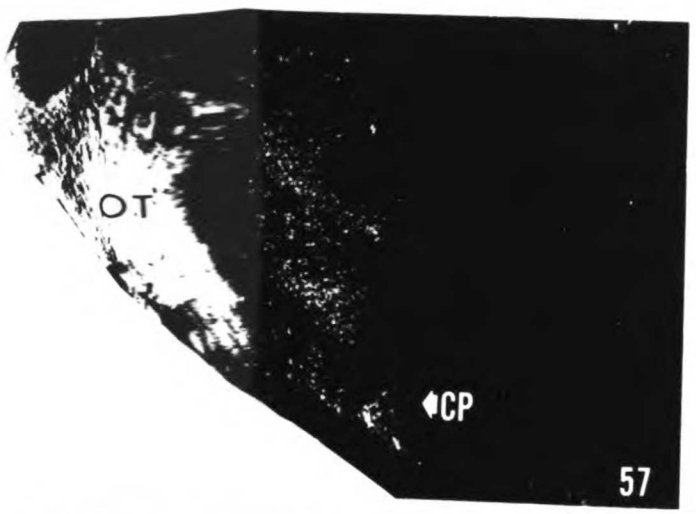

77·73

AII

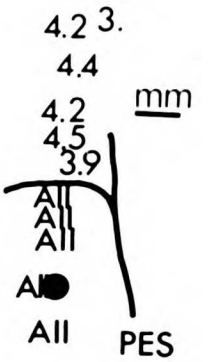

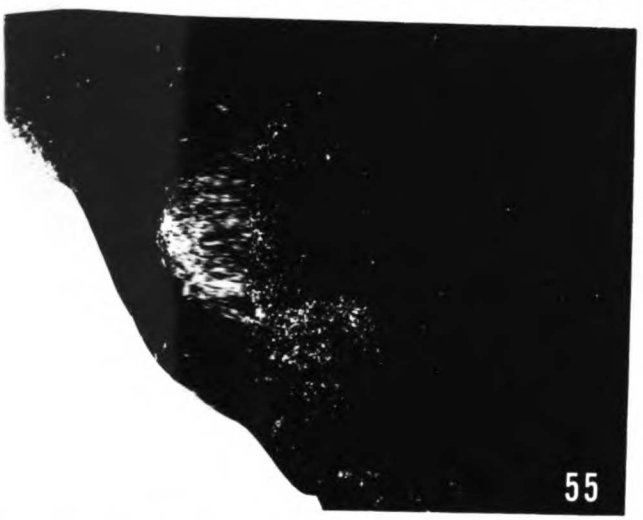

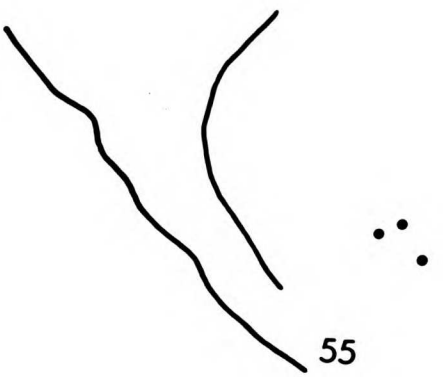

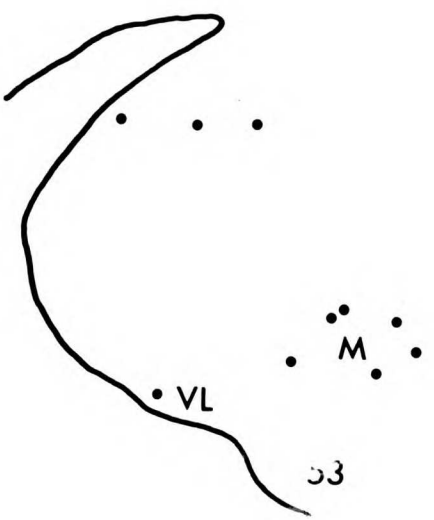

Figure 18

The results in this figure are from the same experiment as Figure 17 and represent the more caudal levels of the MGB. The sections on the left have been processed for autoradiography, the adjacent sections on the right for HRP. Section 50 is taken from the position of the middle and caudal thirds of the MGB, section 48 from the caudal third of MGB, and section 46 from the posterior pole of the caudal third of the MGB.

The numbers in the adjacent section 48's indicate four subregions of Dc that contain both labelled HRP granule containing cells (as indicated by the section on the right) and autoradiographic labelling (as indicated by the section on the left). For all sections, there is a general coincidence of the spatial disposition of the two labels. This is especially true considering adjacent sections are being compared and that the ARG processed sections are slightly more shrunken than the HRP sections due to the larger numbers of processing steps. An exception to this overlap of tracers is the labelled fibers of passage in sections 57 and 55 of Figure 17 and the labelled BIC fibers in the ventromedial region of section 46. Sections in Figures 17 and 18 are numbered caudal to rostral in 360μ steps. Survival time for autoradiography was 8 days.

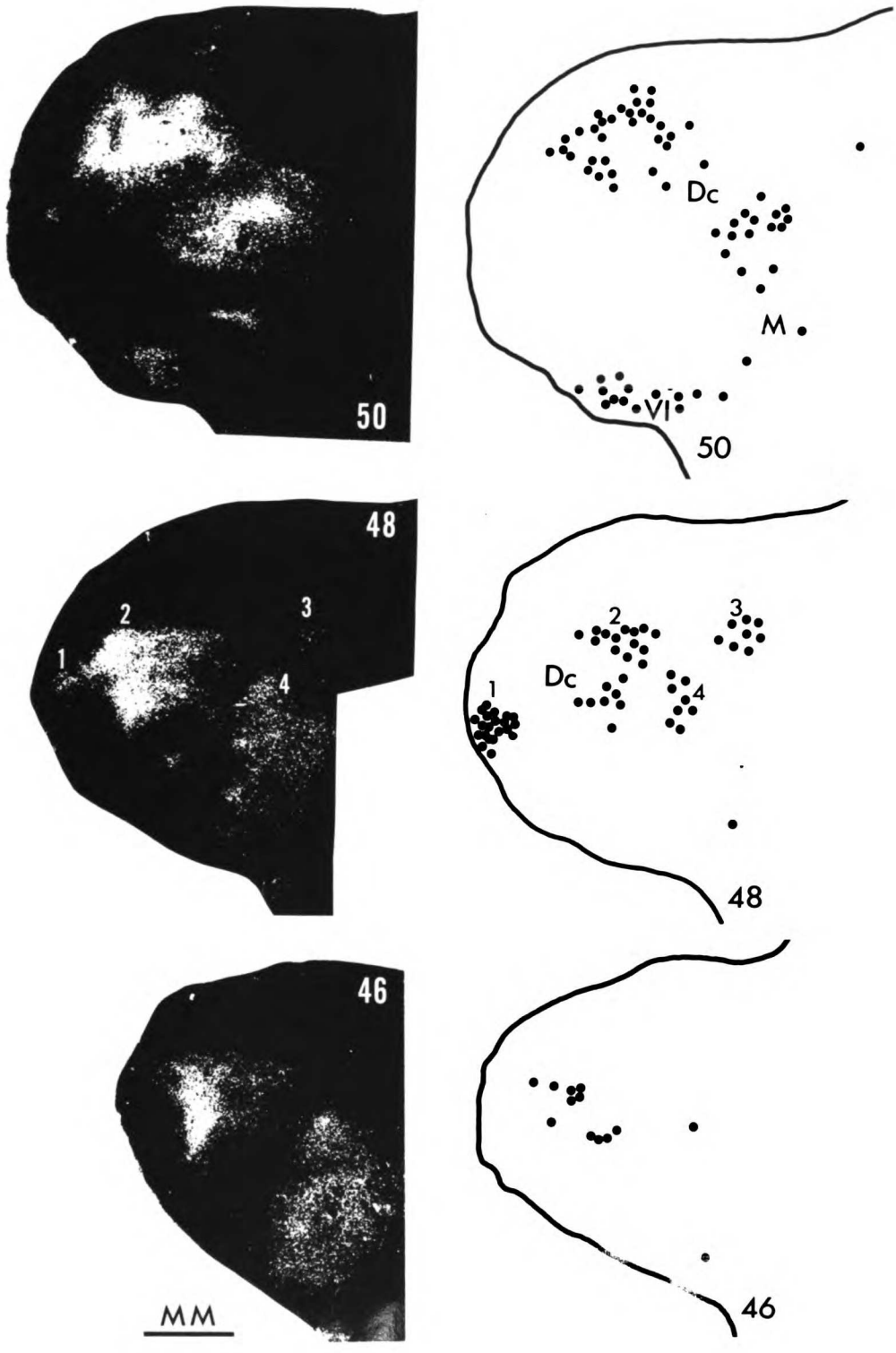
50
Dc
M
VI
50
48
1
2
3
4
48
Dc
1
2
3
4
48
46
MM
46

More rostrally, at about the level of the junction of the posterior and middle thirds of the MGB, a label-free region appeared in the lateral aspect of the MGB (Fig. 18, Sec. 50; Fig. 19, Sec. 10; Fig. 20, Sec. 20, 21, and 22; Fig. 21). This label-free region was the pars lateralis and pars ovoidea of the ventral division. The label-free region was surrounded by a broad band of labelled cells in Dc, VL and M. The cells in VL were of medium size; the cells in M were large and multipolar. This broad, "C" shaped band generally continued for several hundred microns into the middle third of the MGB.

In one case, HRP labelled cells were observed in POl. However, the labelling was very light. This weak labelling might have resulted from spread of the tracer into AI.

Corticothalamic Fiber Projections of AII

In 10 experiments, single microinjections of 3H-l-leucine were placed in physiologically typified AII regions of auditory cortex.

From the injection site, corticothalamic fibers were followed into the thalamus. They followed a course similar to that of AI and AAF fibers. Fibers left the injection site horizontally in the frontal plane and arched dorsomedially. Corticothalamic fibers descended from this bundle in a broad, anastomosing pattern into the internal capsule. The remainder of the corticocortical fibers continued into the corpus callosum.

The AII corticothalamics swept lateral and ventral to the anterior third of LGN and passed through the reticular nucleus of the thalamus. In one case a very light dusty pattern of grains was seen in the reticular nucleus. However, a majority of the labelling in this region had the stringy appearance of fibers passing through the nucleus. Thus, it was difficult to assess unequivocally whether or not there was any descending termination in the reticular nucleus. The fibers converged along the lateral edge of the caudal PO1 and rostral MGB and descended in fasicles. There was very light autoradiographic labelling in the lateral portion of PO1, seen only in one experiment. (Again, as with the single AII HRP injection case, this may have been due to spread of tracer to a bordering field).

In the rostral third of the MGB, in the short survival cases, very light label was sometimes noted along the lateral aspect of the MGB. In the long survival case, this label was more apparent and occurred in fasicles in regions that were free of cell bodies. The tissue in these fasicular regions also transmitted more light under dark field illumination, in a manner typical of fiber bundles cut in cross section. It is thus believed that this lateral label was at least principally of fibers descending to more caudal regions of the MGB.

In the one long survival case, fiber labelling was also noted in the dorsal aspect of the cerebral peduncle (Fig. 17, Sec. 57). These fibers are probably destined for the pontine nuclei and were situated in the

region of the cerebral peduncle where corticopontine fibers of temporal, occipital and parietal origin are located (Brodal '67). Also, descending fibers were noted in the BIC in the caudal MGB (Fig. 18, Sec. 46). These labelled fibers could be followed in the BIC to the inferior colliculus.

Terminal Field Labelling in MGB after AII Injections of Tritiated Amino Acids

Heavy labelling was observed in the middle and posterior thirds of the MGB after single injections of 3H-l-leucine into AII. The autoradiographic label was of a similar pattern to the HRP label and was noted in the Dc, VL and M subdivisions of the geniculate body. The heaviest label was over Dc, followed by VL (Fig. 17, 18 and 19).

When following the labelling caudorostrally in frontal sections, above background autoradiographic grains were first seen in the caudal pole of the MGB in Dc. The labelling in Dc had an intricate and complex pattern, with regions of light and heavy label (e.g., see Fig. 18, Sec. 48 and 50; Fig. 19). More rostrally, the lateral region of the MGB, over pars lateralis and pars ovoidea , was free of label (Fig. 18, Sec. 50). At this level, label was recorded in Dc, M and VL and surrounded the label-free region. Rostral to this level, the label over Dc, M and VL attenuated. The faint label, which occassionally appeared in the lateral aspect of the MGB and was believed to be descending fibers cut transversely, began at about this level (Fig. 17, Sec. 53 and 55).

Reciprocity of Thalamocortical and Corticothalamic Connections

It is apparent from the descriptions above, that the thalamocortical and corticothalamic patterns of labelling were quite similar. In 10 cases, both antrograde and retrograde tracers were injected at single loci in AII. These experiments demonstrated that the projections to and from Dc, VL and M were (with certain reservations) reciprocal (Fig. 17, 18 and 19).

The general strength of labelling of the two tracers in MGB subdivisions coincided. Thus, for both tracers, Dc had the heaviest labelling, followed by VL. Labelling in M was the lightest. Also, regions in Dc where HRP cells were clumped generally had heavier ARG labelling than surrounding areas of Dc (see Fig. 18, Sec. 48 and 50).

Variations in the pattern of label densities of the two tracers were often observed within the MGB subdivisions connected to AII. That is, over, some HRP labelled cell regions within an MGB subdivision, labelling was very dense; over other (even adjacent) cell regions within the same subdivision the corticothalamic projection was very light (see Fig. 18, Sec. 48; Fig. 19, Sec. 10). Thus, the AII corticothalamic and thalamocortical projections were reciprocal in the sense that all labelled cells were overlain with above background ARG label. However, the relative strength of the ascending and descending connections was often regionally variable.

Topographic Organization

Examination of several single injection cases revealed no apparent topography of AII projections to and from MGB nuclei. In these cases, injections were made at various positions along the rostrocaudal dimension of the field with respect to the cochleotopic organization of AI. Also, in these cases, injections were made from sites near the AI-AII border to positions about 3mm ventral to AI.

In one case, two injections were made in AII at different loci. Both were about 1mm from the AI-AII border, one being ventral to the site of representation of 2 KHz in AI, and the other ventral to the site of representation of 11 KHz (Fig. 19). There was no obvious difference between MGB labelling in this case as compared with single injection cases.

Thus a topography of projection could not be demonstrated in this material. The connections of AII with Dc occupy large regions of this nucleus. Each locus in AII gives and receives projections to and from several apparently separated regions within Dc (Fig. 18, 19 and 20). However, the entire nucleus is never occupied by either label after single AII injections (Fig. 18, 19, 20, and 21). Thus, there is available space within Dc for a limited topography of this complex projection, and this hypothetical topography might be elucidated by other means.

Figure 19

An example of the connections of two different loci in AII with the MGB. In this experiment, .15µl of a mixture of HRP and 3H-l-leucine was injected at the two different loci in AII. A) indicates the position of the two injections. Both were made about 1mm from the AI-AII border, at referenced positions of 2 and 11 kHz with respect to AI. B) shows adjacent sections processed for HRP (left) and autoradiography (right). Numbering is caudal to rostral in 200 µ steps. Note that any topography of connectivity with respect to the two injection sites is difficult to discern within this complex projection pattern. The two patterns of label are, in general, similar. However, within subregions of a thalamic nucleus there is often a variation in the densities of distribution of the two tracers (for instance Dc of sections 10).

CASE 76-140
AII INJ.
HRP & TAA

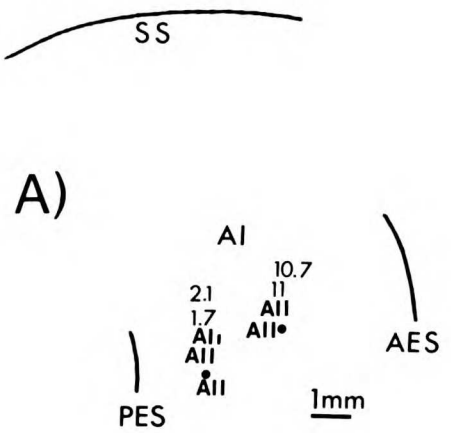

B) HRP

ARG

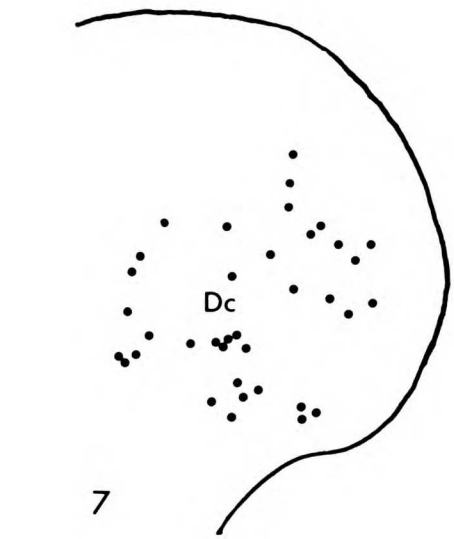

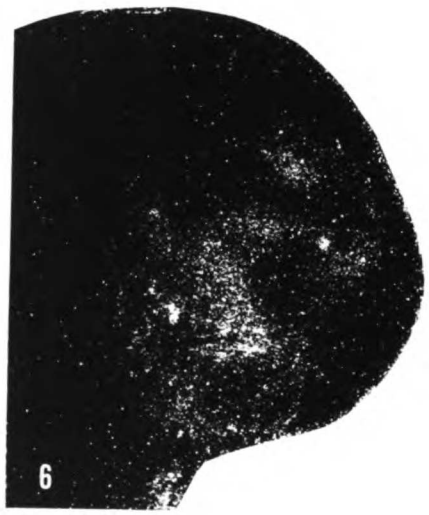

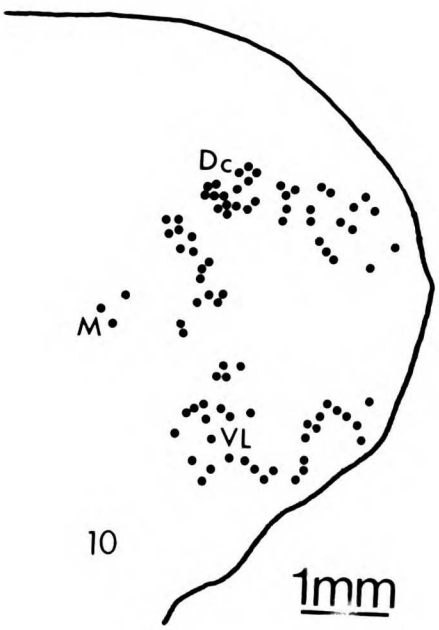

The AII Connections in Relation to AI Connections

An examination of the AII connections with the MGB indicates that AII does not give or receive projections from several regions of the MGB to which AI is connected. To test this observation directly, the two-tracer paridigm that was used to compare the AAF and AI projections was again employed to directly compare the AII and AI projection arrays. Since the connections of AI and MGB nuclei are highly reciprocal, their relation to the thalamocortical projection arrays of AII (and, within the limits of MGB subdivisions, the corticothalamic projection arrays of AII) was demonstrated by placing anterograde tracer in one field (AI) and retrograde tracer in the other (AII). The data presented here were from 4 such AI and AII injection experiments.

A large extent of the AII projection was shown to reside in regions of the MGB caudal to the thalamic origins of the AI projection (Fig. 20, Sec. 22-26). Label in this exclusive caudal region was contained within the Dc.

Proceding rostrally, when the AI projection did begin, the ventral division components of that projection fell within the label-free region of the AII projection (Fig. 20, Sec. 21 and 20; Fig. 21). The Dc component of the AII projection at this level appeared just dorsal to the AI projection to pars lateralis (Fig. 21; Fig.20). The Vl component bordered the AI projection to pars ovoidea ventrally (Fig. 20; Fig. 21).

Figure 20

An example of direct comparisons made, in single hemispheres, of the connections of AI and AII with the MGB. In this experiment, .2µl of 3H-l-leucine (2µ Curies) was injected at a 6 kHz locus in AI and .2µl of HRP was injected into AII about 1mm ventral the AI-AII border. The surface view of the cortex in the upper part of the figure indicates the positions of the injection sites. The darkfield photomicrographs on the right are of frontal sections through the tritiated amino acid (TAA) and HRP injection sites. The sections on the left, in the lower part of the figure, have been processed for HRP with each dot representing an HRP containing neuron. These HRP sections indicate the pattern of the AII thalamocortical projections and the general pattern of the AII cortico-thalamic projection. The adjacent sections on the right are darkfield photographs of the caudal extent of the AI corticothalamic projection. Since AI is reciprocally connected to the MGB, this also indicates the caudal extent of the AI thalamocortical pattern. Note that the connections of the two cortical fields with the MGB are largely segregated, the exception being the medial division. Sections numbered rostral to caudal in 200µ steps.

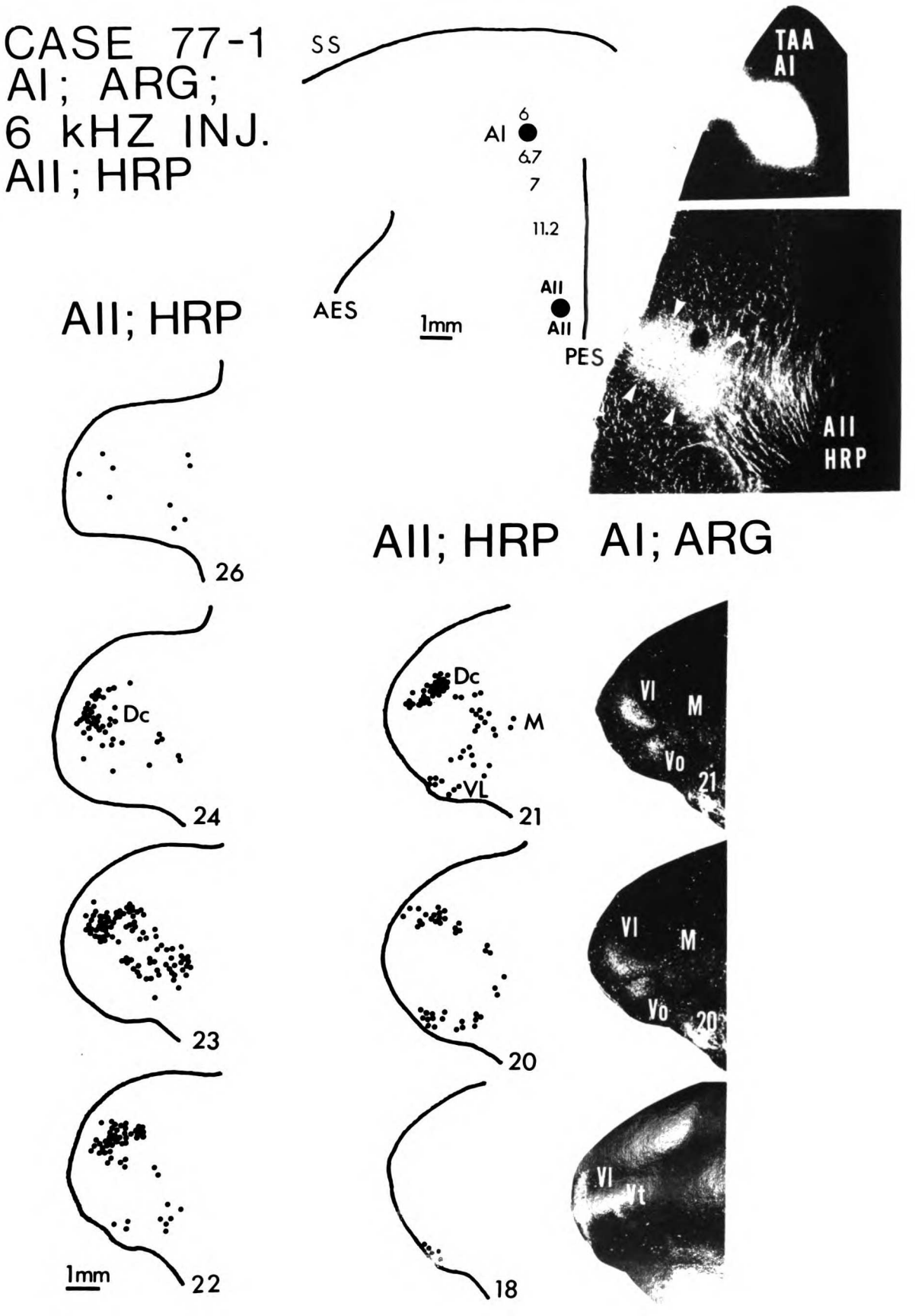
CASE 77-1
AI; ARG;
6 kHZ INJ.
AII; HRP
SS
AI
6
6.7
7
11.2
AII
AII
AES
PES
1mm
TAA
AI
AII
HRP
AII; HRP
AI; ARG
26
Dc
24
23
22
1mm
Dc
M
VL
21
20
18
VI
M
Vo
21
VI
M
Vo
20
VI
Vt

Figure 21

This darkfield photomicrograph is of a section from the experiment in Figure 20, and has been processed for both ARG and HRP. Autoradiographic label, representing the structure of the AI connections, is apparent in the ventral division (Vl, Vo). A group of HRP containing cells, representing the structure of the AII connections, is apparent in the caudal dorsal division, just dorsal to Vl. That the two labelling patterns in the ventral and dorsal divisions are segregated is apparent in these dually processed sections.

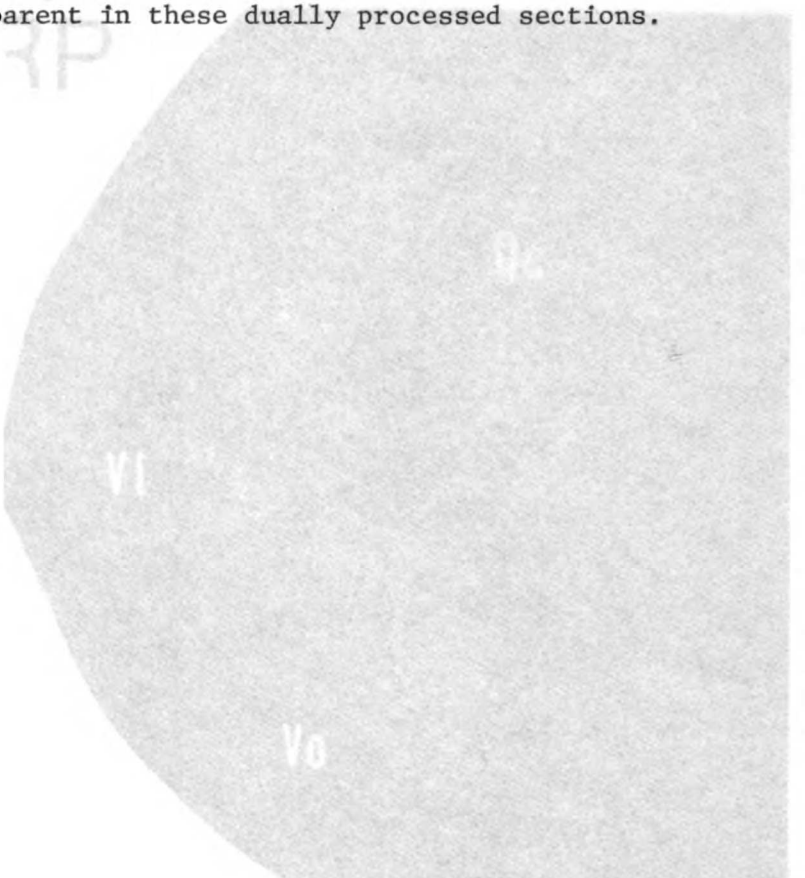

CASE 77-1; LEFT MGB
COMBINED SECTION
AI-ARG
AII-HRP

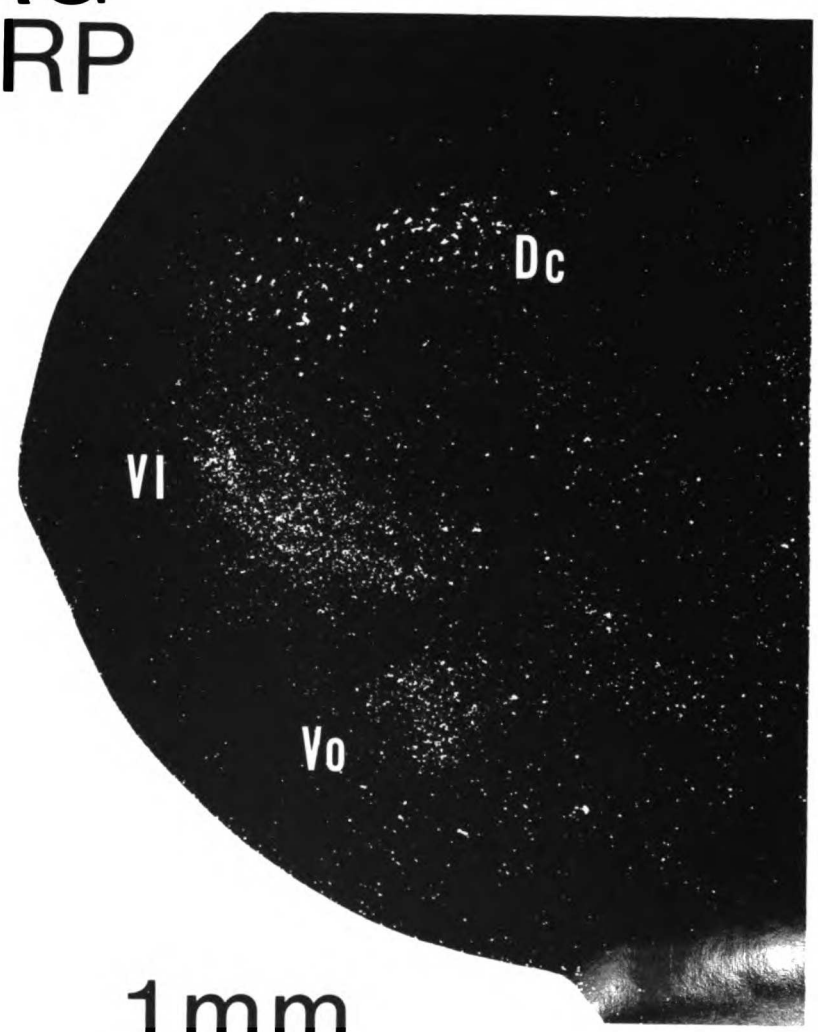

1mm

In one case, there were also lightly stained HRP cells in Vo and Vt after an AII injection (Fig. 21). However, this injection was made close to the AI-AII border and possibly represented a diffusion of tracer across the border. In other two tracer/two field experiments in which HRP was injected into AII loci 2mm from AI, no overlap in Vo and Vt was seen.

Thus, AI and AII appear to have largely separated projection arrays with AI interconnected with the middle and anterior thirds of the MGB and AII interconnected with the posterior and middle thirds. In the middle third, there is an overlap of the two reciprocal projections restricted to the medial division.

Summary

1) AII gives and receives projections from the middle and posterior thirds of the MGB. These connections are with the Dc, VL and M subdivisions of the MGB.

2) The thalamocortical and corticothalamic projections are reciprocal.

3) No clear topography of connections was apparent from the examination of material from this series of experiments in which injections were introduced at different, physiologically defined locations of AII (referenced to the AI topography).

4) The AI and AII projecting regions were largely segregated. The only region of overlap was in the medial division.

Corticotectal projections

The corticotectal projections of AI, AII, and AAF were investigated by placing microinjections of anterograde tracers at physiologically defined loci in these fields. The results presented here were obtained from experiments performed in 37 himispheres of 26 cats. Sixteen experiments were performed in AI, ten in AII and 11 in AAF.

Retrograde tracing experiments were also performed in 26 of these hemispheres. Two studies were made of AI, 14 of AII and 10 of AAF. Injections of HRP into these three fields never produced retrograde labelling in the IC or in any other mesencephalic structure. It thus appears that the described projections from the thalamus are the only direct, ascending sensory projections to these three auditory cortical fields. Since the direct connections of the IC with AI, AII and AAF are only corticofugal, all the results to be discussed were obtained by anterograde tracing of labelled proteins resulting from tritiated amino acid microinjections into these three cortical fields.

AI Corticotectal projection

After single injections of 3H-l-leucine into AI in cases with short survival times (2 days), label only appeared in the caudal half of the inferior colliculi. The ARG label was seen bilaterally in the dorsomedial divisions (ICC-dm) of the central nuclei (ICC) and ipsilaterally in the pericentral nucleus (ICP). The ARG label in both the ICC-dm and ICP was distributed to form continuous sheets, tilted down laterally (see Fig. 22).

With longer survival times (8 to 18 days), ARG label within other regions of the mesencephalon was seen. Most, but probably not all, of this labelling was of cortical efferent fibers. Most of these labelled fibers appeared to be destined for ICC-dm and ICP.

Path of Fibers to the Caudal IC after AI Injections

In long-survival anterograde tracing experiments, a continuous array of autoradiographic label was seen from the caudal pole of the MGB to the sheetlike terminal labelling in the central and (ipsilateral) pericentral nuclei in the caudal inferior colliculi. Four successful long survival experiments were performed. In every case, the results were virtually identical.

Labelled fibers were followed within the ipsilateral brachium of the inferior colliculus (BIC). The contralateral BIC was free of label. The labelled fibers in the BIC were scattered diffusely throughout it; i.e., no restricted topography within the fiber path was evident in this material. There was apparent terminal labelling in the nucleus of the brachium of the inferior colliculus medial and adjacent to the brachium.

Some labelled fibers were always seen (in frontal sections) extending up from the BIC to pass between the superficial and intermediate layers of the ipsilateral superior colliculus at its most caudal and lateral extent. (However, unequivocal terminal field labelling was not seen within the superior colliculus.) These fibers appeared to follow a caudomedially

directed course, to enter the rostral aspect of the collicular commisure (CC).

Light apparent terminal label was seen in the rostral pole of the IC in the region of the rostral aspect of the external nucleus (ICX). The path of fibers from the BIC to this region was not evident. This labelled field extended quite far anteriorly, lateral to the periaquaductal gray and medial to the nucleus of the BIC. In the most anterior aspect of this apparent terminal field, label may have extended into the midbrain tegmentum rostral to the ICX.

At the level of the anterior pole of the ipsilateral central nucleus of the inferior colliculus, many labelled fibers from the BIC passed dorsally and medially. Most of these medially directed fibers descended into the ipsilateral dorsomedial region of the IC. Others entered the collicular commisure and could be followed into the contralateral dorsomedial division of the ICC. A second group of fibers passed over the top of the ipsilateral central nucleus, and could be traced caudally in a dorsolateral position within the pericentral nucleus. This group of fibers was continuous with ARG labelled fields in the dorsolateral and caudal aspects of the ICP. In these long survival cases, other laterally situated labelled fibers coursed ventrally to the lateral region of the external nucleus and, more ventrally and posteriorly, the region of the nucleus sagulum. Unequivocal terminal fields were not observed in either structure. The fiber

labelling in the lateral aspect of the external nucleus may be fibers of the BIC. These labelled fibers appeared to be destined for terminal fields in the part of the ICP that covers the caudal aspect of the IC.

The dorsolateral and dorsomedial projecting fiber tracts of the ipsilateral IC continued posteriorly, and were continuous with the much denser terminal labelling in the ICP and the ICC-dm of the caudal inferior colliculus. Likewise, the contralateral dorsomedial fiber label was continuous posteriorly with the caudal, sheetlike terminal label field of the dorsomedial division of the contralateral ICC. No labelling was noted in the contralateral ICP, ICX, or BIC.

AI Projection onto ICP and the Dorsomedial Division of ICC

Terminal fields in ICP and ICC-dm were apparent in the caudal half of the IC with the most dense labelling in the more caudal regions. The basic pattern of labelling was the same in all 16 experiments, regardless of the survival times used. (However, apparent terminal labelling appeared relatively more rostrally with progressively longer survival times.) The ARG grains in the ipsilateral ICP and the dorsomedial division formed sharply defined sheets (see Fig. 22). The contralateral projection to the dorsomedial division also formed a sheet that occupied a similar (but reversed) position and orientation re the ipsilateral ICC-dm projection. This contralateral label was always fainter. The orientation of the ICC-dm sheet was dorsomedial to ventrolateral in the frontal plane (see Fig. 22). This orientation, in the frontal plane, paralleled the orientation of the

Figure 22

A representative example of the projection of a locus in AI to the inferior colliculus. In this experiment, .25µl of 3H-l-leucine was injected at an 11 kHz locus in AI. A) shows, on the cortical surface, the site of injection within AI and a frontal section darkfield photomicrograph through the center of the injection site. B) are frontal sections through the inferior colliculus. The stippling indicates above background autoradiographic labelling. The sections are numbered caudal to rostral, in 120µ steps, beginning at the caudal pole of the inferior colliculus. C) is a darkfield photograph of a frontal section through the MGB. The three dimensional structure of the projection is in the form of two sheets of labelled terminals in ICP and ICC-dm of the ipsilateral IC and a sheet of labelled terminals in ICC-dm of the contralateral IC.

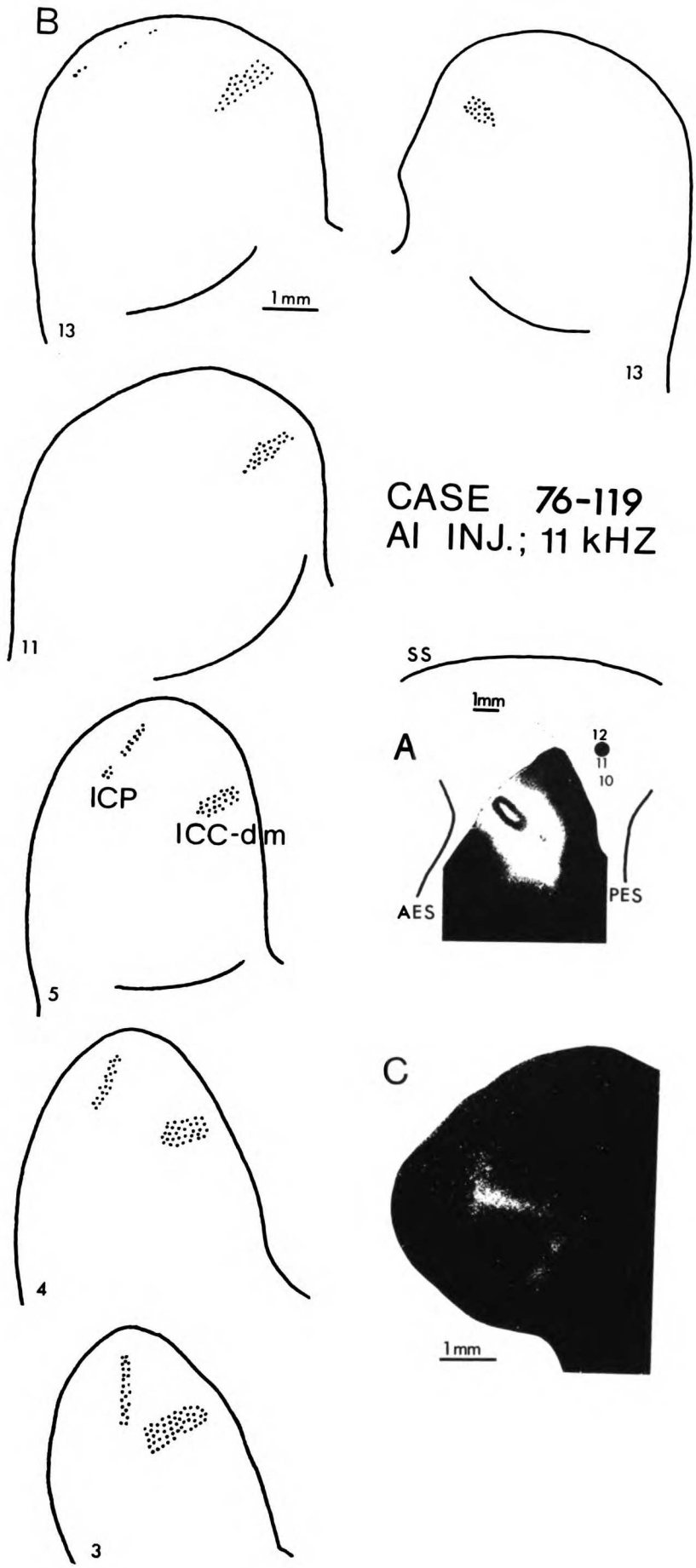
B
1mm
13
13
CASE 76-119
AI INJ.; 11 kHZ
11
SS
1mm
A
12
11
10
ICP
ICC-dm
AES
PES
5
C
4
1mm
3

cellular laminae of the adjacent ventrolateral ICC (Rockel & Jones '73) and also paralleled the isofrequency contours of the ICC (Merzenich & Reid '74).

In proceeding from its rostral to caudal extent, the sheet of ARG label in ICC-dm shifted its degree of lateral tilt within the IC (see Fig. 25 and 27). Rostrally, the laminar array of label was oriented relatively more dorsoventrally and the dorsal aspect of the sheet of label was located more laterally within the IC. Caudally, the sheet acquired a relatively more horizontal orientation and the dorsal aspect of the sheet was placed more medially in the IC. This shift appeared in both ICC-dm's of this bilateral projection.

Anteriorly, the ICP ARG terminal label also formed a distinct sheet, obliquely oriented dorsomedial to ventrolateral. Labelling in the ICP was located in its deeper aspect. Posteriorly, particularily in the region of the ICP which covers the dorsocaudal surface of the IC, the ICP terminal sheet often rotated so that in frontal sections, it had a nearly vertical orientation (see Fig. 22). The ICC-dm and ICP projections always came into close apposition at their ventrolateral edges in the extreme caudal pole of the IC (see Fig. 22, Sec. 3; Fig. 25, Sec. 29 & 32; Fig. 27, Sec. 16). No projections from the ipsilateral AI to the contralateral ICP were ever recorded.

Topographic Organization of the AI Corticotectal Projection

The projections to ICC-dm and ICP are both topographically organized with respect to the cochleotopic representational order in AI. Injections introduced at the sites of representation of successively more apical (low frequency) cochlear locations in AI resulted in sheets of ARG label that were located at successively more dorsomedial positions in ICP; and in sheets of label that were located in successively more dorsolateral positions in the ICC-dm. There was an apparent frequency reversal in the topographic projection from AI to ICC-dm and ICP along their mutual border, with injections at the AI sites of representation of lowest frequencies projecting along this border.

Figure 23 is an example of an experiment that demonstrates the topographic organization of the AI projection onto the IC. In this case, injections were placed in the left AI auditory field at 22 kHz locus and in the right AI at two 2.4 kHz loci. In the right IC, a continuous sheet of ARG label was seen that passed through ICC-dm (dm_2). This ARG labelled sheet resulted from the injections at the 2.4 kHz representation in the right AI. In the left IC there were two foci of label in ICC-dm in sections 10 and 11. The more ventral focus of ARG label (dm_1) resulted from the 22 kHz place injection in the AI tonotopic representation of the left cortex. The more dorsal focus of ARG label (dm_2) resulted from the injections at the 2.4 kHz representation in the contralateral AI. (ARG labelling from the 22 kHz place injection in the left AI did not appear bilaterally in ICC-dm as was sometimes the case in short-survival experiments.) Examination of these sections

Figure 23

A representative example of the topographic organization of the corticotectal projection re the cochleotopic order of AI. In this experiment, .3 μl of 3H-l-leucine was injected at a 22 kHz locus in the left AI auditory field, and at two positions along a 2.4 kHz isofrequency contour in the right AI. A) shows surface views of the left and right cortical surfaces with the injection sites represented by the black spots. B) is a darkfield photograph of a frontal section through both MGB's. Labelling in the left and right MGB's indicates the cochleotopic organization of the ventral division, with the basal end represented dorsomedially. C) are sections through the two ICs with stippling indicating areas of above background autoradiographic labelling. The subscripts indicate labelling from the higher (1) frequency place injection and lower (2) frequency place injection. Section numbering is caudal to rostral, in 200μ steps, beginning at the caudal pole of the IC. D) are darkfield photomicrographs of the right IC drawn in C. Notice the topographic organization in ICC-dm and ICP, with the higher frequency representational region of AI projecting relatively more medioventrally in ICC-dm and ventrolaterally in ICP. Also, the patterns of label are similar for a single locus injection and two injections made along an isofrequency contour.

CASE 76-141

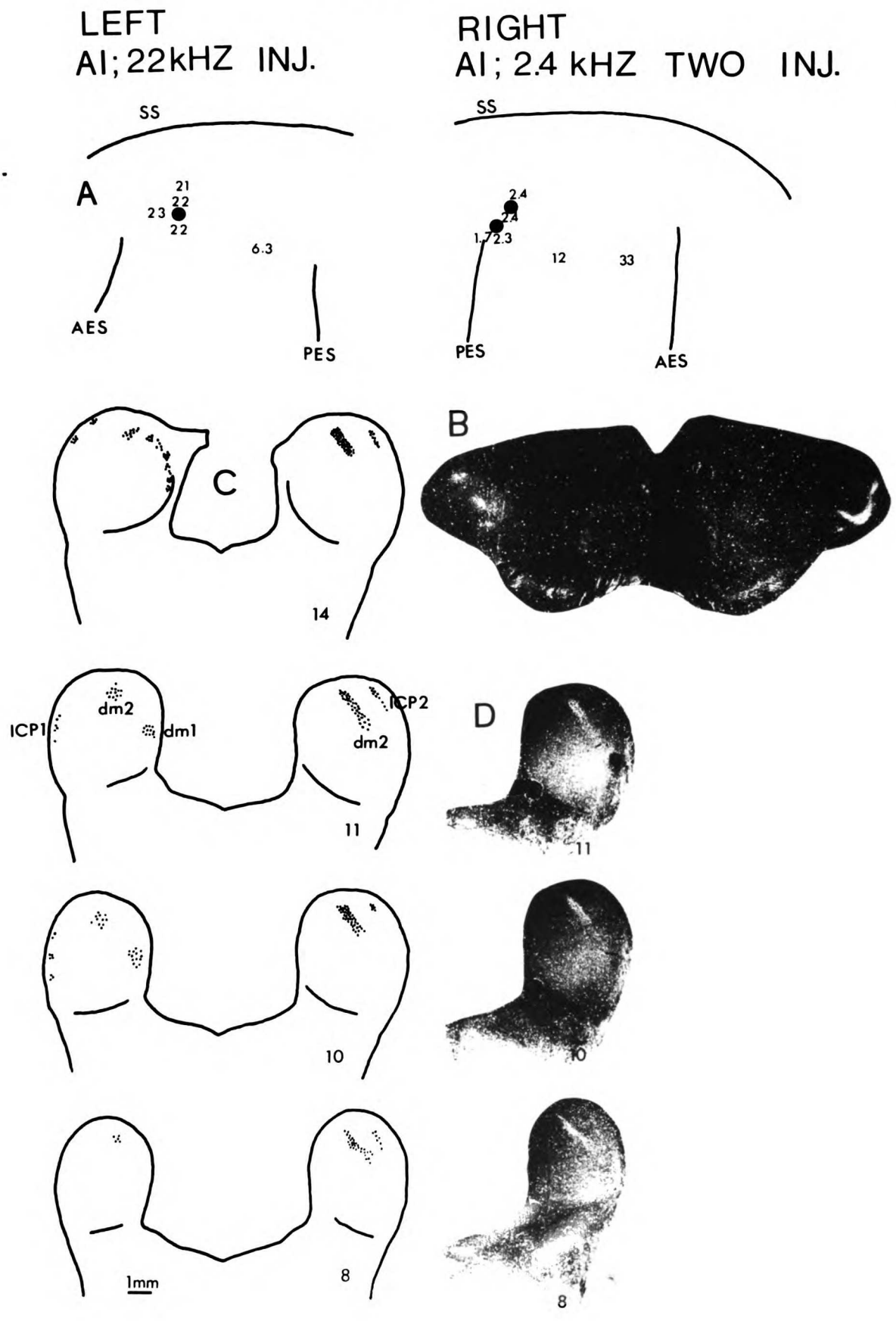
LEFT
AI; 22kHZ INJ.
RIGHT
AI; 2.4 kHZ TWO INJ.
SS
SS
A
21
22
23
22
6.3
AES
PES
2.4
2.4
1.7
2.3
12
33
PES
AES
B
C
14
ICP1
dm2
dm1
ICP2
dm2
11
D
11
10
10
1mm
8
8

demonstrated that the lower frequency place injections in the right cortex produced more dorsal and lateral ARG label in ICC-dm with respect to the ARG label that resulted from the higher frequency place injection in the left cortex. This was particularily apparent in the left IC of sections 10 and 11, where the projection from the location of the relatively lower frequency representation of the contralateral AI (dm_2) was directly comparable with the more dorsal and lateral projection from the location of the relatively higher frequency representation of the ipsilateral AI (dm_1). Examination of these sections also indicated that the projection from the lower frequency representation of the right AI occupied a more dorsal and medial position in the right ICP (ICP_2) than the projection to the left ICP (ICP_1) from the relatively higher frequency representation of the left AI.

In three experiments, injections were placed at two widely separated locations re the cochleotopic representation of single AI fields. This resulted in two parallel sheets of label in both the ipsilateral and contralateral dorsomedial divisions (see Figs. 25, 26 and 27). In two of the cases (in which the two injection sites were very widely separated) there was also two distinct sheets of label passing through the ipsilateral ICP (see Figs. 25 and 27). These experiments directly demonstrate that there exists a topographic organization of projection into the ICC-dm and ICP with respect to the cochleotopic organization of AI. The topographic organization appears to be slightly more restricted for ICC-dm than for ICP (see Fig. 26). These two injection experiments also demonstrate that the

Figure 24

In this figure, the relative positions of the corticotectal projections in the ICC, as a function of the best frequency positions of the AI injections, are compared with the best frequency-relative position microelectrode recording data obtained from the ICC in the study of Merzenich and Reid '74. In A), the relative depth of the projections in the ICC is plotted (solid dots) against the best frequency determinations of the cortical injection sites. The relative depth of best frequency determinations from recordings in the ICC are also plotted on this graph (dotted line). These two plots are similar indicating that the topographic (cochleotopic) order of the projection is in a relative register with the cochleotopic organization of the ICC. In B) the relative depths of the anatomical and recording data are plotted against one another. If the two sets of data were exact, they would fall along a line of a 45° angle. Instead, the data points form a straight line that indicates a 30° greater depth for the recording data with each comparison. The proportional variation is consistent with a proportional shrinkage of the tissue during fixation. C) indicates three examples of how the twelve anatomical data points were obtained. The projections to ICC-dm from the same levels in IC were superimposed. Measurements were made from a line approximately perpendicular to the projection laminae. The measurements were made referenced to the lowest frequency place projection from AI.

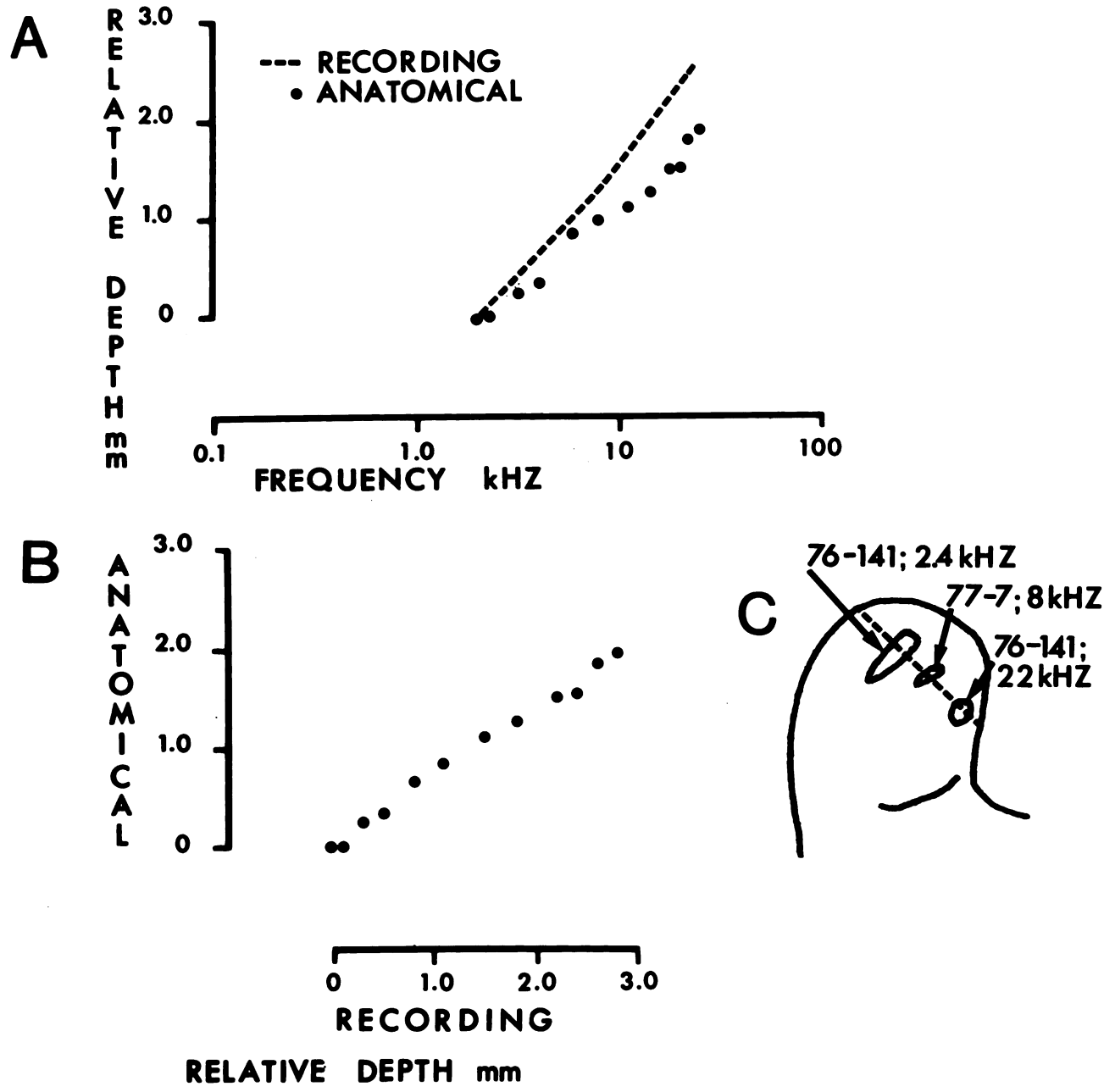
A
RELATIVE DEPTH mm
3.0
2.0
1.0
0
--- RECORDING
• ANATOMICAL
0.1
1.0
10
100
FREQUENCY kHZ
B
ANATOMICAL
3.0
2.0
1.0
0
0
1.0
2.0
3.0
RECORDING
RELATIVE DEPTH mm
C
76-141; 2.4 kHZ
77-7; 8 kHZ
76-141;
22 kHZ

Figure 25

A representative example of this systematic topography of the AI corticotectal projection onto the IC re the cochleotopic order in AI. Subscripts indicate labelling as a result of injections (.5µl) at (1) an 18.5 kHz locus in AI and (2) a 2 kHz locus in AI. Higher frequency positions in AI project to more ventromedial positions in ICC-dm and more ventrolateral positions in ICP. The laminar projections in ICC-dm are longer for relatively lower frequency representational loci in AI (see section 21). The ICP and ICC-dm ARG sheets come into close apposition more rostrally after injections of TAA in relatively lower frequency representations of AI (see section 29). Sections numbered rostral to caudal in 30µ steps.

77·45; AI INJECTIONS
1) 18.5 KHZ 2) 2 KHZ

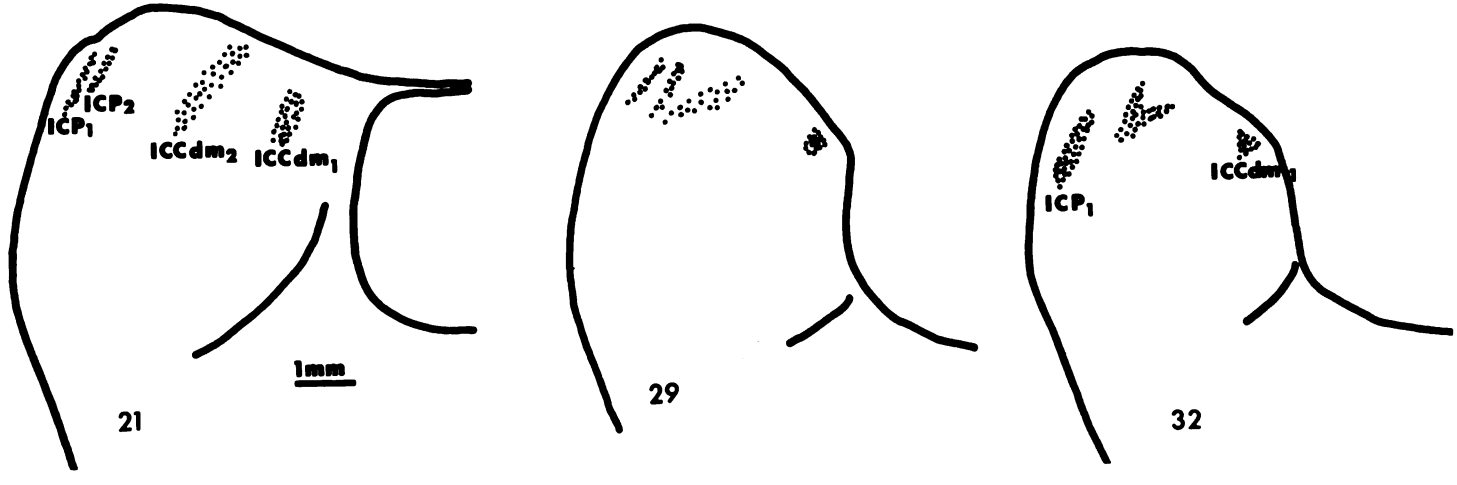

Figure 26

Another example of the systematic topography of the AI projection onto the IC. In this experiment, two 3H-1-leucine injections (.2µl) were made at 20 and 24 kHz best frequency loci in AI. Thus, these injections were placed relatively short distances from one another re the cochleotopic order in AI. This produced two closely spaced sheets of label in ICC-dm but only one (rather fat) sheet of label in ICP. This suggests that the topographic organization of the projection onto ICC-dm is slightly more restricted (less divergent across the cochleotopic order) than the projection onto ICP.

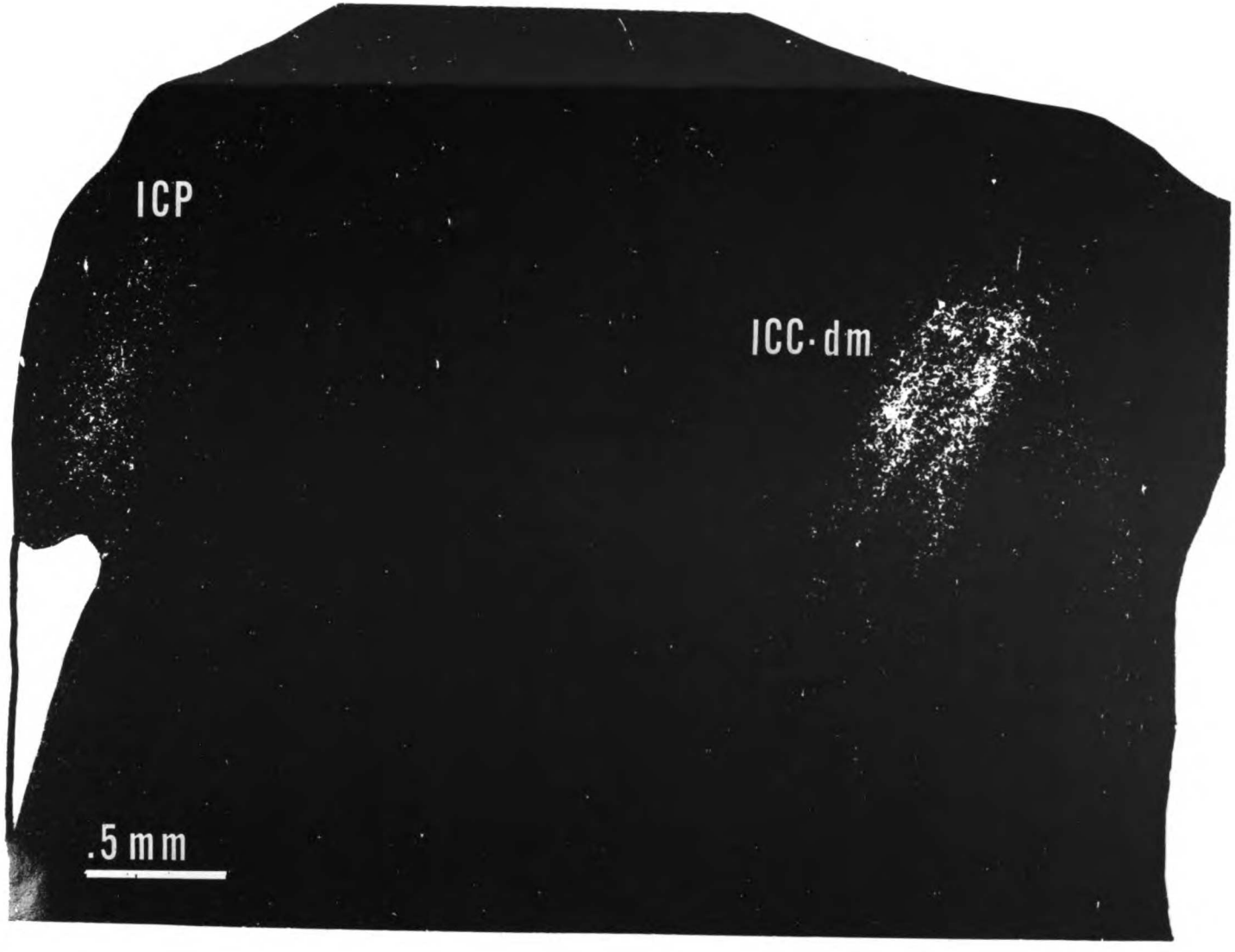
ICP
ICC-dm
.5 mm

Figure 27

An example of the topography of the corticotectal projection from AI re its cochleotopic organization. In this experiment, injections of 3H-l-proline were made along almost the entire extent of a 6 kHz isofrequency contour and at a 2 kHz locus in AI. On the right are frontal sections through the ICC with stippling indicating above background, autoradiographic labelling. On the left is a darkfield photomicrograph of one of the drawn sections on the right. Note the two laminae in ICP and ICC-dm. The more medial lamina in ICC-dm and the more lateral lamina in ICP represent the higher frequency place injections in AI. These results again demonstrate the form of the projection from an isofrequency lamina in AI is similar to the form of the projection from a locus in AI.

CASE 77-4

A1 INJECTIONS: 6 KHZ LAMINA
2 KHZ LOCUS

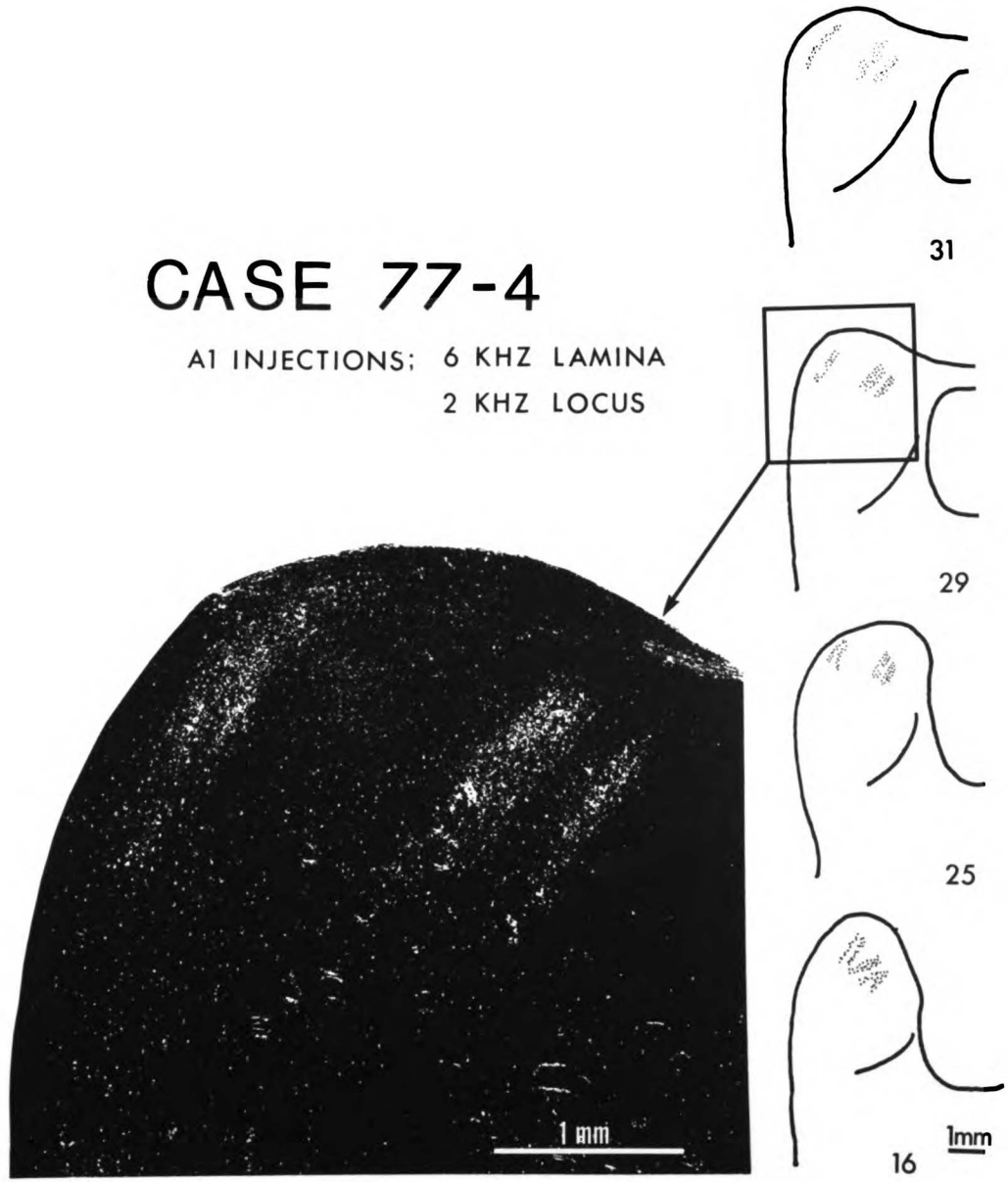

laminar terminal fields in ICC-dm and ICP come into close apposition with one another at successively more rostral levels with single injections into successively higher best frequency representations in AI (see Fig. 25, Sec. 29 and Fig. 27, Sec. 16).

In three experiments, two, three and four injections were made along isofrequency contours in AI. In all these cases, the same pattern of projection in the IC was seen as with single injection cases. Multiple injections along an isofrequency contour produced only one sheet of label in the ipsilateral ICP and single sheets in the ipsilateral and contralateral ICC-dm (i.e., see Fig. 23, Sec. 11, 10 and 8 of row D). The dimensions of the sheets were also the same as with single injections. The length of the laminae seen in the frontal section did not increase, nor did labelling extend more rostrally after multiple injections along a contour. Thus, isofrequency bands in AI project to single restricted slabs in ICC-dm and ICP. These slabs in the IC probably represent the same best frequencies as the projecting bands in cortex. Each sector of the projecting cortical band projects throughout the full extent of the target region in ICC-dm and ICP.

Injections at lower best frequency loci in AI produced bilateral laminae in ICC-dm which were longer when viewed in the frontal place (i.e., see Fig. 23; Fig. 24C and Fig. 25). This is consistent with the idea that a larger volume of the dorsomedial division is committed to the representation of the lower frequency regions of the cochlea (FitzPatrick '75). However, it must be emphasized that injections at all places in the

cochleotopic representation of AI produced labelling in the dorsomedial aspect of ICC (presumably, but not unequivocally, restricted to ICC-dm). This is consistent with the interpretation that there is a complete or nearly complete representation of the cochlea within ICC-dm.

An analysis was made of the locations of the ICC-dm label arrays resulting from injections of tracer at several different positions re the cochleotopic representation in AI (see Fig. 24). This analysis demonstrated that the AI laminar projections within ICC-dm were properly positioned to be in register with the dorsal aspect of the physiologically defined, homotypic isofrequency laminae of the cochleotopic representation of the ICC (Merzenich & Reid '74).

The relative positions of the sheetlike terminal arrays of the cortical projections onto the ICC were determined for 12 different frequency locations in the tonotopic map in AI. Each projection was photographed at the same level in the ipsilateral IC (at approximately the junction of the middle and caudal thirds) and a tracing was made of the IC and the projection. These tracings were combined onto one IC in the same manner as shown in the inset (C) of Figure 24 for three of these experiments. The distances between the centers of these parallel laminar projections and the center of the lowest best frequency place projection (2 kHz) were measured along an axis approximately perpendicular to the laminae (the dotted line in 24C). The axis of the microelectrode penetrations in the experiments of Merzenich & Reid '74 were also approximately perpendicular to the isofrequency contours of the ICC.

On the graph in A of Figure 24, the ICC relative depth vs. best frequency recording data of Merzenich and Reid '74 is represented by the dotted line. The black dots represent the relative depth of the ARG terminal arrays in the ICC, obtained as described above, against the best frequency representational sites of the tracer injections in AI. This graph shows that the topographic organization of the AI terminal projection laminae in the ICC, with respect to the cochleotopic organization of AI, is structurally very similar to the cochleotopic organization of the isofrequency contours within the ICC. However, the anatomical points consistently fell on the short side in terms of relative depth in the ICC when compared to the depth of the homotypic best frequency determinations in the ICC.

In the graph in B of Figure 24, the relative anatomical depths of the projections in the ICC have been plotted against the relative depths of the ICC recording data for homotypic best frequencies in AI and the ICC. The fact that this plot is roughly linear demonstrates that the two sets of data vary in a proportional fashion with the anatomical projection depths being about 30% less at all frequencies. This proportional compression is consistent with the interpretation that the variation is due to a proportional shrinkage of the tissue resulting from profusion fixation and the additional processing of the tissue that is required for autoradiography. Thus, the cochleotopic organization of the ICC and the topographic organization of the terminal fields of the AI projection onto the ICC, with respect to the cochleotopic organization of AI, are very similar if not identical along the axis perpendicular to the isofrequency contours.

The isofrequency contours of the ICC extend continuously through the ventrolateral (ICC-vl) and dorsomedial divisions of the nucleus (Merzenich & Reid '74). That is, neurons with approximately the same best frequencies are located along single planes that subtend the two divisions of the ICC. The orientation of these isofrequency planes parallel the orientations of the morphological laminations (Morest '64b) observed in ICC-vl (Rockel & Jones '73, Merzenich & Reid '74). The orientation of the laminar AI projections onto the largely non-morphologically laminated ICC-dm (Rockel & Jones '73) are of similar orientation to both the isofrequency contours of the ICC and morphological laminations of ICC-vl. The analysis above, demonstrates that the cochleotopic order of the ICC-dm projections and the isofrequency contours are also very similar. Thus, this data is consistent with the interpretation that the parallel laminar AI projections to ICC-dm fall along the dorsal aspects of parallel, homotypic isofrequency contours that subtend both the dorsomedial and ventrolateral divisions of the ICC. This data also suggests that the laminar projections to the presumably non-morphologically laminated ICC-dm form continuous planes with the morphological laminations in ICC-vl.

Fiber Projection of AII onto the Tectum

Long survival experiments demonstrated that the corticotectal fibers from AII follow a path similar to those from AI. Fibers pass caudal to the MGB in the brachium of the inferior colliculus. Labelled fibers were scattered difusely throughout the brachium. There was very light label over the nucleus of the BIC.

At the rostral pole of the IC, fibers passed dorsomedially from the brachium. Some entered the collicular commissure and coursed into the contralateral inferior colliculus. In the contralateral IC, these fibers ended in a terminal field just medial and dorsal to the ICC

However, the bulk of the medially directed fibers passed caudally, in the ipsilateral IC, dorsal and medial to the ICC. This medial projection produced apparent terminal field labelling along most of the rostrocaudal extent of the IC, with this label being heaviest caudally.

The remaining lateral labelled fibers of the ipsilateral IC passed caudally into a continuous terminal field in the lateral and posterior aspects of the ICP. This was the same region of the ICP that was labelled after AI injections although larger areas of the ICP appeared to be labelled after AII injections. In long survival experiments, some labelled fibers were seen coursing ventrally in the ICX but no ARG terminal field was apparent in this region. Labelled fibers, without unequivocal terminal field labelling, were also seen within the nucleus sagulum. No label was seen in the ipsilateral ICC, or within the contralateral BIC, ICP, ICC or ICX.

Distribution of Terminal Fields in the IC after AII Injections

After single injections of 3H-l-leucine into AII, three sheets of label were seen passing rostrocaudally in the IC. Two sheets were located in the ipsilateral IC; one was located medially and the other laterally

Figure 28

An example of labelling in the IC after an AII injection of 3H-l-leucine. In this experiment, an injection of .25µl of 3H-l-leucine was made into AII 2mm from the AI-AII border. Sections are numbered caudal to rostral in 120µ steps; the caudal pole of the IC begins at section 12. Survival time was 8 days. "d" and "l" indicate dorsal and lateral orientations. This figure indicates the structure of the AII projection onto the caudal IC. In sections 19 and 16, the projections to ICP-l and ICP-m are apparent. In section 14, the ICP-m label swings laterally, dorsal to ICC to meet the ICP-l label. Note that ICC is not labelled after AII injections.

77·73, IC

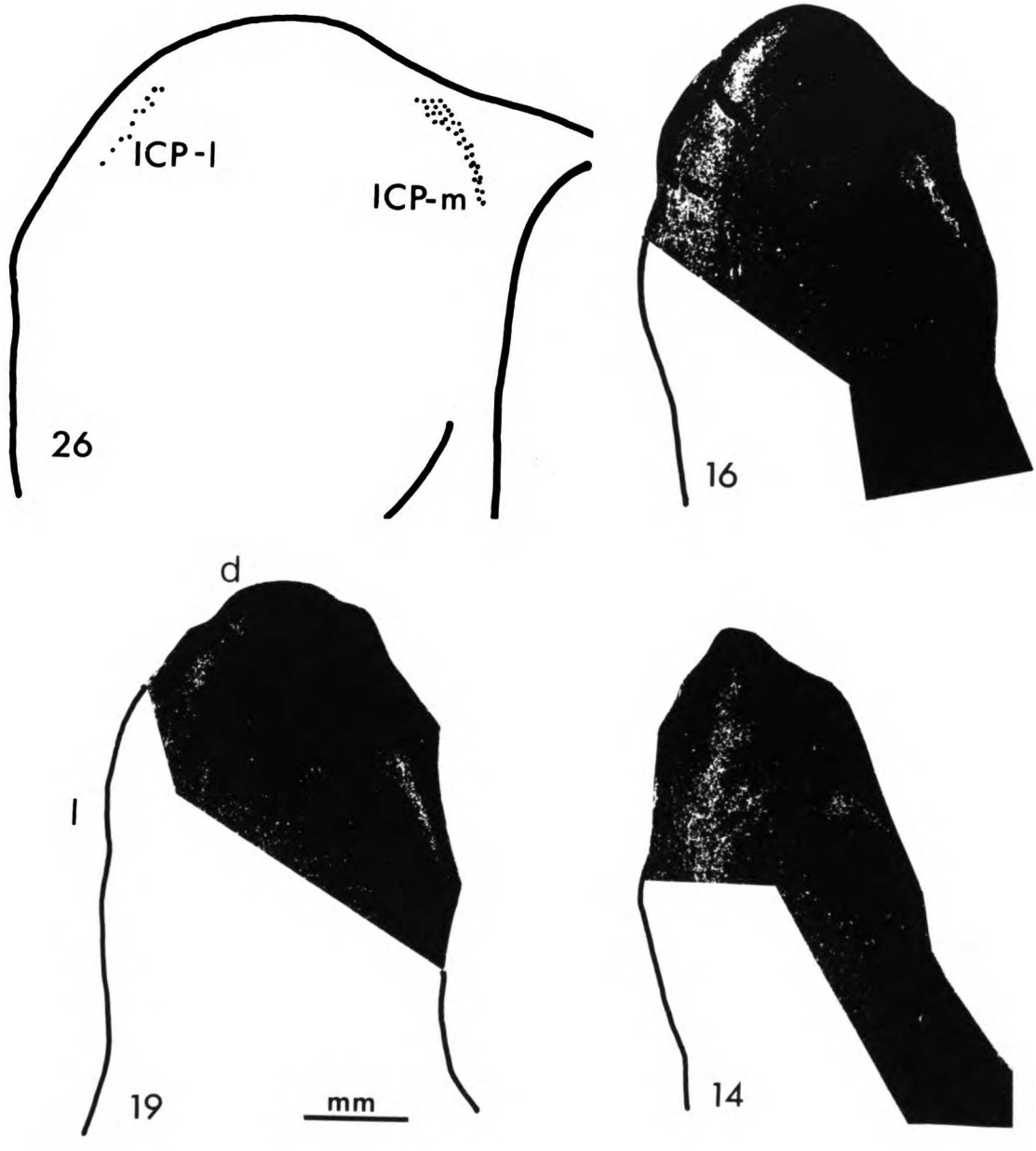

(see Fig. 29, Sec. 10, Case 76-140 and Fig. 28, Sec. 19). A third corresponding medial sheet was located in the contralateral IC.

The ipsilateral and contralateral medial ARG label arrays were in the form of thin sheets, adjacent to the dorsomedial edge of the ICC. There was no label in the adjacent ICC. These two projections were roughly mirror symmetrical; however, the ipsilateral medial sheet was much more heavily labelled than the contralateral one. It is difficult to assign this medial sheet of ARG label to a previously described subdivision of the IC. The rostral region of the label could be classified as existing over the lateral margins of the intercommisural nucleus (Geneic & Morest '71). However, most of the labelled sheet was caudal to the IC commissure (and caudal to the "intercommissural nucleus"). The cells in the region over which label was evident were smaller, more tightly packed, and slightly lighter staining with Nissl stains than were the cells of the adjacent dorsomedial division of the ICC; the cytoarchitectonic boundary between ICC-dm and this narrow strip is relatively distinct. Rostrally, these neurons formed a thin layer sandwiched between ICC-dm and the periaquaductal gray. Caudally, these neurons appeared as a thin superficial lamina covering the dorsomedial surface of the ICC-dm and bordering the fourth ventricle. This cell region was continuous dorsally with the dorsal aspect of the ICP and is in a region that is sometimes included in the definition of the ICP (e.g., see Rockel & Jones' 73, '73a). In this study, this region of label will therefore be called the medial part of the pericentral nucleus of the inferior colliculus (ICP-m).

Figure 29

Two examples of labelling in the IC after injections of 3H-l-leucine into AII and short survival periods (2 days). In the experiment on the left, two injections of .15μl (1.5μC) 3H-l-leucine were made into AII at two topographically different loci. The caudal injection was made 1mm from the AI-AII border referenced to a 1.7 kHz position in AI. The rostral injection was made about 1mm from the AI-AII border referenced to an 11 kHz position in AI. The loci of these injections are indicated by black spots on the cortical surface in A. The dark-field photograph is of a frontal section through one of the injection sites. B are drawings of frontal sections with stippling indicating above background autoradiographic labelling. The numbering of sections is caudal to rostral, in 200μ steps, beginning at the caudal pole of the IC. In the experiment represented on the right of the figure, an injection of .2μl (2μC) of 3H-l-leucine was made into AII. The injection was made 1mm from the AI-AII border, referenced to a 10 kHz region in AI. A) is a view of the cortical surface. The darkfield photograph in A is of a frontal section taken through the center of the injection site. B) is drawings of frontal sections through the caudal IC. The sections are numbered caudal to rostral in 150μ steps, beginning with the caudal pole of the IC. Both these experiments represented in this figure were of short survival times (2 days). The labelling is much lighter than with longer survival experiments but of the same pattern (i.e., see Figure 28). Labelling is always lighter in the IC for AII injections when compared to AI injections.

CASE 76-140
TWO AII INJ.

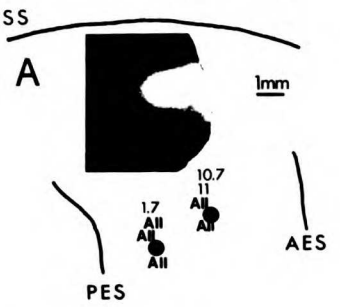

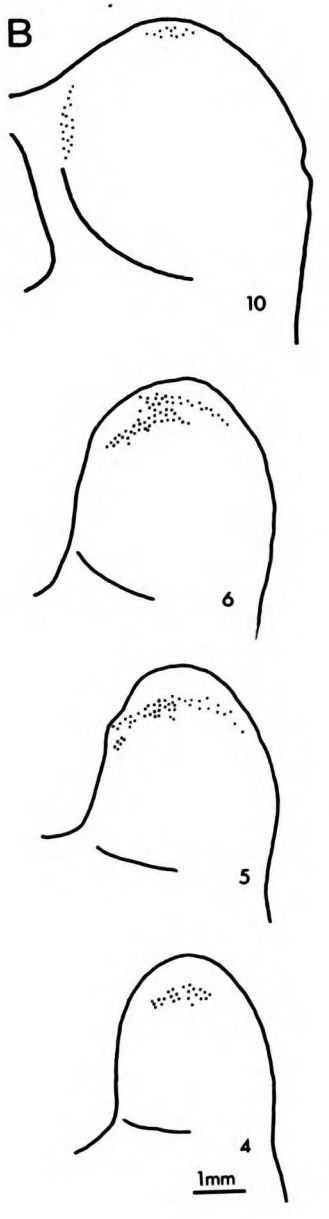

CASE 76-32
AII INJ.

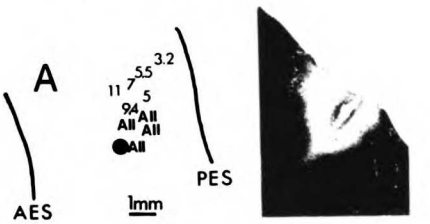

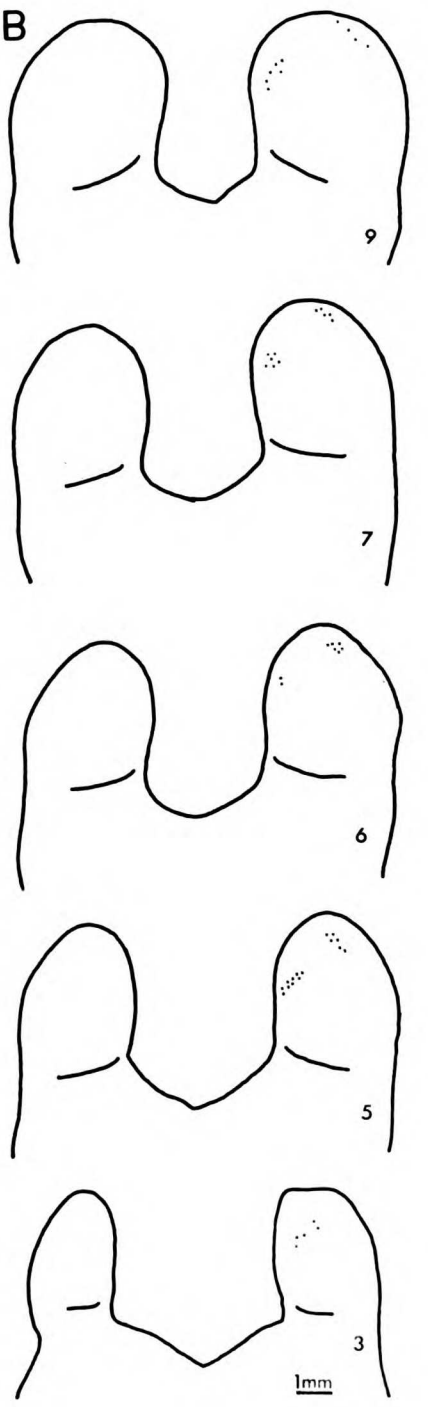

The ipsilateral lateral sheet of the label was located then, in the lateral part of the ICP (ICP-l) (see Fig. 28). This is the same region which was labelled after AI injections, although the labelling appeared to cover larger areas of this part of the nucleus after AII injections.

In the posterior pole of the IC, the sheet of label in ICP-l of the ipsilateral IC obtained a nearly vertical orientation. At this caudal level, the label in ICP-m arched across the dorsal surface of the ICC and merged with the ICP-l component of label (see Fig. 28, Sec. 14). Further caudally, where frontal sections only contained the ICP, label was seen scattered throughout the nucleus. The intensity of labelling in the IC after AII injections was much less than after AI injections.

The overall corticotectal projection pattern of AI and AII is different, then, in several aspects. AI projects to the dorsomedial division of ICC, and to the lateral ICP. The ICC-dm projection is bilateral, while the ICP projection is wholly ipsilateral. By contrast, AII does not project to ICC. It does project to the lateral aspect of ICP (again only ipsilaterally) in the AI projecting region. In addition, AII projects to the medial aspect of ICP, and like the AI projection to the ICC, this descending projection is bilateral. The AI projection to IC was always stronger. It was quite apparent autoradiographically after short survival times, whereas the AII projection could be fully appreciated only after longer survival periods.

AAF Corticotectal Projections

Injections of anterograde tracer into AAF produced a pattern of label in the IC that was similar to that produced with AI injections, except that the AAF projection was much weaker than the AI projection. In fact, of 11 injection cases in AAF which produced a prominent pattern of labelling in the MGB typical of AAF injections, only 4 of these cases resulted in above background labelling in the IC.

The labelling, after AAF injections, consisted of single sheets of autoradiographic grains passing rostrocaudally through ICC-dm and ICP in the caudal ipsilateral IC. In contrast to the AI projection, a contralateral ICC-dm sheet of label was not seen.

In two experiments, two injections of tracer were placed at cochleotopically dissimilar positions in AAF. In both cases, this resulted in two laminae of label in the ipsilateral ICC-dm. The laminae were in approximately the same positions in ICC-dm that would have been occupied by label had the injections been placed instead in cochleotopically homologous regions of AI.

Figure 30 indicates the relation of the topography of the AAF corticotectal projection with respect to the topography of the AI projection. In the AI of the left hemisphere an injection of 3H-l-leucine was made at an 8 kHz locus. In the right hemisphere, single injections were made at 2 and between 15 and 20 kHz loci in AAF. The typical AI projection to ICP

Figure 30

An example of the form and systematic topography of the projections of loci in AAF onto the IC. In this experiment, an injection of .25µl of 3H-l-leucine (2.5µC) was made into an 8 kHz locus in the left AI. In the contralateral hemisphere two .2µl injections of a mixture of HRP and 3H-l-leucine (2µC) were made at a 1.7 kHz locus and at a higher frequency locus between 11 and 20 kHz. A) shows surface views of the auditory cortex of the two hemispheres and a darkfield photograph of the AI injection site. B) is a darkfield photograph of the AI projection onto the MGB. C) are drawings of frontal sections through the two IC's. ICC-dm_1 represents labelling resulting from the 1.7 kHz AAF injection, ICC-dm_3 the higher frequency AAF injection, and ICC-dm_2 the 8 kHz AI injection. The darkfield on the right is of the left IC of section 57. The form and systematic topography of the projections of loci in AAF onto the ipsilateral ICC-dm are similar to the projections from AI loci. However, the ARG labelling after AAF injections is always much lighter.

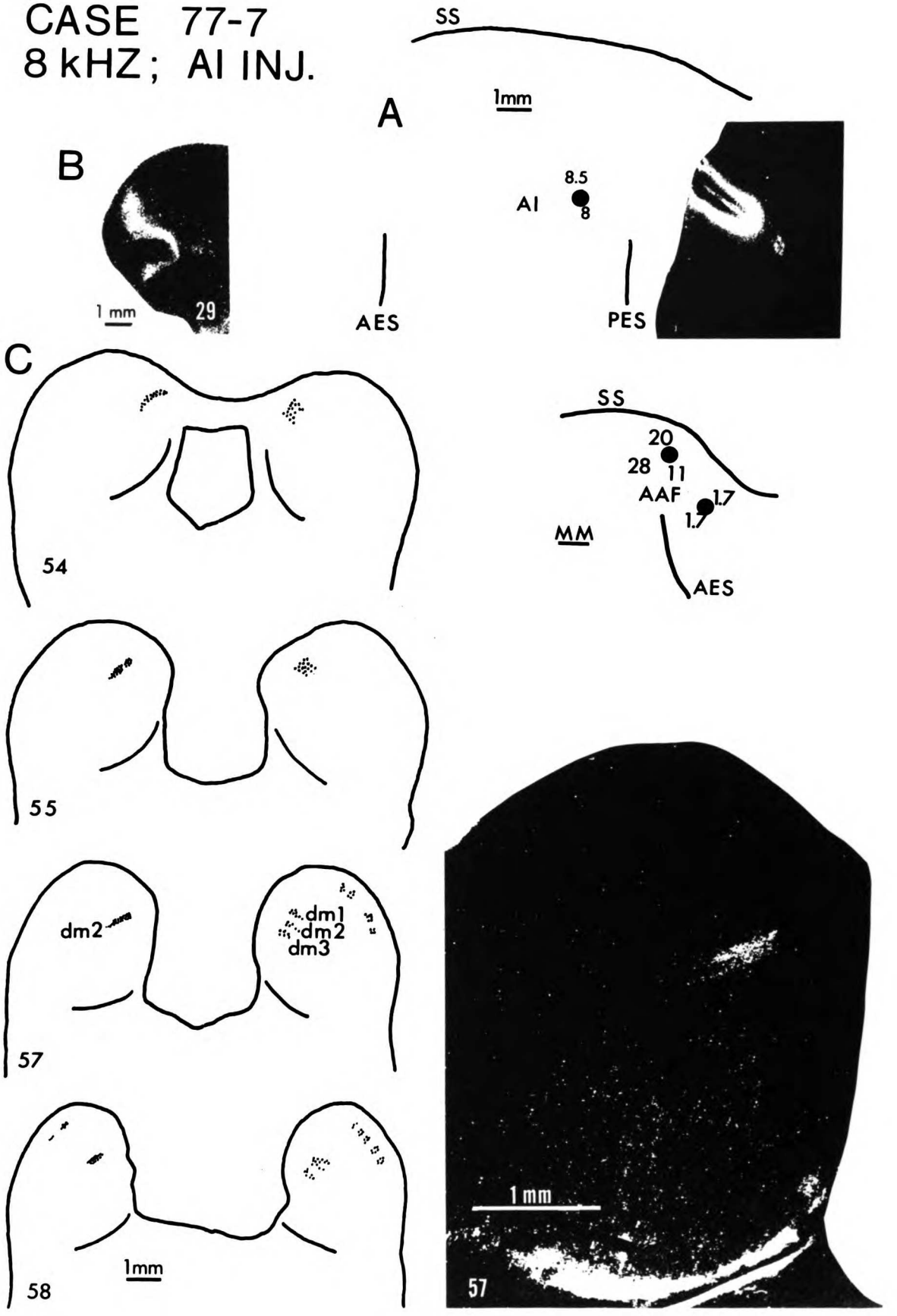
CASE 77-7
8 kHZ; AI INJ.
SS
1mm
A
B
8.5
AI
8
1 mm
29
AES
PES
C
SS
20
28
11
AAF
1.7
1.7
MM
AES
54
55
dm2
dm1
dm2
dm3
57
1mm
58
1 mm
57

and ICC-dm is indicated in the left IC. In the right IC, the lighter contralateral laminar projection to ICC-dm from AI (dm_2), is flanked dorsally and ventrally by two lightly labelled laminae that become apparent in caudal sections. The more dorsal lamina (dm_1) resulted from the injection at the lower frequency representation in AAF and the more ventral lamina (dm_3) resulted from the injection into the higher frequency representation of AAF. There is also a projection to the ICP of the right IC from AAF with dorsal and ventral components (which appeared banded). Thus, the projection of AAF to IC appears to be quite similar in pattern to the AI projection, and in topographic register with respect to the topographic order of the AI projection to the ICC-dm.

No Terminal Projections to the Superior Colliculus from AI, AII or AAF

In 37 experiments, the entire rostral to caudal extent of the superior colliculus (SC) was examined, in serial frontal sections, for autoradiographic labelling after injections of tritiated amino acids into the auditory cortex. In all, 16 experiments involved AI injections, ten involved AII injections and 11 involved AAF injections.

In 36 of these cases, no apparent terminal labelling was seen in SC. In one case labelling was seen in the SC after very large, multiple injections of 3H-l-proline in AI and a long survival period. In this case, there was light labelling in the intermediate and deep layers of SC. In many other long survival cases where large injections of leucine were made into AI, no terminal label in SC was noted. It thus appears that either the projection

from AI to SC is very meager and the tracer technique is not sensitive enough (even after long exposure periods of three to four months) to indicate the projection; or that AI does not project to SC and the one case of labelling seen with proline was due to transsynaptic transport or spread of the tracer in cortex to adjacent fields.

The apparent lack of a projection from AI, AAF or AII onto SC was a surprising result, since auditory responses are commonly recorded in the deeper layers of SC and it is often assumed to be a result of a convergence of visual and auditory corticotectal projections. However, some other auditory cortical fields, not investigated in these experiments, may project onto SC.

Conclusions

1) The major finding of these experiments is that the corticotectal projection from AI onto the dorsomedial division of the ICC (described by others) follows a precise topographic organization as a function of the best frequency site of injection and with respect to the cochleotopic organization of the ICC. This investigation also demonstrated that the pericentral nucleus receives a topographically organized projection from AI. There is an apparent topographic low frequency reversal between the ICC-dm and ICP projections at their mutual border with the projection from the lowest frequency representational site in AI ending in both nuclei along this border.

2) These experiments provide further evidence that the presumably morphologically nonlaminated dorsomedial division is functionally continuous

with the morphologically laminated ventrolateral division with respect to the isofrequency contours of the ICC. This is suggested by the orientation of the laminar projection to ICC-dm and the topographic organization of the projection with respect to the cochleotopic organization of AI and the ICC.

3) Single injections in AI, AAF, and AII produce labelling that is geometrically in the form of continuous sheets in the IC.

4) These experiments indicate that AI and AII have a common ipsilateral-only projections to the lateral aspect of ICP, and different bilateral projections to ICC-dm and ICPm, respectively. The projections of AI and AAF to the IC were very similar, although the AAF projection was far weaker, and no contralateral ICC-dm projection was evident.

5) Although all three fields project to the IC, the projection from AI gauged in terms of ARG methodology, was by far the heaviest.

6) Injections in apical (low frequency) regions of the cochleotopic representation in AI produce longer laminae in ICC-dm than injections in more basal regions.

DISCUSSION

Discussion

Relations to previous studies -- thalamocortical and corticothalamic connectivity

Previous studies of the connections of auditory cortex with the thalamus were largely concerned with identifying the specific nuclei of the MGB that were connected with specific auditory cortical fields. Within this context, there is a wide variability in the reported patterns of connections of the various fields with the MGB. These studies were hampered by three major problems: 1) There was no method employed for the identification of the cortical field whose connections were presumably being studied. In previous studies, the sulcul patterns on the cat cortex and the evoked potential maps of Woolsey '60 were used to determine the position of the cortical fields. This is an imprecise approach, since the position of cortical fields in relation to the sulcal patterns varies from animal to animal (Merzenich et al., '75, '77). Also, the AI designated by Woolsey '60 is an overestimation of the actual size of AI (Merzenich et al., '77) and includes a major portion of AAF (Knight '77). Ep probably contains two auditory cortical fields and a major part of the suprasylvian fringe is actually the lower frequency representational region of AAF. Thus, although most of the cortical lesions or injections of tracer probably included a portion of the cortical field of study, they also appeared to have included other cortical fields as well. 2) In cases where lesions were made in the various nuclei of the MGB, the lesions probably involved fibers of passage from the other nuclei as well as damage to the nuclei that were traversed by the lesion probe to reach the lesion site. Thus,

for example, lesions anywhere in the MGB produced large areas of degeneration across many cortical fields with little regional, fine detail (Wilson and Cragg '69; Niimi and Naito '74). 3) Different investigators used different parcellations of the MGB. Although most investigators used parcellations according to Rioch '29 or Morest '64, or mixtures of the two parcellations, there are extensive variations in the areas of designation between studies.

The present study has enabled a much more precise definition of the connections of several cortical fields with specific nuclei in the MGB. This was made possible by circumventing the problems inherent in the previous investigations. 1) The position and boundaries of each cortical field was determined prior to the injection of tracers using the microelectrode recording techniques. This ensured that the tracer spread was always entirely limited to single, identified cortical fields. 2) Since injections of tracers were made only in the cortex (and since tritiated amino acids are not picked up and transported by damaged fibers) this eliminated the problems of fibers of passage inherent in MGB (and possibly cortical) lesion studies. 3) Once these ambiguities were resolved, it became apparent that the connectional patterns strictly conformed to the parcellations of the MGB made by Cajal '55 and later elaborated by Morest '64. Furthermore, partial filling of the proximal dendrites of HRP labelled neurons in the MGB added more morphological data to the Nissl counterstaining data and facilitated the definition of the target nuclei.

Therefore, the use of the microelectrode recording technique as an anatomical control and the use of the newer anterograde and retrograde tracing techniques, has provided an exact knowledge of the nuclei of the MGB that are connected to specific auditory cortical fields. In the following section, the previous studies are briefly reviewed in relation to these findings.

The methodological approach adapted in this study enlarged the scope of the investigation beyond that of most previous studies. The electrophysiological mapping provided information on the position of the injections re the functional architecture of the cortical fields. This enabled the determination of the topography of the connections. In all experiments, the projections were analyzed from serial sections enabling a three dimensional reconstruction of the form of the connectional terminal and cell arrays. The two tracer/two field protocol provided an exact comparison of the connections of different cortical fields with no ambiguity about differences or similarities in the projecting regions. All these findings will be covered in later sections of the discussion.

AI

This study demonstrated that AI gives and receives highly ordered projections from the Dd, Vl, Vo and M subdivisions of the MGB. The heaviest projections (both thalamocortical and corticothalamic) are those reciprocally connecting Vl and AI. The projections to and from the ventral division to a locus in AI are, three dimensionally, in the form of a sheet passing rostrocaudally through Vl and Vo, and a column passing rostrocaudally through

Dd and M (Fig. 31,B). A complex reciprocal pattern of connectivity was also noted between POl and AI. Since the arrays of HRP labelled neurons or ARG labelled terminals are always continuous through POl and Dd it is quite likely that POl is a part of the MGB (see later section on POl).

The connections between AI and the thalamus of cat have previously been studied using the techniques of Marchi degeneration (Woollward and Harpman '39, Ades '41), retrograde degeneration (Mettler '32, Rose and Woolsey '49, Neff et al., '56, Diamond and Neff '57, Rose and Woolsey '58, Diamond et al., '58, Locke '61, and Jones and Powell '71), anterograde degeneration (after lesions in the MGB-Wilson and Cragg '69, Sousa Pinto '73, Niimi and Naito '74; after lesions in AI - Rasmussen '64, Kasama et al., '66, Diamond et al., '69, Van Noort '69, Jones and Powell '71, Pontes et al., '75), retrograde (HRP) tracing (Winer et al., '77, Merzenich and Colwell '79) and anterograde (ARG) tracing (Pontes et al., '75, Colwell and Merzenich '79). Retrograde degeneration was quite extensive in the rostral half of MGp after AI lesions but little or no degeneration was noted in MGm (Rose and Woolsey '49, '58, Neff et al., 56, Diamond and Neff '57, Diamond et al., '58, Locke '61). Lesions to MGp and particularily V1 produced anterograde degeneration in large regions of auditory cortex (Wilson and Cragg '69, Niimi and Naito '74); however, the degeneration in cortex always appeared heaviest in the region of AI (Sousa Pinto '73, Niimi and Naito '74). These results are probably a reflection of the strong thalamocortical projection of V1 to AI.

Figure 31

A schematic representation of the connections between the IC, MGB and AI. A) indicates that a locus in the ICC diverges to M, Dd and Vl. A cochleotopically homotypic locus in AI has the same overlapping pattern of connections, both corticothalamic and thalamocortical, with the MGB. AI also projects to the dorsomedial aspect of the ICC along a presumably cochleotopically homotypic isofrequency contour subtending the ICC and a presumably cochleotopically homotypic isofrequency contour in ICP. B) represents the three dimensional form of the projection of a locus in AI onto the MGB and IC. The projection onto the MGB is in the form of a column of terminals extending through Dd and M and a sheet of terminals extending through the ventral division. This sheet is folded caudally and includes Vl, Vt and Vo. The pattern of the labelled terminals is the same as the pattern of neurons in the MGB that project onto the same cortical locus. The projection onto the IC is in the form of sheets of terminals in ICC-dm (ICC) and ICP. The projection to ICC-dm is bilateral but was observed only ipsilaterally to ICP. There is a question as to whether there are terminal endings in the ipsilateral ICX although labelled fibers were seen in the nucleus. C) shows the very gross pattern of connections between the IC, MGB and AI. The MGB receives bilateral projections from the IC and is reciprocally connected to the ipsilateral AI. AI projects bilaterally to the IC and is thus indirectly, reciprocally connected to AI through connections with the MGB.

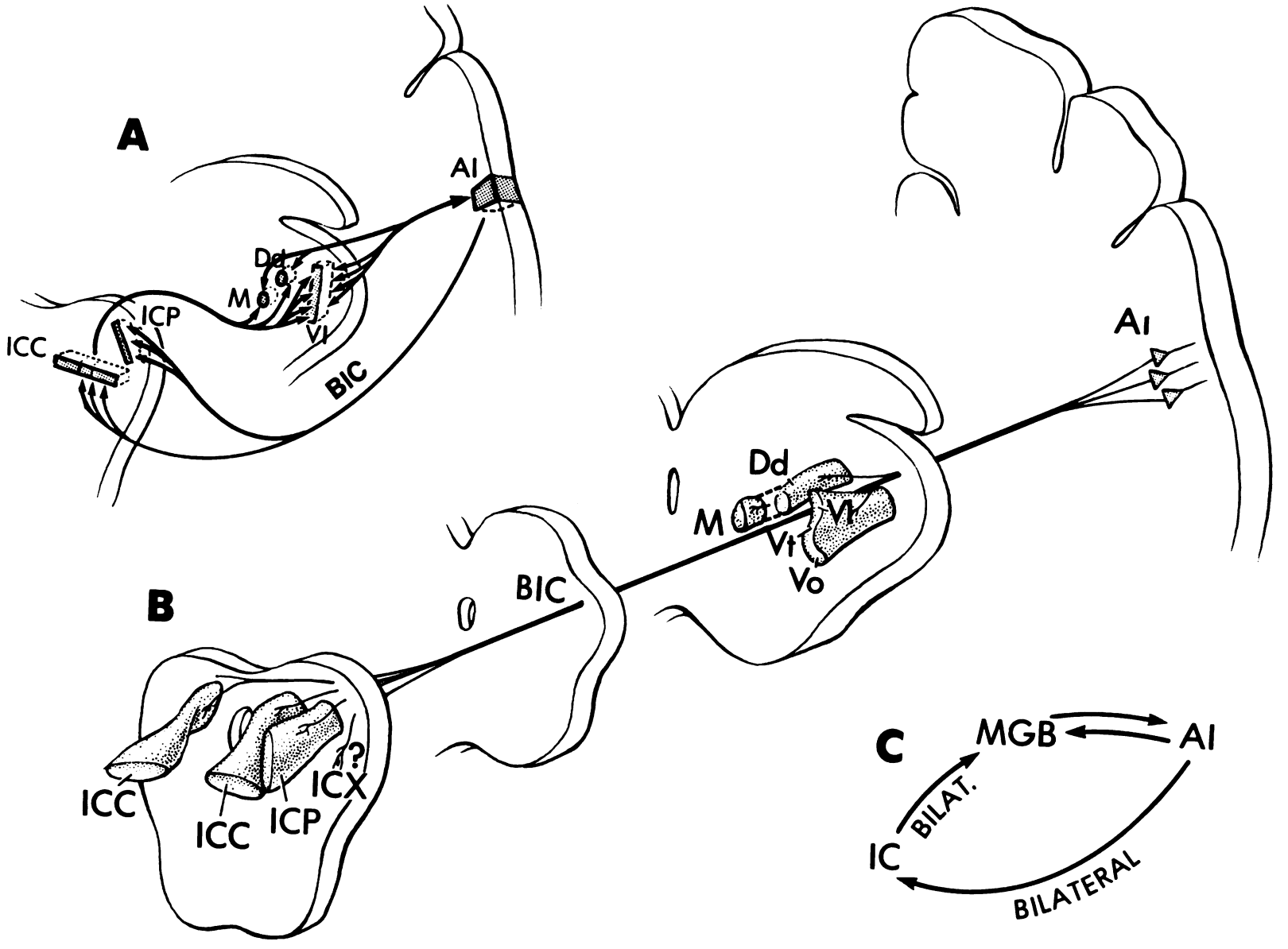
A
AI
Dd
M
ICP
ICC
Vl
BIC
B
BIC
Dd
M
Vt
Vo
AI
ICC
ICC
ICP
ICX
?
C
MGB
AI
BILAT.
IC
BILATERAL

After lesions in AI, anterograde degeneration was recorded in MGp (Kasama et al., '66, Van Noort '69), MGm and PO1 (Jones and Powell '71). Diamond et al., '69 and Pontes et al., '75 noted degeneration in V1, Vo, Dd and the "magnocellular" division (which probably includes the medial division). Tritiated amino acid injections into AI produced labelling in these same subdivisions of the MGB (Pontes et al., '75). HRP injections in AI produced labelled cells in the ventral, dorsal, and medial divisions of MGB and in the anterior and medial parts of the posterior group (Winer et al., '77). Thus, the corticothalamic patterns of projection recorded by Diamond et al., '69 and Pontes et al., '75 are consistent with the corticothalamic projection reported here and the thalamocortical pattern reported by Winer et al., '77 is in part similar to the present findings.

A more extensive study has recently been made of the thalamocortical and corticothalamic connections of AI using the anterograde and retrograde tracing techniques (Colwell and Merzenich '79, Merzenich et al., '79). These investigators also used the microelectrode recording technique as an anatomical control (as we did in the present study). The present results are consistent with those of Colwell and Merzenich '79 and Merzenich et al., '79. Only a few additions will be mentioned: 1) Often the array of label (whether autoradiographic silver grains or HRP filled neurons) in Dd and M appeared as a continuous column that extended through both nuclei. This was particularly true with injections into the higher frequency representations in AI. Colwell and Merzenich '79 reported that the labelling in the two nuclei always appeared separated. 2) The laminar

projection to and from the ventral division was rostrally in the form of a single lamina in Vl. In approximately the middle of the MGB it was divided into two laminae: a dorsal one located in Vl and a ventral one located in Vo. Further caudally these two laminae joined to form a single folded sheet. Since the laminar projection was continuous rostrocaudally through these transitions, the division of Vl into Vl and Vo produced a hole in the otherwise continuous sheetlike projection. 3) ARG or HRP label in Vt is present rostral to the division of Vl into Vl and Vo. In small injection cases, the label in Vt appears as a column, oriented rostrocaudally. Caudally, this column is incorporated in the most medial aspect of the folded sheet projection in the caudal part of the ventral division. 4) HRP labelled cells in Vo and Vt are of similar morphology. This similarity of cell types probably indicated that Vt is the dorsal aspect of pars ovoidea and may correspond to the "transitional" zone of Morest '65. The cells in Vo and Vt are of mixed sizes and shapes, consistent with the observations of Cajal '55. They appear to be of different morphology from the cells in Vl with many labelled cells in Vo and Vt being larger than those of Vl. However, the apparent differences in the appearance of the cells in pars ovoidea from the cells in pars lateralis could result from the different (laminar) orientations of the cell bodies and their processes in the two nuclei (Morest '65).

AII

AII gives and receives projections to and from the Dc, VL and M subdivisions of the MGB. The projections to and from Dc are the strongest

followed by VL. The connections with Dc show regional variations, as indicated by the anterograde and retrograde tracers being concentrated into subgroups within the nucleus.

Lesions in AII produced little or no retrograde degeneration in the MGB (Rose and Woolsey '49, Diamond et al., '58). Anterograde degeneration studies indicate that AII projects to the caudal pole (Dc) of the MGB (Pontes et al., '75), as well as other components of the dorsal division. Diamond et al., '69 reported that AII lesions produced the same pattern of anterograde degeneration as AI lesions; however, their lesions probably encroached on AI or one of the other cochleotopically organized cortical fields. Lesions of the caudal pole (Dc) of the MGB produced anterograde degeneration in AII (Sousa Pinto '73, Niimi and Naito '74). HRP injections in AII produced labelled cells in the "caudal", dorsal and magnocellular divisions (Winer et al., '77). TAA injections in AII produced ARG label in the caudal pole of the MGB (Dc), Vl, "magnocellular part", Ds and Dd (Pontes et al., '75). Thus, many of these studies are in agreement that AII gives and receives projections from the caudal pole of the MGB. These observations probably correspond to the reciprocal connections of AII with Dc of the present findings. The reports of thalamocortical (Winer et al., '77) and corticothalamic (Pontes et al., '75) connections with the "magnocellular" region probably corresponds to the reciprocal connections with the medial division. There is only one report of a thalamocortical projection from VL. Other reported connections probably reflect involvement of other cortical fields.

AAF

The connections of AAF with the auditory thalamus are somewhat similar to the AI connections. AAF is reciprocally connected with both POl and MGB. The reciprocal connections with the MGB are limited to the Dd, Vl, Vo and M subdivisions. However, the connections of AAF differ from AI in that the projections to and from Dd are the strongest. The connections with Vl (which were the strongest for AI) are very weak for AAF. Moreover, the thalamocortically projecting arrays of neurons in Vl are much more discontinuous in pattern after AAF HRP injections than after AI injections, and often tend to be grouped within a single restricted column in Vl.

Since AAF has only recently been discovered (Merzenich et al., '75, Knight '77), no previous connectional studies have been conducted in this cortical field. However, the connectivity of the dorsal aspect of the anterior ectosylvian gyrus, in the approximate region of the location of AAF, has been examined in some previous studies.

Rose and Woolsey '58 found that PO was preserved after cortical ablations that included most of the auditory cortex. However, when the ablation was extended to SII, and included the region of AAF as well, the anterior region of the posterior group (POl) degenerated. Waller recorded retrograde degeneration in the rostral aspect of the small celled region (principle division, probably Vl) of MGB after a lesion restricted to the dorsal part of the anterior ectosylvian gyrus (probably AAF). A lesion in the region of AAF produced scanty anterograde degeneration in the magno-

cellular division (Pontes et al., '75). Lesions to the MGB produce anterograde degeneration undoubtedly extending across AAF (Wilson and Cragg '69). Lesions restricted to MGp (probably Vl) also produced degeneration in AAF (Niimi and Naito '74) that was less pronounced than that recorded in AI. Thus, taken together, these earlier data indicated that AAF probably received projections from POl, was reciprocally connected to Vl and projected onto the medial division. These data, in terms of MGB subdivisions, confirm portions of the results of the present study of the connections of the AAF.

Corticogeniculate Fiber Path

The corticogeniculate fibers pass from the injection site into the internal capsule. They pass ventral to the LGN and through the reticular nucleus of thalamus to enter the auditory dorsal thalamus. These observations are in general agreement with those of Diamond et al., '69.

However, this pathway appears to be different from the one reported after MGB lesions using the Marchi degeneration (Woollard and Harpman '39) and anterograde (Sousa Pinto '73) degeneration techniques. These authors reported that the thalamocortical fibers traverse the putamen or pass around it. The fibers also pass dorsal, caudal or posterior to the claustrum, but not through it, to reach the auditory cortex. These reports raise the possibility that the geniculocortical pathway lies ventral and lateral to the corticogeniculate pathway. This result is interesting considering the general spatial coincidence, in the MGB of the arrays of

cells that project into a locus in the cortex and the terminal fields that are received from the same cortical locus (see the section on "descending control").

Corticotectal projections -- relations to previous studies

The corticotectal projections from AI loci terminate in the IC in the form of distinct sheets of terminals in the dorsomedial division of the central nucleus and in the pericentral nucleus. There may also be a projection to the external nucleus; however, unequivocal terminal field labelling is not apparent in this region. Only the projection to ICC-dm is bilateral and it is less intense on the contralateral side(Fig. 31B). Injections into AII produced a sheet of label in the lateral region of ICP and a second thin sheet of label in the medial aspect of ICP. Whereas the lateral label was definitely of the appearance equated with terminal fields, the medial labelling may be of fibers passing to the posterior surface of the ICP. There is no projection to the central nucleus from AII. Again, a projection to the external nucleus is uncertain. Only the labelling in the medial aspect of the ICP was bilateral. Injections into AAF rarely produced labelling in the IC. When labelling did occur it was of the same basic pattern as seen after AI injections, although much lighter. It is possible that this labelling is a result of trans-synaptic transport from the ipsilateral AI since it has been shown that AAF projects in a restricted fashion to cochleotopically homotypic locations in AI (Imig and Reale '77). In any case, the projection from AI to the inferior colliculus appears to be the strongest of the corticotectal projections studied in terms of the methodology that was used.

The corticotectal projection has been studied previously in the cat by recording anterograde degeneration following large lesions in the auditory cortex (Massopust and Ordy '62, Rasmussen '64, Kasuma et al., '66, Diamond et al., '69, Van Noort '69, Rockel and Jones '73, Cooper and Young '76). Generally, these lesions included several auditory fields. However, the pattern of projection that was consistently reported was similar to the composite of the patterns of AI (or AAF) and AII projections reported here. The corticotectal projection was reported to be bilateral (Rasmussen '64, Kasuma et al., '66, Diamond et al., '69, Rockel and Jones '73, Cooper and Young '76). Ipsilaterally, degeneration was noted in regions that correspond to the ICP, ICC-dm and ICX (Massopust and Ordy '62, Kasuma et al., '66, Van Noort '69, Diamond et al., '69, Rockel and Jones '73, Cooper and Young '76). However, there is some question as to the certainty of the degeneration in ICX being of terminal fields (Diamond et al., '69). A projection to the contralateral ICC-dm was also reported and noted to be less intense than the ipsilateral projection (Rockel and Jones '73).

More restricted lesions were also made in some of these studies. Small lesions, presumably within AI, produced bilateral degeneration in the ICC-dm that was quite restricted (Rockel and Jones '73). Diamond et al., '69 reported that AI lesions produced sheetlike degeneration in the ICC-dm with the fibers oriented in rows coursing dorsomedially to ventrolaterally. Lesions to the insular-temporal region produced a pattern of degeneration in the IC similar to the AII pattern of projection seen in the present study. Thus, in terms of the subdivisions of the ICC which

receive projections from the auditory cortex, the data reported here is consistent with previous, but less specific, degeneration studies.

Fiber path from the auditory cortex to the IC

In these experiments, after AI or AII injections and long survival periods, the same basic pattern of fiber projection was observed. Labelled fibers were traced from the BIC within the MGB, through the ipsilateral BIC, to the inferior colliculus. At the level of the rostral IC, fibers passed through the ICP dorsal to the ICC and entered the collicular commisure. These fibers ended in terminal fields in the contralateral colliculus more caudally. Other medially directed fibers entered either the ipsilateral ICC-dm (after AI injections) or the medial aspect of the ipsilateral ICP (after AII injections) and ended caudally in terminal fields. Still other fibers maintained a lateral orientation and ended in terminal fields in the lateral aspect of the ipsilateral ICP. Other laterally located fibers entered the ICX but appeared to remain within the BIC in this region and terminate caudally along the posterior surface of ICP. Apparent terminal label was noted in the nucleus of the brachium and in the aspect of the ICX which borders the ICC rostrally (some of this label probably also extends rostral to the ICX into the midbrain tegmentum).

This course of the corticotectal fibers was described in anterograde degeneration experiments following (usually large) lesions in the auditory cortex (Diamond et al., '69, Rockel and Jones '73, Kasuma et al., '66). Of particular interest is the fact that AI or AII TAA injections (of this study) or the large cortical lesions (of previous studies) which involve several

auditory cortical fields, all produce the same pattern of fiber disposition. This indicates that probably most (if not all) auditory corticotectally projecting cortical fields send fibers along the same pathways and that they differ only in the patterns of their terminal arrays in the IC.

Also of interest is the fact that the corticotectal fibers appear to reach the inferior colliculus by passing through the MGB. Ades '41, using the Marchi method, made lesions of the MGB and noted degenerating fibers entering the IC. Van Noort '69 also made lesions of the MGB and reported anterograde degeneration in the IC that was of the same pattern as resulted from cortical lesions. From his evidence, Van Noort '69 proposed a geniculotectal projection. However, the lesions in these studies probably interrupted corticotectal fibers passing through the MGB. Recent experiments in which HRP was injected into the ICC (and in some cases the ICP) did not produce HRP labelled cells in the MGB, although lower brainstem auditory nuclei projecting to the IC were always labelled (Andersen et al., '79). This suggests that there is not a geniculotectal projection, since many of these injections were in the regions of degeneration noted by Van Noort after MGB lesions.

Each cortical field has a unique pattern of connections with the MGB and IC

The two tracer/two field protocol revealed that AI and AII have connections with the MGB which are largely segregated. AI and AAF differ considerably in the details of their connectivity with the ventral division. The connections of AI and AII with the IC are also different with AI

projecting onto the ICC and lateral ICP, and AII projecting onto the lateral and medial aspects of the ICP. Although AI and AII overlap in their projection onto the lateral aspect of ICP, the AII projection appears to be more divergent. The ARG labelling in the IC after AI and AAF injections differed in terms of their relative strengths with AI being much stronger.

Each cortical field is connected to several nuclei in the thalamus and the IC

In previous studies, the arguement has been that either each auditory cortical field is connected to several subdivisions of the MGB (Diamond et al., '69, Winer et al., '77) or that each cortical field is connected to only one thalamic subdivision (Sousa Pinto '73, Pontes et al., '75). In these experiments, electrophysiological mapping prior to the injection of tracers insured that the tracers did not difuse into adjacent cortical fields. Thus it is certain that AI, AII and AAF each receive projections from and project to several subdivisions of the MGB. Also, the same subdivisions converge onto any small cortical locus in these three fields. This convergence must have important implications in the processing of auditory information. Likewise, very small loci in any of these cortical fields diverge onto the several subdivisions of the thalamus from which they receive their projections. (As will be covered in another section, as the cortical injections into AI or AAF become smaller, certain details in the pattern of the projection become more apparent in Vl. However, the projections to and from every subdivision always remain, even with extremely small injections.)

Although every field receives projections from several subdivisions of the MGB, each studied cortical field also had a single different subdivision to which it is most strongly connected. Thus, AI is most strongly interconnected (thalamocortically and corticothalamically) to Vl, AAF to Dd, and AII to Dc. It is possible that each strongly connected subdivision shares some common functional feature (e.g., is excitatory) that is different from the several other, less strongly connected subdivisions (e.g., are inhibitory).

AI, AII and AAF are parallel processors

Each of the cortical fields studied have strong and direct connections with the MGB. The electrophysiological recordings in these fields indicate that they are activated by auditory stimuli with approximately the same latencies. These two lines of evidence demonstrate that AI, AII and AAF are processing auditory information in parallel as it arises along the auditory neuroaxis.

AI has been considered, by some investigators, as the "primary" auditory field and AII and other surrounding auditory cortical areas "association" fields. Earlier speculations about cortical structure and function proposed that the primary auditory cortical fields received direct projections from the thalamus and the "association" fields relied on the "primary" field for their activation (Ades '43, Bremer '53). However, Rose and Woolsey ('49, '58) demonstrated that many auditory cortical fields received direct projections from the MGB. Experiments in which AI has been

ablated bilaterally (Downman et al., '60), or where AII has been isolated surgically (Kiang '55) directly demonstrated that AII does not require AI for activation. Similar experiments in the visual system (Sperry '55) and somatosensory motor system (Lashley '50) have also shown that the corticocortical "association" connections are not as essential as previously imagined for cortical function outside the "primary" areas. However, the ipsilateral AAF and AI are strongly, reciprocally connected corticocortically (Imig and Reale '77, Andersen '78). AII is also strongly, reciprocally interconnected with several auditory cortical fields (Andersen '78). There are also reciprocal collosal connections between the two AIs, the AIIs, the AAFs, AI and AAF, and AAF and AI (Imig and Reale, '77; Andersen '78). Thus, although these three fields receive unique and direct mixtures of auditory information from the thalamus, they are not independent, in that activity in one cortical field would presumably influence the activity in others via corticocortical interconnections.

Finally, it is of interest that the descending connections are also arranged in parallel. Thus the corticothalamic projections end only on the regions of thalamus that are projecting to that cortical field. Also, the patterns of projection of AI and AII onto the IC are different. The descending corticotectal projection of an auditory cortical field may be controlling only the regions in the IC that will project, via the thalamus, onto that cortical field.

Essential and sustaining projections

To explain the results of their retrograde lesion studies, Rose and

Woolsey ('49, '58) proposed the concepts of "essential" and "sustaining" thalamocortical projections. An "essential" projection from a thalamic nucleus to cortex existed if destruction of one cortical field produced marked degeneration in the nucleus. A "sustaining" projection was present if destruction of either of two (or more) cortical areas produced little or no degeneration in a thalamic nucleus; while destruction of both (or all) areas together produced marked degeneration. There are several possible explanations for the sustaining projection results. Rose and Woolsey ('58) favored the idea that cells of several thalamic nuclei send collateral axons to more than one auditory field and that any set of these collaterals can maintain the integrity of the cells. Another is that a thalamic cell emits a collateral to an adjacent thalamic nucleus that was an essential projection for one of the fields. Thus a thalamic cell can be sustained by the thalamic cells of another nucleus even after its thalamocortical axon has been destroyed but will degenerate if the sustaining thalamic nucleus degenerates (Rose and Woolsey '58). There are several other possibilities, two of which will be presented after the examination of the results presented here with those of the earlier lesion work. This comparison will indicate that, whatever the actual nature of the sustaining scheme may be, it must involve the divergence of projections from the thalamic nucleus to all the cortical fields that "sustain" the projection.

After lesions of AI alone, the anterior aspect of the principle division, in the region of the ventral division, completely degenerated

(Rose and Woolsey '49, 58, Diamond et al., '58). This is consistent with the present results, which demonstrate that a major target of projection of the laminated aspect of the ventral division (Vo and Vl) is AI (see Figure 32A). Destruction of AI coupled with lesions to Ep (and AII) produced even greater degeneration in the anterior aspect of MGp (the ventral division) (Rose and Woolsey '49, '58, Diamond et al., '58). In one case presented here, injections of tracers in a cochleotopically organized field (possibly the ventral posterior auditory field - VPAF) near the AII, Ep border of Woolsey '60 produced a sparse HRP labelled cell array in the laminated ventral division. FitzPatrick et al., '77 have examined the thalamocortical connections of the posterior auditory field (PAF), which is a cochleotopically organized field in Ep. They found it to be connected to the ventral division. AAF also receives a sparse projection from the ventral division and was included in the anterior part of the AII cortex in the older parcellations of the cortex (Woolsey and Walzl '42). Thus, although Vl and Vo project primarily to AI, they also project to several cortical fields near AI. Thus, expanding the lesions to include these fields would, predictably, increase degeneration in Vl and Vo (see Fig. 32A).

Lesions to AAF (which included SII) or AI alone produced only spotty degeneration in the "anterior" posterior group (POl). (The "anterior" aspect of the posterior group of Rose and Woolsey ('58) may include the anterior aspect of Dd in the present study (see Figure 32E)).

Figure 32

The reciprocal connections of the various subdivisions of auditory thalamus with several cortical fields as elucidated by this study, Diamond et al. '58, Diamond et al. '69 and FitzPatrick et al. '77.

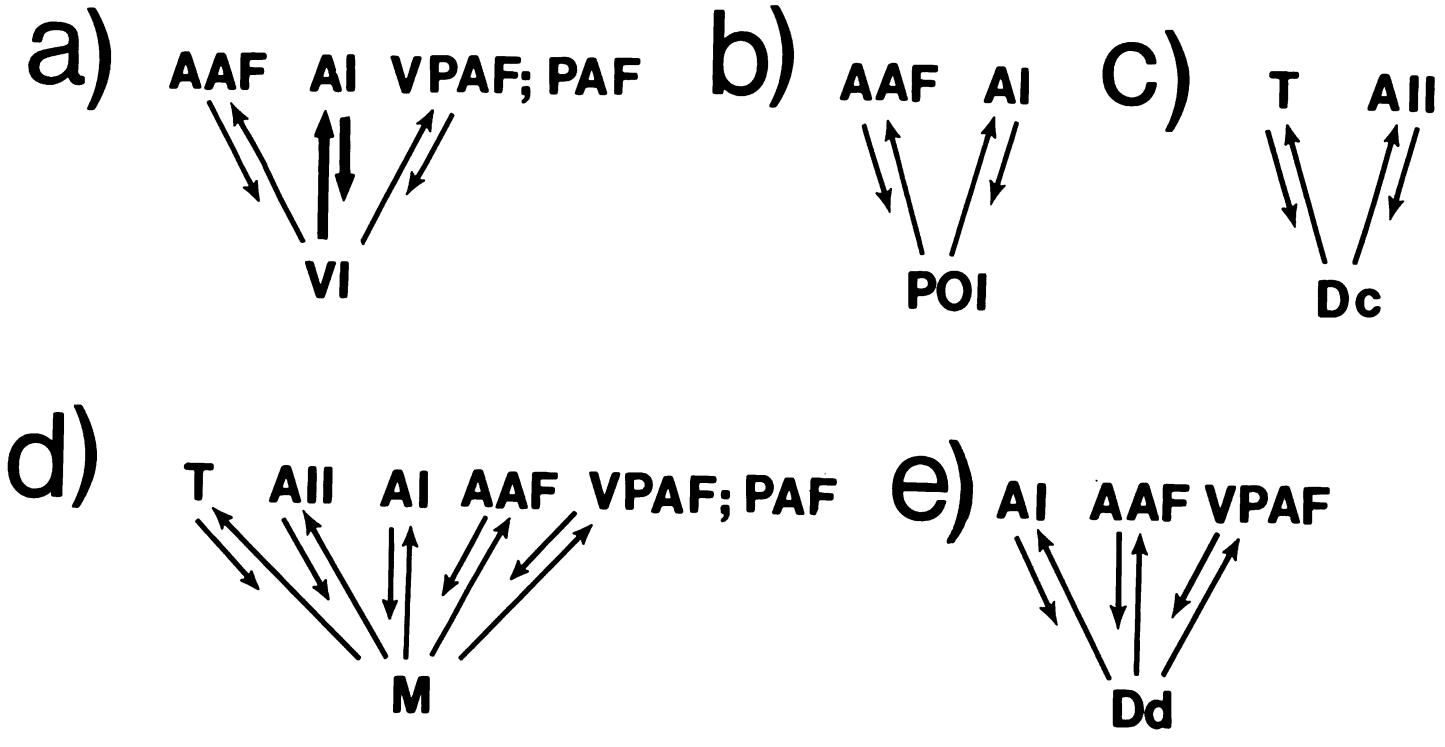
a)
AAF
AI
VPAF; PAF
VI
b)
AAF
AI
POI
c)
T
AII
Dc
d)
T
AII
AI
AAF
VPAF; PAF
M
e)
AI
AAF
VPAF
Dd

However, when the lesion included both AAF (including SII) and AI, then POl degenerated (Rose and Woolsey '58). The present data indicates that AAF and AI both receive projections from POl (see Figure 32B).

Lesions of AII or the insular-temporal (I-T) region alone produced partial degeneration in the caudal aspect of MGp (Dc) (Diamond et al., '58). When lesions included both these fields, the caudal pole of the MGB completely degenerated (Diamond et al., '58, Rose and Woolsey '58). Thus, AII and IT receive a "sustaining" projection from the caudal MGB (Dc). The present results show that AII is strongly connected to Dc. Other studies have indicated that the temporal cortex (T) is strongly connected to the caudal MGB (Diamond et al., '69, Cranford et al., '76, Winer et al., '77). Thus, Dc also appears to diverge to its two sustaining cortical regions (see Figure 32C).

Finally, MGm did not degenerate unless most of the auditory cortex, including AI, AII, Ep and I-T, was ablated (Rose and Woolsey '58, Diamond et al., '58, Locke '61). The present experiments indicate that every cortical field studied (including AI, AAF, AII and the cochleotopically organized field posterior AI) receives a projection from the medial division. PAF also receives a projection from M (FitzPatrick et al., '77). Other investigators have noted that every studied auditory cortical field appears to be connected to M (Diamond et al., '69, Winer '77). Thus M projects to every auditory field that must be ablated before it will degenerate (see Fig. 32D).

This comparison between the present results of the connections of several auditory fields and the previous lesion results relevant to sustaining and essential projections, verifies that each thalamic nucleus projects to the subset of cortical fields that must be lesioned to produce degeneration. Conversely, the projections of an MGB subdivision appear to be limited to the cortical fields that must be lesioned to produce degeneration. Thus, any explanation of the sustaining phenomenon must take into account the divergence of the thalamocortical projections of an MGB subdivision that includes, and appears to be limited to, the sustaining cortical fields. In this context, the idea of bifurcating collaterals to the sustaining fields is still the most attractive hypothesis. On the other hand, this data suggests that a sustaining collateral to another thalamic nucleus is not. However, collaterals that end on cells of the same thalamic nucleus could also conceivably sustain a projection, within the framework of the present results, since subsets of cells within the nucleus may project to different sustaining fields. Thus a collateral from a neuron projecting to one sustaining field, that has been lesioned, could conceivably be maintained by a cell within that nucleus that projects to the other sustaining field(s). Since the thalamocortical and corticothalamic connections of all the fields studied are reciprocal (this appears to be true of auditory cortical fields and, possibly, of cortical fields in general; see section of "descending control") the overlapping corticothalamic projections might also conceivably account for the sustaining phenomenon (see Figure 32). Thus, for instance, a lesion to AI might destroy the axons of many of the cells in POl, but the corticothalamic

projection from AAF onto these cells would maintain their integrity. Thus only after a lesion to AAF as well (which would destroy this cortico-thalamic projection) would the POl cells degenerate. Of course, all these possibilities are speculative, and the true explanation of "sustaining" projections is still unresolved.

Two systems hypothesis

Although each cortical field examined had overall a unique pattern of connectivity, two basic patterns of connectivity were recorded. One pattern of connectivity is limited mostly to the rostral aspect of the MGB. This pattern is comprised of the morphologically laminated nuclei of the ventral division (Vo and Vl) laterally and Dd and M medially. This general pattern may also include POl. The cortical fields exhibiting this pattern of connectivity include AI, AAF and a cochleotopically organized field posterior to AI (possibly VPAF). This general pattern of connectivity also seems to apply to PAF (FitzPatrick et al., '77). Since all these cortical fields share the common feature of being cochleotopically organized, this pattern of connectivity will be referred to as the "cochleo-topic pattern" or "cochleotopic system".

On the other hand, the AII cortical field gives and receives projections from the predominently more caudal aspects of the MGB. AII is connected to the Dc, VL and M subdivisions of the MGB. The two tracer/ two field experiments demonstrated that the connections of some of the "cochleotopic pattern" fields (AI and AAF) with the MGB and the connections of AII with the MGB are largely segregated with the only overlap occurring

in M. Previous studies indicate that the temporal region of cortex gives and receives projections from the MGB in a similar pattern to the AII connections (Cranford et al., '76, Diamond et al., '58, Winer et al., '77, Diamond et al., '69, Waller '40). (The insular region does not appear to be directly connected to the MGB (Winer et al., '77)). Since AII and T have a rather diffuse pattern of connections with the MGB and since AII and probably T have broadly tuned neurons, this pattern of connections will be referred to as the "diffuse pattern" or "diffuse system".

Thus, there are two general, largely segregated systems of connections between the MGB and auditory cortex. The cortical fields of the "cochleotopic system" include AI, AAF, and probably PAF and VPAF. The cortical fields of the "diffuse system" include AII and the temporal cortex.

Topography of connections of the "cochleotopic" and "diffuse" systems

There is a systematic topography of the connections between the "cochleotopic pattern" cortical fields and the MGB, with respect to the cochleotopic organization of each field. The two tracer/two field experiments showed that the AI and AAF projections to and from all the component MGB nuclei overlaped for connections with cochleotopically homotypic loci in the two fields. Furthermore, these overlapping connections varied in location in the MGB nuclei in the same systematic fashion with respect to the cochleotopic representations in the two

fields. Thus, for example, lower frequency sites of representation in both AI and AAF give and receive projections from more medial and ventral regions of Dd than do the higher frequency representational sites. Although only one experiment was performed to examine the connections of the cochleotopically organized field posterior to AI, this low frequency site injection produced a pattern of anterograde and retrograde label that was typical of low frequency site injections in AI and AAF. Thus, all cortical fields of the "cochleotopic pattern" have a similar topographic (cochleotopic) organization of connections.

Also the geometries of connectivity of the "cochleotopic pattern" fields are in general similar. Thus, for example, single loci in AI or AAF project in the form of a sheet of terminals in the ventral division and a column of terminals in Dd. These geometries of connectivity, in general, appear to reflect the cochleotopic organizations of the component nuclei (and will be covered in more detail in a later section).

On the other hand, a systematic topography of connections similar to that seen in the "cochleotopic system" was not found in the topography of the AII cortical field connections with the MGB. The connections appeared more complicated and divergent, with, for instance, several regions of Dc being reciprocally connected to single loci in AII. A systematic order of connections for the cortical fields of the "diffuse system", as well as a functional order within these cortical fields, is at present unknown.

Extension of the two systems hypothesis

The segregation of connections into a cochleotopic system and a diffuse system appears to extend beyond the thalamocortical-corticothalamic loop. There is evidence for two ascending systems of connection from the IC to the MGB. The projection of the central nucleus onto the medial geniculate is of the same form and systematic topography (i.e., cochleotopic organization) as the thalamocortical and corticothalamic connections of AI (Andersen et al., '78). The pericentral nucleus, on the other hand, appears to project to Dc and other regions of the MGB that project to AII (unpublished observation).

The segregation into two systems may include the corticotectal projections as well. AI projects onto the ICC whereas AII does not. The topography of the AI projections onto the central nucleus, with respect to the cochelotopic organization in AI, is apparently in register with the cochleotopic organization of the central nucleus of the IC. AII projects to the lateral and medial aspects of the pericentral nucleus. Although the AII corticotectal projection to the lateral aspect of the ICP overlaps with the AI projection to the same region, it appears to be more divergent from single cortical loci than the AI projection. AI does not project to the medial aspect of ICP.

Thus, there appear to be two largely segregated and parallel auditory projection systems connecting the IC, MGB, and auditory cortex. From the ICC, information in the "cochleotopic system" passes to the rostral thalamus, and is reciprocally connected with the "cochleotopic pattern" cortical fields

(e.g., AAF, AI). The topographic organization of connections remains consistent with the recorded cochleotopic organization of the IC, MGB and cortical fields throughout this ascending system. The recurrent cortico-collicular and corticothalamic projections of the "cochleotopic system" cortical fields also maintain a very strict and systematic topographic order, with respect to the cochleotopic organizations of the target nuclei. The cortico-collicular projections of AI may control at least a portion of the input from the central nucleus (dorsomedial division) of the inferior colliculus to the "cochleotopic system" cortical fields.

From the ICP, information in the "diffuse system" passes to caudal regions of the MGB that are exclusively and reciprocally connected to the "diffuse system" cortical fields (e.g., AII and T). The AII cortico-collicular pathway projects back onto the ICP, and thus may control the ascending input to at least part of the "diffuse system" at the collicular level. Since AI projects to the lateral aspect of the ICP, this "cochleotopic system" cortical field may control at least some of the input to the "diffuse system" cortical fields at the level of the inferior colliculus.

The two systems of connections overlap in the medial division of the MGB. There are still other possible links in these two largely segregated systems. Since injections of anterograde tracer in the ICP also spread into the ICC, it is not known whether the ICP projects to the "cochleotopic system" subdivisions of the MGB as well as the "diffuse system" subdivisions

(Andersen et al., '79). It is also not known in what way or to what extent the two systems are segregated below the IC. Most anatomical studies to date suggest that all or nearly all the lower brainstem auditory nuclei project into the central nucleus (see Roth '77, Roth et al., '77, Van Noort '69, Osen '72). The ascending projections to ICP are unknown (Rockel and Jones '73, Harrison and Howe '76).

Functional properties of the two connectional systems

One aspect of the two connectional systems is the similarity in physiological properties of the neurons of the component nuclei within each system. All nuclei and cortical fields in the "cochleotopic system" that have been investigated contain cells with sharp tuning curves. These nuclei include the central nucleus of the inferior colliculus (Roth et al., '78, Roth '77, Rose et al., '63, Merzenich and Reid '74), the pars lateralis and pars ovoidea of the MGB (Aitkin and Webster '72), and the cortical fields AI, AAF, PAF and VPAF (Merzenich et al., '75, Knight '77, Reale and Imig '77, Andersen, Merzenich, Middlebrooks and Patterson unpublished observations). On the other hand, the component nuclei of the "diffuse system" that have been investigated have neurons with broad tuning curves. These include ICP (Rose et al., '63, Merzenich and Reid '74, Aitkin et al., '75), AII (Merzenich et al., '75, Hind '63, and this study) and probably T (this study). One thalamic nucleus (M) projects to cortical fields in both systems. It is interesting to note that M neurons have broad tuning curves (Aitkin '73), while at the same time M appears to be topographically organized.

A second similarity of physiology within the "cochleotopic system" is the strict cochleotopic organization of most of the component nuclei. The ICC and pars lateralis of the MGB as well as the cortical fields AI, AAF, PAF and VPAF have all been demonstrated to be strictly tonotopically organized. This is probably also the case for Dd (Gross et al., '74) and Vo (Aitkin and Webster '72). On the other hand, a cochleotopic organization for the "diffuse system" cortical fields (AII and probably T) was not apparent, although such an organization may be obscured as a consequence of the broad tuning curves of its neurons. A possible exception to this distinction has been recorded in ICP, which is cochleotopically organized yet is probably a major component in the ascending "diffuse pattern" system.

The distinction of two parallel and largely segregated systems of connections between nuclei that contain neurons of sharp tuning characteristics ("cochleotopic system") and nuclei that contain neurons of broad tuning characteristics ("diffuse system"), produced some interesting questions. For instance, what are the sources of ascending input to the ICP and how do they differ from the ascending projections to ICC? The eighth nerve appears to be comprised of a generally uniform population of sharply tuned fibers that differ from one another mainly in the best (critical) frequencies of their tuning curves. This would indicate that the broader tuning of the "diffuse system" neurons is derived from a convergence somewhere in the brainstem of eighth nerve fiber input from different locations along the basilar membrane. Presumably this convergence takes place in the projection of the lower brainstem auditory nuclei, whose neurons are in general sharply tuned, onto the ICP.

It is possible, since there are two receptor classes in the cochlea, that the "cochleotopic system" represents inner hair cell input that is processed separately from outer hair cell -- "diffuse system" input. However, this appears unlikely since this would imply a segregated region in the brainstem below the ICP that contains neurons with broad tuning properties. Such a region has not yet been found.

That there are two connectionally largely segregated systems whose neurons have different response properties indicates that these two systems are functionally different. However, what function each system serves is at present not known. Since the "cochleotopic system" preserves frequency information in an orderly manner, at least the information is present for frequency discrimination and analysis. The broad tuning of the "diffuse system" neurons is a response property that would be predicted for feature detectors of spectrally complex sounds. However, there is at present no data to support either of these speculations.

Whether one or both of these systems is involved in sound localization is also an open question. The recent findings of binaural response segregation in AI (Imig and Adrian '77, Imig and Brugge '78, Middlebrooks et al., '78), and the psychophysical and neurophysiological evidence that binaural intensity and time cues must be in register with respect to the frequency of stimulation at the two ears, suggests that the "cochleotopic system" may be important in processing sound localization information. On the other hand, Knudsen and Konishi '78 have shown in the owl that there are two functionally segregated regions in the homologue to the mammalian

inferior colliculus (MLD). The one region is noncochleotopic and contains a systematic map of the auditory space. The other region is cochleotopically organized and is not space mapped. By analogy, this would suggest that the "diffuse system" may be involved in sound localizing. It is interesting that the space mapped region of the owl contains predominantly neurons that discharged to the onset of the sound stimulus and the tonotopic region predominantly neurons that discharged in a sustained fashion to sound stimulation (Knudsen and Konishi '78). This same segregation in response properties has been noted between the ICP (onset) and the ICC (sustained) in the cat (Merzenich and Reid '74). These observations suggest similarities between the space mapped region of owl and the ICP -- "diffuse system" of the cat and the tonotopic region of the owl and the ICC -- "cochleotopic system" of the cat.

The topography of connections of AI and AAF reflects the cochleotopic organizations of the projecting and target nuclei

There is a systematic variation in the order of connections between AI and AAF and the nuclei of the MGB and IC. The topography of these connections is in every case consistent with the interpretation that loci in these two cortical fields are interconnected with cochleotopically homotypic regions of the MGB and IC. The systematic topography of connections between AI and the MGB observed in this study are consistent with the reports of Colwell and Merzenich '78.

V1 The thalamocortical and corticothalamic connections of AI and AAF with pars lateralis are ordered such that the relatively higher frequency

representational loci in these two fields are connected to relatively more medial aspects of the nucleus. The experiments of Aitkin and Webster '72 and Rose and Woolsey '58 indicate that pars lateralis is cochleotopically organized with the higher frequencies represented more medially. Thus, this topography and the order of the physiological response characteristics of the neurons are consistent with the idea that cochleotopically corresponding regions of pars lateralis and these two cortical fields are interconnected. The thalamocortical and corticothalamic connections of loci from these two fields with pars lateralis are, in general, in the form of sheets of source neurons and sheets of terminals in pars lateralis. These sheets are oriented such that they appear to parallel the described morphological laminations in Vl (Morest '65). The orientation and systematic topography of these connections provide further support for the contention that the laminar structure of Vl is a morphological substrate for the tonotopic organization of Vl (Morest '64, Aitkin and Webster '72).

Dd The dorsolateral aspect of Dd is interconnected with the higher frequency representational regions of AI and AAF, whereas the ventromedial aspect of Dd is interconnected with the lower frequency representational regions. This implied cochleotopic order in Dd is consistent, at least in part, with the recording data of Gross et al., '74 derived in squirrel monkey. The connections of the highest frequency regions of the cortical fields with Vl and Dd appear to share a common border between the two thalamic nuclei. This suggests a high frequency reversal between Vl and Dd.

Such a reversal has been recorded by Gross et al., '74.

M Successively higher frequency representational regions in AI and AAF are reciprocally connected to successively more dorsal and rostral aspects of the medial division. Extensive microelectrode maps of M have not been made to determine its organization. However, a cochleotopic organization is suggested by the data of Aitkin ('73), which indicate that neurons of similar best frequencies in M tend to be grouped together.

Vo The higher frequency representational regions of AI and AAF are connected to relatively more medial and dorsal regions of Vo. There is a close apposition of anterograde or retrograde labelling between Vl and Vo after very low frequency injections in AI and AAF. This suggests that there is a low frequency reversal between these two nuclei. The laminar pattern of thalamocortical and corticothalamic connections in Vo does not conform to the described spiral laminations in Vo (Morest '65). Thus, little can be said at the present time about the possibility of the laminae in Vo being a morphological representation of a tonotopic organization in Vo.

Dc, VL The thalamic nuclei which were exclusively connected to AII (Dc and VL) did not have a readily apparent topographic relationship to that field. This may explain, at least in part, the difficulty in defining a tonotopic organization in AII. In other words, the topography of connections between AII and the MGB may follow rules of organization

which are much more complex than the cochleotopic organizational pattern. The connections of Dc with a locus in AII, although complex, never involved the entire volume of the nucleus. Thus, there is space available for a topography of connections. The form and/or existance of such a topography requires further study.

ICC-dm There is an exquisitely restricted order to the projections from AI onto the ICC-dm. Relatively higher frequency representational loci in AI project as continuous sheets of terminals to relatively more ventral, medial and caudal positions in ICC-dm. ICC-dm does not appear to be a morphologically laminated structure (Rockel and Jones '73). However, the orientation of the sheets of terminal arrays derived from loci in AI are of the proper orientation to be continuous with the described morphological laminations in the ventrolateral division of the ICC.

Also, a comparison was made of the relative dimensions of the systematic topographies of the AI projection with the relative dimensions of the cochleotopic organization of the ICC (taken from the recording data of Merzenich and Reid '74). This compairson showed that the two systematic organizations were proportionally very similar (see Figure 24). This similarity is consistent with the interpretation that loci in AI project in a highly ordered manner to cochleotopically homotypic laminae in ICC-dm.

ICP Relatively higher frequency representational regions of AI project to more ventral, lateral and caudal regions of the lateral aspect of ICP. The topography of this projection, with respect to the cochleotopic

order of AI, is in approximate register with the cochleotopic organization of the ICP (Rose et al., '63, Merzenich and Reid '74, Aitkin et al., '75). It is still surprising that this nucleus, which contains relatively broadly tuned neurons, maintains this very highly ordered connectional topography, especially since other experimental data suggest that the ICP projects to regions of the MGB that are exclusively connected to AII (Andersen et al., '79). The AII connections with the MGB do not appear to have a cochleotopic topography, nor does AII appear to contain an orderly representation of the cochlea.

Thus, the topography of connections between AI or AAF and Vl, Vo, Dd and M and between AI and ICC-dm and ICP are in every case ordered, such that they reflect the cochleotopic organizations of both the projecting nucleus and the target nucleus. In other words, only cochleotopically homotypic regions of cortex (AI and AAF) and these subdivisions of the MGB and IC appear to be interconnected. This systematic topography of connections between component nuclei in the "cochleotopic system", thus all appear to be cochleotopically organized.

The cochleotopic organization of connections between nuclei is probably the major substrate that preserves the sharp tuning and cochleotopic organization of response properties of neurons from the cochlear nuclei to the cortex.

As indicated by this study and Andersen et al., '78, there is a precise, systematic topography of connections between the ICC, MGB and the cortical fields AI and AAF (see Figure 31A). The order of these connections is consistent with the interpretation that only cochleotopically homotypic regions of these three levels of the auditory system are interconnected. Likewise, the projections of the lateral and medial superior olivary nuclei and the cochlear nuclei onto the central nucleus of the inferior colliculus is also systematic and apparently cochleotopically rendered (Roth et al., '78; Roth '77). The projection of eighth nerve fibers onto the cochlear nuclei is also systematic and presumably cochleotopic (Lorente de No '33; Rose '60) and the LSO and MSO derive a systematic input directly or indirectly from the cochlear nuclei (see Harrison and Howe '76).

Thus, this strict maintenance of a cochleotopic segregation of connections can account for the maintenance of sharp tuning and the cochleotopic organization of best frequencies that are properties of the neuron populations in AI and AAF. Thus, for instance, lateral inhibition is not a necessary mechanism for the maintenance of sharp tuning curves or cochleotopic organization in the higher levels of the auditory neuroaxis.

It is interesting that the descending connections of AI (and AAF) also appear to be in register with the cochleotopic

organization of the ascending auditory neuroaxis (see Figure 31A). This is true of both the corticothalamic and corticotectal projections. The reciprocal corticocortical connections of AI with the ipsilateral AAF and contralateral AI and AAF also appear to be cochleotopically ordered (Imig and Reale '77; Andersen '78).

However, not all the connections of AI or AAF with other neural structures appear to be cochleotopically organized. The projections of these cortical fields onto the ipsilateral putamen, although restricted, do not appear to exhibit a cochleotopic topography (Andersen '78). It, of course, would be interesting to know what new arrangements of connections takes place in the transformation from a cochleotopic to a noncochleotopic order.

Considerations of the development of a cochleotopic organization of connections along the auditory neuroaxis

A remarkable feature of the auditory system is the maintenance of orderly (cochleotopic) topographies in such a complex fabric of connections. Thus, at the levels of the IC, MGB and cortex, single auditory nuclei of the "cochleotopic system" project to several other auditory nuclei. Likewise, they receive projections from several of the same and/or different auditory nuclei. Yet, in the face of this remarkable structural complexity, there is a strict maintenance of a presumably cochleotopic order of connectivity throughout each element of this system.

How such an exquisitely ordered system is achieved developmentally is certainly deserving of experimental inquiry.

Divergent-Convergent form of projection

One fascinating feature of these results is the geometric form of the projections. The thalamocortical and corticothalamic projections from and to the ventral division to and from a locus in AI are in the form of sheets of neurons and terminals that pass through Vl and Vo. In other words, a sheet of neurons in the ventral division converge on a small approximately spherical volume in AI. Likewise, this same small spherical volume of cortical tissue projects divergently back onto the projecting cells in the ventral division in the form of a sheet of terminals. These three dimensional forms of connections between a locus in AI and the ventral division are consistent with those reported by Colwell and Merzenich '78. The AAF projection onto the ventral division were, similarily, in the form of divergent sheets of terminals. However, the ventral division (convergent) projects arrays of neurons onto loci in AAF were discontinuous in form and in some experiments approximated a sheet of projecting neurons but in other experiments more closely resembled a column of projecting cells. The divergent locus-to-sheet projection form was also noted in the projections of AI and possibly AAF to ICC-dm; and in the projections of AI, AII and possibly AAF to the ICP.

An interesting feature of these geometries of projection is that they appear, at least in most cases, to be in precise cochleotopic register.

Similar best frequencies are represented along radial slabs in AI and AAF (Merzenich et al., '75; Knight '77) and along sheets in ICC (Merzenich and Reid '74; FitzPatrick '75). Best frequencies also appear, from the examination of recording data of Aitkin and Webster ('72) and Rose and Woolsey ('58), to be represented along sheets in V1. The form and orientation of the sheets of labelled terminals or neurons in V1 and the sheets of labelled terminals in ICC-dm are oriented approximately parallel to the isofrequency contours. Thus, the divergent projections appear to be from a locus to an isofrequency contour of the same best frequency and the convergent projections from a sheet of neurons of approximately the same best frequency onto a locus in cortex of similar best frequency representation. The locus-to-sheet divergence from AI to ICP also appears to be of proper orientation and topography to be in register with the cochleotopic organization of ICP. (Although three dimensional recording maps have not been made in the ICP, it is quite probably that the sheets of terminals also coincide with isofrequency contours within the structure).

A column-to-locus convergence in the projections from Dd-M onto loci in AI of AAF was also noted. There was also a locus-to-column divergence from loci in AI and AAF into columns extending through Dd and M. Similar forms of connections between Dd and loci in AI were noted by Colwell and Merzenich '78. The columnar profiles in Dd-M were topographically organized with respect to the cochleotopic order in AI and the presumed cochelotopic order in Dd-M (Gross et al., '74). Thus, the convergence and divergence to

and from loci in AAF and AI from and to Dd-M appears to be in the form of homotypic isofrequency columns.

When multiple injections were made along an isofrequency slab in AI or AAF, the same general divergent and convergent labelling in the IC and MGB was obtained as with single injections. This indicates that sectors along an isofrequency slab in cortex have similar patterns of connections with the same isofrequency contours and columns in the MGB and IC. A slight qualification to this rule is the thalamocortical and corticothalamic connections of V1 with AI and the corticothalamic connections of AAF. When small injections were made, a periodicity of thalamocortical and corticothalamic labelling was noted in V1. However, even this periodic light and heavy irregularity of the V1 connections was contained within the form of the isofrequency contour.

It has already been proposed that isofrequency contours represent a form of spatial processing (Merzenich et al., '77). The cochlear epithelium is essentially a line, since it is only 4 hair cells wide and thousands of hair cells long. Thus, best frequency positions along this line are represented as points. In the above examples, the best frequency point has been expanded along a column or sheet, adding one or two dimensions of representation. These expansions probably signify some derived form of spatial processing. The convergent and divergent patterns of connections, described above, may constitute the method by which spatial processing is accomplished. Models of neural processing usually assume that processing is

accomplished by microcircuits within a nucleus. Once this processing has been accomplished, the transformed product is relayed to the next nucleus. The microcircuits of the second nucleus then further processes this data. The highly complex convergent and divergent patterns of connection, indicated by these experiments, suggest that connections between nuclei are not simply for relay purposes. In such a model, processing is also accomplished by the divergent and convergent patterns of connections between nuclei. Thus, for example, a locus in AI receives input from a sheet of neurons in the ventral division. The convergence of an activity profile across this sheet onto a restricted locus in cortex may be a method for processing neural data. The ventral division input at a locus in AI is also combined with input derived from a column of neurons passing through Dd and M. Moreover, the convergent projection samples from continuous arrays of neurons which pass through morphologically distinct cell groups. The sheet in the ventral division is continuous through both Vo and Vl and the medially placed column passes through both Dd and M. Thus, the convergence of a lamina in the ventral division (or a column in Dd-M) combines the activity of two morphologically distinct nuclei at the cortical locus.

There are, in some projections, even higher levels of complexity within the geometries of the convergent and divergent patterns described above that further suggest that the pattern of connections between nuclei subserve a spatial processing function. Small injections into cortex indicate that there are periodic densities in the corticothalamic and thalamocortical connections of AI with the caudal aspect of Vl and in the

corticothalamic connections of AAF with the caudal V1. (It will be shown in the next section that these periodicities of light and heavy connectivity may have a role in binaural processing). The thalamocortical connections of V1 with AAF are also very complex and can take the form of a column or can approximate the form of a sheet.

The locus-to-column, locus-to-sheet divergence and column-to-locus convergence has been noted at lower levels along the auditory neuroaxis. Columns of neurons in the LSO and MSO converge onto single loci in the ICC (Roth et al., '78). Loci in the ICC diverge to sheets in the ventral division and columns in M-Dd (Andersen et al., '78). It is remarkable that the form and cochleotopic order of the ICC to MGB projection appear to be identical to the MGB to AI projection. Thus, a locus in the ICC diverges to form a complex pattern of terminals in the MGB. This pattern of terminals delimits the arrays of neurons in the MGB that converge on a cochleotopically homptypic locus in AI. Also, the ICC locus to MGB terminal arrays presumably occupy the same regions of the MGB as the corticothalamic terminals from the cochleotopically homotypic loci in AI.

Thus, the convergent and divergent pattern of connections, with one or two added dimensions for the frequency domain, apparently exists at all levels of the auditory neuroaxis. The locus-to-sheet pattern of connections appears to be unique for the auditory system since the nuclei of the visual and somatosensory systems are connected locus-to-locus or locus-to-column (Merzenich et al., '77).

Possible microstructure of the divergent projections from AI and ICC onto Vl

It is interesting that the ICC to MGB, MGB to AI and AI to MGB connections all overlap spatially in the MGB. An isofrequency contour in the ventral division contains the array of terminals from a homotypic best frequency locus in the ICC, the array of projecting neurons that converge on a homotypic best frequency locus in AI, and the array of corticothalamic terminals originating from a homotypic best frequency locus in AI. Likewise, any Dd-M column contains the collicular-thalamic and corticothalamic terminals and thalamocortical projecting cells of homotypic best frequency loci of ICC and AI. This exact spatial match of the convergence of ICC loci onto the MGB with the convergence of the MGB onto loci in AI and the divergence of AI loci onto the MGB is an important factor to any consideration of the processing that is being achieved by the auditory thalamus.

Some clue to the processing that is being achieved by this spatial match may be discerned from the orientations of the preterminal processes of the ICC to MGB and AI to MGB projections (see Fig. 33).

Within Vl, the tectothalamic fibers sweep laterally and rostrodorsally parallel to the laminar structure of the nucleus (Morest '65). The terminal fields are elongated, restricted to the laminar structure and form dense pericellular nests along the perikaryon and proximal dendrites (Morest '65). Descending cortical efferents enter the anterior pole of the MGB and distribute extensively within the ventral division (Cajal '55). The descending axons run longitudinally along the morpho-

Figure 33

A) The possible path of tectothalamic fibers (dotted lines) and corticothalamic fibers (solid lines) within the MGB. B) The possible orientation of the tectothalamic (t.t.) and corticothalamic fibers (c.t.) with respect to one another in Vl. The labelled fibers are drawn as three groups to correspond to the banding in Vl that often occurs with 3H-l-leucine injections into AI or the ICC. r: rostral; l: lateral.

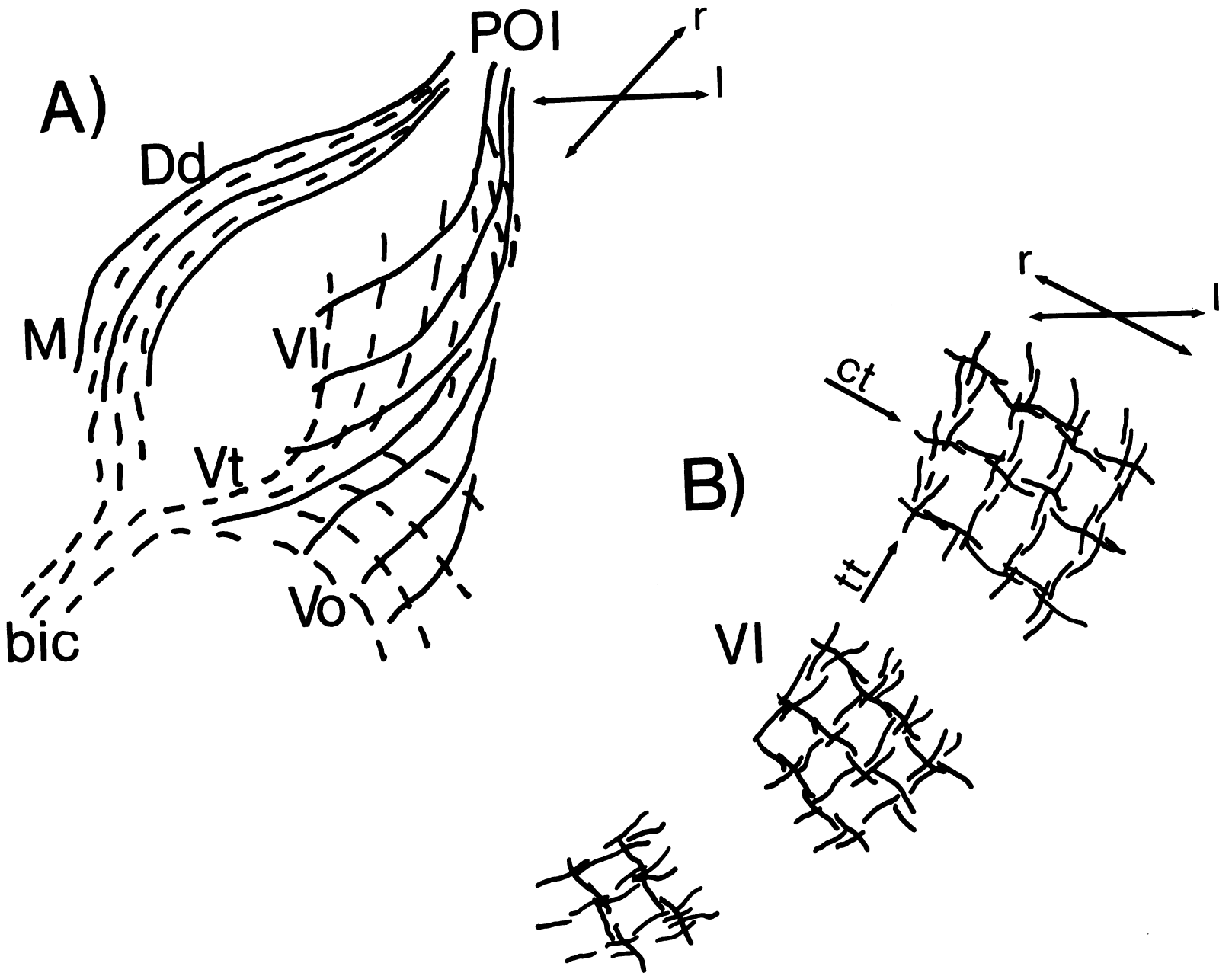
A)
POI
r
l
Dd
M
Vl
Vt
Vo
bic
B)
r
l
ct
tt
Vl

logical laminations in the ventral division, perpendicular to the ascending fibers (Morest '65). They appear to end on more distal segments of the dendrites of the cells in the ventral division (Morest '65). Since ARG labelling, is the present experiments, was not seen in the superior acoustic pathway after AI injections, it is possible that the cortico-geniculate fibers to Vl run through Vl before terminating in the nucleus. Slow flow AII experiments demonstrated that the cortical efferents run in fasicles through the anterior region of the ventral division before distributing terminal fields to the caudal regions of the MGB. Slow flow experiments were not performed in AI, so the path in the MGB of the descending AI to Vl fibers is not known for certain.

The terminal field labelling in Vl after AI injections appeared different than after ICC injections. The cortical efferent ARG labelling was dusty and homogeneous in appearence whereas the tectal efferent labelling was discontinuous in nature. The different appearence of the labelling may be attributed to two factors: 1) the distribution of the terminals on the Vl relay neurons is different with the tectothalamics ending on the perikaryon and proximal dendrites while the corticothalamics end on the distal dendrites (Morest '65); 2) the orientation of the preterminal fibers and fields is different with the tectothalamics oriented more parrallel to the plane of section and the corticothalamics oriented more perpendicular to the plane of section.

After lesions in the IC, degenerating fibers were seen through the

entire extent of the magnocellular division (M-Dd) and extending into POl (Moore and Goldberg '63). Labelling, after AI injections, appeared along rostrocaudal columns in Dd-M but not in the superior acoustic pathway. Thus the ICC to MGB projection may send preterminal fibers caudorostrally through M-Dd whereas the AI to MGB projection may send fibers in the opposite, rostrocaudal direction through the same Dd-M column. Therefore, while the tectothalamic and corticothalamic preterminal fibers in Vl appear to be oriented obliquely (or even normal to one another), in Dd-M they appear to run parrallel to one another but in different directions (see Fig. 33).

The probable distribution of projections to and form loci in the MGB

The convergent, divergent pattern of connections allows predictions of the form of projections to and from loci in the MGB. A locus in AI projects onto an isofrequency sheet in the ventral division and the neurons of that sheet converge onto the same locus. Each sector of the isofrequency slab in AI will give and receive connections to and from the same isofrequency sheet in the ventral division. Thus a locus in Vl or Vo projects along an isofrequency contour in AI. Conversely, that locus receives projections from the same contour. Every position within the isofrequency sheet in the ventral division has connections along the same isofrequency contour in AI.

When very small injections are made into AI, a periodic pattern of dense and light connections was observed along the sheet in Vl. When

reconstructed three dimensionally, these discontinuities are in the form of parallel columns that pass rostrocaudally through Vl. The periodic thalamocortical and corticothalamic patterns of discontinuous connections in Vl, for a single locus in cortex, are directly superimposable. Since large injections produce a continuous pattern of labelling, this suggests that there are two units in cortex that alternate in the densities of their connections. From this structural information, it can be inferred that there are two alternating subunits in Vl as well. Thus each Vl locus that comprizes a single subunit is probably connected both thalamocortically and corticothalamically to alternating subunits in AI.

Predictions for the connections of a locus in the ventral division with AAF are somewhat different than for AI. The label in Vo and Vl after AAF injections was similar in form to the ARG label after AI injections but much less dense. If this labelling is indicative of a weak corticothalamic projection and not trans-synaptic labelling, then an array of neurons in AAF projecting onto a locus in Vo or Vl lys along an isofrequency contour in AAF but the numbers of projecting neurons is probably much less than the numbers of neurons in AI projecting onto a locus in the ventral division. A locus in AAF receives projections from discontinuous arrays of neurons in the ventral division that are confined within an isofrequency sheet. Thus a locus in the ventral division probably projects in a discontinuous manner along an isofrequency contour in AAF.

Single loci in AI or AAF give and receive projections to and from single columns passing through Dd-M. Any position along an isofrequency slab in cortex converges and diverges from and to the same column. Thus,

a locus in Dd-M projects along an isofrequency contour in both AI and AAF. Likewise it receives projections from across the AI and AAF isofrequency contours. All of these predicted connections of a locus in the MGB with AAF and AI can be varified by injections of anterograde and retrograde tracers placed in the MGB.

The convergence of AI onto a locus in ICP or ICC-dm can also be predicted form this data. A locus in AI projects to single sheets in ICC-dm and ICP. Any locus along an isofrequency contour in AI projects into the same sheets in ICC-dm and ICP. Thus entire isofrequency contours in AI project onto single loci in ICC-dm and ICP. (Since the corticotectal projection from AAF appears to be of the same form as the AI projection but relatively weaker, fewer neurons probably converge from contours in this field onto loci in the ICC-dm and ICP (if this weak labelling is not due to trans-synaptic transport.) This pattern of connections can be verified by injections of retrograde tracer in the IC.

Single loci anywhere in either ICC-dm or ICC-vl diverge to sheets of terminals in the ventral division and single columns through M-Dd (Andersen et al. '79). The label in MGB is probably cochleotopically homotypic with the injection site in the ICC. Thus loci in Vo, Vl, Dd and M probably all receive a convergent projection from sheets of neurons aligned along isofrequency contours that pass continuously through ICC-dm and ICC-vl. These patterns of connection can be varified by

injections of retrograde tracer in the various subdivisions of the MGB.

Finally, the layers of cortex that receive projections from loci in the MGB or give projections to loci in the MGB and IC can be inferred from some previous work. The thalamocortical projection terminates primarily in layers IV and III (Sousa Pinto '73, Niimi and Naito '74). There may be differential projections from the ventral and medial divisions (of rat) with the ventral division projecting to III and IV and the medial division to all layers (Ryugo and Killacky '74). The cortico-thalamic projection appears to arise from cells in layer V (Ravizza et al., '76). The callosal connections of AI arise from layers III, IV and VI (Andersen '79, Imig and Brugge '78). Thus the cortical layers in AI that receive thalamocortical input and are the source of the corticothalamic projection are also the layers that project trans-callosally.

Possible segregation of binaural response properties by a parallel segregation of connections

Recently Imig and Adrian '77, Imig and Brugge '78 and Middlebrooks et al., '78 have shown that there is a segregation of two major binaural response classes in AI. Moreover, this segregation is in the form of repeating slabs that are oriented approximately normal to the isofrequency contours (Middlebrooks et al., '78). The two basic binaural response classes are cells that are excited by stimulation of either ear (EE) and cells that are excited by the contralateral ear stimulation and the

contralateral exitatory response is inhibited by simultaneous stimulation of the ipsilateral ear (EI).

The binaural segregation of response classes is reflected in the callosal connections of the two AI's. Multiple injections or single injections of HRP or tritiated amino acids produce alternating slabs of light and dense labelling in the contralateral AI (Imig and Brugge '78, Andersen '78). The areas of dense autoradiographic labelling or HRP labelling corresponds to the EE regions (Imig and Brugge '78). Combined injections of HRP and 3H-l-leucine at single loci in AI produce banded patterns of light and heavy labelling for both tracers in the contralateral AI that are superimposable (Andersen '78). Thus, a single locus in AI is reciprocally connected more strongly to EE slabs than to EI slabs.

Single small injections of anterograde and retrograde tracers (at high frequency representational sites) indicated that there are periodic discontinuities in the thalamocortical and corticothalamic connections of loci in AI with Vl and in the corticothalamic connections of AAF with Vl. These discontinuities are periodic light and heavy regions of connectivity in the caudal aspect of pars lateralis, where it assumes a folded sheet form with pars ovoidea. Reconstructions indicate that, in three dimensions, these discontinuities are in the form of parallel columns oriented rostrocaudally. The corticothalamic and thalamocortical periodic patterns in Vl are superimposable (reciprocal) for connections with single loci in AI.

The fact that large AI cortical injections produce a continuous sheet of label in V1 whereas small injections produce banding, suggests that there are repeating subunits in cortex that have alternating banding patterns of connection with V1. It is probable that these repeating subunits are the EE and EI slabs. Thus, the banding in V1 may result from single small injections in cortex being restricted mostly to only one binaural response slab. This would suggest that V1 also contains binaural response slabs that are oriented normal to the isofrequency contours of V1. The binaural response segregation in AI would then be maintained by the segregation of connections between the EE and EI regions in V1 and AI. Interestingly, single injections of 3H-l-leucine in the ICC can result in a similar banded pattern of labelling in V1 (Andersen et al., 78). A segregation of binaural response properties has been noted in the ICC by Roth et al., '78. Thus it is possible that there is a segregation in binaural response properties that passes, in parallel and through a segregation of connections, from the ICC through V1 to AI. It is also possible that this segregated system may begin at the lower brainstem auditory nuclei since binaural responses of the EE and EI type have been recorded in these structures (Goldberg and Brown '69, Brugge et al. '70, and Boudreau and Tsuchitani '70) and these structures appear to project in a segregated fashion, re the EI and EE classifications, onto the ICC (Roth et al., '78).

POl may be a subdivision of the MGB

Injections of tracers in AAF or AI produced thalamocortical and cortico-thalamic cell and terminal arrays in the thalamus that were always continous

through PO1 into Dd. It has been noted that PO1 and Dd are very similar cyto-archetectonically (Rose and Woolsey '58, Diamond et al. '69). Also, PO1 contains predominently sound sensitive units with sharp tuning curves (Phillips and Irvine '76). Thus, PO1 could be considered a component nucleus of the MGB.

Descending Projections

Reciprocal structure of the thalamocortical and corticothalamic projections The results of these experiments indicated that all connections of AI with the MGB and PO1 are reciprocal and were consistent with the reports of Colwell and Merzenich '78. The connections of AAF with Dd-M and PO1 were also found to be precisely reciprocal. However, the labelling in V1 after injections in single loci in AAF was continuous for the autoradiography but spotty for the HRP. If some or all of the ARG labelling is not due to trans-synaptic transport through AI, this very interesting result indicates that there is a difference in the pattern of the corticothalamic and thalamocortical connections of AAF loci with V1. The corticothalamic projection of AAF is identical to the AI cortico-thalamic projection in form (although much weaker). Since the 2 tracer/ 2 field experiments indicated that similar restricted sectors of V1 give and receive projections to and from homotypic loci in AI and AAF, the AAF corticothalamic projection could have a modulating influence over most or all the AI projecting secter of V1 for homotypic cortical loci. Moreover, since AAF and AI are both strongly reciprocally connected to Dd-M and the topography of connections is apparently the same re the

cochleotopic representations in the two fields, either of these two fields can probably modulate the input to the other from the Dd-M complex. This, and the overlap of the corticothalamic and thalamocortical connections of AI and AAF with the ventral division are probable structural substrates (other than the corticocortical connections between AI and AAF) for a strong functional interdependence of these two fields. However, the nature of this presumed functional interdependence is at present unknown. VPAF has a connectional structure similar to AI and AAF and thus is probably also functionally integrated with these cortical fields.

The thalamocortical and corticothalamic connections of AII are also reciprocal with respect to the thalamic nuclei to which they are connected. However, similar to V1 reciprocal connections with AAF, there were variations in the pattern of label densities within the MGB subdivisions connected to AII. Although all regions with HRP labelled neurons were also above background ARG labelled, some HRP labelled regions were heavily ARG labelled whereas others were not so heavily labelled. This variation in the densities of labelling of the two tracers may be a reflection of the techniques used. HRP labels cell bodies and proximal dendrites whereas the autoradiographic terminal label is indicative of the pattern of termination of the corticothalamic projection on the dendrites of the cells. Thus, a locus in AII could project back onto the same cells from which it receives its thalamocortical input but could distribute its terminals along the dendrites of these cells such that there occurs regional variations in the distributions of the two tracers. On the other hand, it is possible that some of the AII corticothalamic projections from an AII locus ends on MGB cells differnt from those projecting onto that locus and this difference is reflected by the different patterns of the densities of

labelling of the two tracers.

These experiments demonstrate that all four cortical fields that were studied are reciprocally connected to the thalamus (with the reservations mentioned above). A reciprocity of thalamocortical connections has been sited extensively by previous investigators (Cajal '03, Ades '41, Diamond et al. '69, Colwell '77). Reciprocal connections (in several species) between thalamus and cortex have been noted in the auditory system (Rasmussen '64, Diamond et al. '69, Horenstein and Yamamoto '76, Colwell and Merzenich '78), the visual system (Jacobson and Trojanowski '75, Colwell '75, Ogren and Hendrickson '76, Tigges et al. '77), the somatosensory system (Linn et al. '78, White and DeAmicis '77), and the motor (frontal eye fields) system (Akert '64-retrograde degeneration compared to Astruc '71-anterograde degeneration). However, in no case to our knowledge, has the connections of several fields within a sensory system been studied in detail with respect to the reciprocity of the connections. These results indicate that each of the four auditory cortical fields studied is reciprocally connected. It is quite likely that all auditory cortical fields will be found to be reciprocally connected with the thalamus. This data and the studies of other areas of cortex sited above, suggest that reciprocity of connectivity is a general rule for all connections between the dorsal thalamus and the cortex.

All connections between auditory fields of the cat that have been investigated have been found to be reciprocal (Imig and Reale '77, Andersen '78, Diamond et al. '68, '68a). Thus, reciprocal

connectivity between cortical fields appears to be a general rule of structure for the auditory system. The similarity of a reciprocal connectivity between auditory cortical fields and the thalamus and a reciprocal connectivity between auditory cortical fields themselves further suggests that the thalamus is an intricate component of the cortex.

Corticotectal descending control The corticotectal projection form AI is interesting in that it appears to be in register with the ascending afferents with respect to the cochleotopic organizations of the corticotectal and ascending connections. Thus, a locus in AI can directly modulate a homotypic locus in ICC-dm without directly effecting cochleotopically dissimilar representational regions.

A second interesting aspect of the corticotectal projection is that it is limited to only those portions of the isofrequency laminae in the ICC that are within ICC-dm. Since both ICC-dm and ICC-vl probably project into the MGB (Andersen et al. '79) this observation indicates that only a portion of the ascending input that passes from the ICC to AI is probably being influenced directly by AI.

Descending projections from the IC There are also descending projections from the IC to the ipsilateral dorsal cochlear nucleus and preolivary nuclei (Rasmussen '64, Van Noort '69, Andersen et al. '79). Combined injections of HRP and 3H-l-leucine in the ICC indicates that the ICC preolivary connections are directly reciprocal (Andersen et al. '79). However, most of the brainstem auditory nuclei that project onto the

ICC do not receive reciprocal descending projections. Also, there does not appear to be a direct, descending pathway from the auditory cortex to the haircells of the cochlea via the ICC since the ICC to preolivary nuclei pathway terminates in the medial preolivary nucleus (Andersen et al. '79) whereas the olivocochlear projections arise mostly from the dorsomedial and dorsolateral preolivary nuclei (Rasmussen '46, '60).

Possible functions of the descending projections Electrical stimulation of auditory cortex reduced or abolished auditory evoked potentials in the IC (Massopust and Ordy '62, Amato et al. '70) and MGB (Amato et al. '70). This suggests that at least the corticotectal projection is inhibitory. On the other hand, the corticotectal (Rockel and Jones '73b) and corticogeniculate (Morest '75) terminals form asymetrical synapses and thus may have an initially excitatory action. However, it is difficult from these data to acess the actual physiological action of these descending pathways given the difficulties in interpretation of population responses (evoked potentials) and the reservations of inferring function from the morphology of synapses.

There are several theories as to the function of reciprocal connections between thalamus and cortex. Cajal's "theory of the expecting action" proposes that, by acting on the thalamus to facilitate afferent impulses, the thalamic projections focus attention (Cajal '55). The thalamocortical-corticothalamic loops can also be the substrates of reverberating circuits (Lorente de No '33a, '34) that could account

for longer acting nervous functions such as short term memory. Narikashvili '75 has argued against such a model on the basis that auditory cortex ablation or cooling does not abolish the rythmic after discharges recorded from the MGB. A knowledge of the functions of the descending projections and particularily of the reciprocal corticothalamic pathway is of extreme importance considering the ubiquity of such projections.

BIBLIOGRAPHY

Abeles, H. and M.H. Goldstein. 1970. Functional architecture in cat auditory cortex: columnar organization and organization according to depth. J. Neurophysiol., 33: 172-187.

Adams, J.C. and D.C. Teas. 1973. Organization of the posterior colliculus. J. Acoust. Soc. Amer., 53: 361.

Ades, H.W. 1941. Connections of the medial geniculate body in the cat. Arch. Neurol. Psychiat., 45: 138-144.

Ades, H.W. 1943. A secondary acoustic area in the cerebral cortex of the cat. J. Neurophysiol., 6: 59-63.

Aitkin, L.M. 1973. Medial geniculate body of the cat: responses to tonal stimuli of neurons in medial division. J. Neurophysiol. 36: 275-283.

Aitkin, L.M., D.J. Anderson and J.F. Brugge. 1970. Tonotopic organization and discharge characteristics of single neurons in nuclei of the lateral lemniscus of the cat. J. Neurophysiol., 33: 421-440.

Aitkin, L.M., H. Dickhaus, W. Schult, and M.Zimmermann. 1978. External nucleus of inferior colliculus: Auditory and spinal somatosensory afferents and their interactions. J. Neurophysiol., 41: 837-847.

Aitkin, L.M. and W.R. Webster. 1972. Medial geniculate body of the cat: organization and responses to tonal stimuli of neurons in the ventral division. J. Neurophysiol., 35: 365-380.

Akert, K. 1964. Comparative anatomy of frontal cortex and thalamo-frontal connections. In: The Frontal Granular Cortex and Behavior. J.M. Warren and K. Akert eds., McGraw-Hill, New York, pp. 372-396.

Altman, J. and M.B. Carpenter. 1961. Fiber projections of the superior colliculus in the cat. J. Comp. Neur., 116: 157-177.

Amato. G., V. LaGrutta and F. Enia. 1970. The control of acoustic input in the medial geniculate body and inferior colliculus by auditory cortex. Experientia, 26: 55-56.

Andersen, R.A. 1978. Auditory cortical fields of cat: direct demonstration of reciprocity between fields; banded cortico-cortical connectivity; similarity of projection onto striatum. Society for Neuroscience Abstracts, 4: 3.

Andersen, R.A., H. Patterson, P. Knight, B. Crandall, and M.M. Merzenich. 1978. Thalamocortical and cortico-thalamic projections to and from physiologically identified loci within the auditory cortical fields AAF, AII and AI. Society for Neuroscience Abstracts, 3: 3.

Andersen, R.A., G.L. Roth, L.M. Aitkin and M.M. Merzenich. 1978. Organization of projection from the central nucleus of the inferior colliculus into the medial geniculate body of cat. J. Acoust. Soc. Amer., 64: S65.

Andersen, R.A., G.L. Roth, L.M. Aitkin and M.M. Merzenich. 1979. The topography of projection of the central nucleus of the inferior colliculus into the medial geniculate body of the cat. In preparation.

Andersen, R.A. and R. Snyder. 1979. Cortico-cortical connections in the auditory cortex of cat. In preparation.

Andersen, R.A., R. Snyder and M.M. Merzenich. Auditory cortico-tectal connections of cat. J. Acoust. Soc. Amer., 62: S86.

Astruc, J. 1971. Corticofugal connections of Area 8 (frontal eye field) in macaca mulatta. Brain Res., 33: 241-256.

Berkley, K.J. 1973. Response properties of cells of ventrobasal complex and posterior group in the cat. J. Neurophysiol., 36: 910-922.

Berman, A.L. 1968. The Brainstem of the Cat. University of Wisconsin Press, Madison.

Boudreau, J.C. and C. Tsuchitani. 1970. Cat superior olive S-segment cell discharge to tonal stimulation. In: Contributions to Sensory Physiology. W.D. Neff, ed., Academic Press, New York, pp. 144-213.

Bremer, F. 1953. Some Problems in Neurophysiology. Athlone Press, London.

Brugge, J.F., D.J. Anderson and L.M. Aitkin. 1970. Responses of neurons in the dorsal nucleus of the lateral lemnicus of the cat to binaural tonal stimulation. J. Neurophysiol., 33: 441-458.

Brugge, J.F., N.A. Dubrovsky, L.M. Aitkin, D.J. Anderson. 1969. Sensitivity of single neurons in the auditory cortex of cat to binaural stimulation: effects of varying interaural time and intensity. J. Neurophysiol., 32: 1005-1024.

Clapton, B.M. and J.A. Winfield. 1973. Tonotopic organization in the inferior colliculus of the rat. Brain Res., 56: 355-358.

Colwell, S.A. 1975. Thalamocortical-corticothalamic reciprocity: a combined anterograde-retrograde tracer study. Brain Res., 92: 443-449.

Colwell, S.A. 1977. Reciprocal Structure in the Medial Geniculate Body. Thesis, U.C. San Francisco.

Colwell, S.A. and M.M. Merzenich. 1975. Organization of thalamocortical and corticothalamic projections to and from physiologically defined loci within primary auditory cortex in the cat. Anat. Rec., 181: 336.

Colwell, S.A. and M.M. Merzenich. 1979. Corticothalamic projections from physiologically defined loci in the cat. Submitted.

Cooper, M.H. and D.A. Young. 1976. Cortical projections to the inferior colliculus of the cat. Exp. Neurol., 51: 488-502.

Cowan, W.M., D.I. Gottlieb, A.E. Hendrickson, J.L. Price, and T.A. Woolsey. 1972. The autoradiographic demonstration of axonal connections in the central nervous system. Brain Res., 37: 21-51.

Cranford, J.L., S.J. Ladner, C.B.G. Campbell, and W.D. Neff. 1976. Efferent projections of the insular and temporal neocortex of the cat. Brain Res., 117: 195-210.

Curry, M.J. 1972. The exteroceptive properties of neurons in the somatic part of the posterior group (PO). Brain Res., 44: 439-462.

Desmedt, J.E. and K. Michelse. 1959. Corticofugal projections from temporal lobe in cat and their possible role in acoustic discrimination. J. of Physiol. (Lond.), 147: 17-18P.

Diamond, I.T., K.L. Chow and W.D. Neff. 1958. Degeneration of caudal medial geniculate body following cortical lesion ventral to auditory area II in the cat. J. Comp. Neur., 109: 349-362.

Diamond, I.T., E.G. Jones and T.P.S. Powell. 1968. Interhemispheric fiber connections of the auditory cortex of the cat. Brain Res., 11: 177-193.

Diamond, I.T., E.G. Jones and T.P.S. Powell. 1968a. The association connections of the auditory cortex of the cat. Brain Res., 11: 560-579.

Diamond, I.T., E.G. Jones., and T.P.S. Powell. 1969. The projection of the auditory cortex upon the diencephalon and brainstem in the cat. Brain Res., 15: 305-340.

Downman, C.B.B., C.N. Woolsey and R.A. Lende. 1960. Auditory areas I, II and EP: cochlear representations, afferent paths and interactions. Bull. Johns Hopkins Hosp., 106: 127-142.

Erulkar, S.D. 1959. The responses of single units of the inferior colliculus of the cat to acoustic stimulation. Proceed. Roy. Soc. B., 150: 336-355.

Evans, E.F., H.F. Ross, and I.C. Whitfield. 1965. The spatial distribution of unit characteristic frequency in the primary auditory cortex of the cat. J. Physiol. (Lond.), 179: 238-247.

FitzPatrick, K.A. 1975. Cellular architecture and topographic organization of the inferior colliculus of the squirrel monkey. J. Comp. Neur., 164: 185-208.

FitzPatrick, K.A., T.J. Imig, and R.A. Reale. 1977. Thalamic projections to the posterior auditory field in cat. Society for Neuroscience Abstracts, 3: 6.

Galambos, R. 1952. Microelectrode studies on medial geniculate body of cat. III response to pure tones. J. Neurophysiol., 15: 381-400.

Galambos, R., J.E. Rose, R.B. Bromiley and J.R. Hughes. 1952. Microelectrode studies on medial geniculate of cat. II response to clicks. J. Neurophysiol., 15: 359-380.

Geisler, C.D., W.S. Rhode and D.W. Hazelton. 1969. Responses of inferior colliculus neurons in the cat to binaural acoustic stimuli having wide-band spectra. J. Neurophysiol. 32: 960-974.

Geniec, P. and D.K. Morest. 1971. The neuronal architecture of the human posterior colliculus. Acta Oto-Laryngologica, Suppl. 295.

Goldberg, J.M. and P.B. Brown. 1969. Response of binaural neurons of dog superior olivary complex to dichotic tonal stimuli: some physiological mechanisms of sound localization. J. Neurophysiol. 32: 613-636.

Goldberg, J.M. and R.Y. Moore. 1967. Ascending projections of the lateral lemniscus in the cat and monkey. J. Comp. Neur. 129: 143-156.

Goldstein, M.H., M. Abeles, R.L. Daly, and J. McIntosh. 1970. Functional architecture in cat primary auditory cortex: tonotopic organization. J. Neurophysiol. 33: 188-197.

Graham, R.C. and M.J. Karnovsky. 1966. The early stages of absorption of injected horseradish peroxidase in the proximal tubules of the mouse kidney: ultrastructural cytochemistry by a new technique. J. Histochem. Cytochem. 14: 291-302.

Gross, N.B., W.S. Lifschitz and D.J. Anderson. 1974. Tonotopic organization of the auditory thalamus of the squirrel monkey (Saimiri sciureus). Brain Res., 65: 323-332.

Hall, J.L. and M.H. Goldstein. 1968. Representation of binaural stimuli by single units in primary auditory cortex of unanesthetized cats. J. Acoust. Soc. Amer., 43: 456-461.

Hand, P. and C.N. Liu. 1966. Efferent projections of the nucleus gracilis. Anat. Record, 154: 353-354.

Hand, P. and T. VanWinkle. 1977. The efferent connections of the feline nucleus cuneatus. J. Comp. Neur., 171: 83-110.

Hanker, J.S., P.E. Yates, C.B. Metz, K.A. Carson, A. Light and A. Rustioni. 1977. A new specific, sensitive and noncarcinogenic reagent for the demonstration of horseradish peroxidase (HRP). Society for Neuroscience Abstracts, 3: 30.

Harrison, J.M. and M.E. Howe. 1974. Anatomy of the afferent auditory nervous system of mammals. In: Handbook of Sensory Physiology, Vol. 5. W.D. Keidel and W.D. Neff, eds., Springer-Verlag, New York, pp. 283-336.

Hedreen, J.C. and S. McGrath. 1977. Observations on labelling of neuronal cell bodies, axons and terminals after injection of horseradish peroxidase into rat brain. J. Comp. Neur., 176: 225-246.

Hendrickson, A.E. 1972. Electron microscopic distribution of axoplasmic transport. J. Comp. Neur., 144: 381-398.

Hind, J.E. 1953. An electrophysiological determination of tonotopic organization in auditory cortex of the cat. J. Neurophysiol., 16: 475-489.

Hind, J.E., J.E. Rose, P.W. Davies, C.N. Woolsey, R.M. Benjamin, W. Welker, and R.F. Thompson. 1960. Unit activity in the auditory cortex. In: Neural Mechanisms of the Auditory and Vestibular Systems. G. Rasmussen and W. Windle, eds. Charles C. Thomas, Springfield, Ill., pp. 201-210.

Horenstein, S. and T. Yamamoto. 1976. The relationship of the feline temporal cortex to the medial geniculate body. Society for Neuroscience Abstracts, 2: 31.

Hotta, T. and K. Kameda. 1963. Interactions between somatic and visual or auditory responses in the thalamus of the cat. Exp. Neurol., 8: 1-13.

Imig, T.J. and H.O. Adrian. 1978. Binaural columns in the primary field (AI) of cat auditory cortex. Brain Res., 138: 241-257.

Imig, T.J. and J.F. Brugge. 1978. Sources and terminations of callosal axons related to binaural and frequency maps in primary auditory cortex of the cat. J. Comp. Neur., 182: 637-660.

Imig, T.J. and R.A. Reale. 1977. The origins and targets of corticocortical connections related to tonotopic maps of cat auditory cortex. Society for Neuroscience Abstracts, 3: 8.

Imig, T.J., M.A. Ruggero, L.M. Kitzes, E. Javel, and J.F. Brugge. 1977. Organization of auditory cortex in the owl monkey (Aotus trivirgatus). J. Comp. Neur. 171: 111-128.

Jacobson, S. and J.Q. Trojanowski. 1975. Corticothalamic neurons and terminal fields, an investigation in rat using horseradish peroxidase and autoradiography. Brain Res., 85: 385-401.

Jane, J.A. and D.M. Schroeder. 1971. A comparison of dorsal column nuclei and spinal afferents in the European hedgehog (Erinuceus europaeus). Exp. Neurol., 30: 1-17.

Jones. E.G. and T.P.S. Powell. 1971. An analysis of the posterior group of thalamic nuclei on the basis of its afferent connections. J. Comp. Neur., 143: 185-216.

Kasama, T., K. Otani and E. Kawana. 1966. Projections of the motor, somatic sensory, auditory and visual cortices in cats. In: Correlative Neurosciences Vol. 21 A. T. Tokizane and J.P. Schade, eds., Elsevier, New York, pp. 292-322.

Kiang, N.Y.S. Referred to by C.N. Woolsey, 1960, in: Neural Mechanisms of the Auditory and Vestibular Systems. G. Rasmussen and W. Windle, eds., Charles C. Thomas, Springfield, Ill., pp. 165-180 (1955).

Knight, P.A. 1977. Representation of the cochlea within the anterior auditory field (AAF) of the cat. Brain Res., 130: 447-467.

Knudsen, E.I. and M. Konishi. 1978. Space and frequency are represented separately in auditory midbrain of the owl. J. Neurophysiol., 41: 870-884.

Kutsuko, Y., T. Watanabe, and N. Maruyama. 1959. Activity of auditory neurons in upper levels of brain of cat. J. Neurophysiol., 22: 343-359.

Lashley, K.S. 1950. In search of the engram. In: Symp. Soc. Exp. Biol., 4. Cambridge Univ. Press, New York.

LaVail, J.H. and M.M. LaVail. 1972. Retrograde axonal transport in the central nervous system. Science, 176: 1416-1417.

LaVail, J.H., K.R. Winston and A. Tish. 1973. A method based on retrograde axonal transport of protein for identification of cell bodies of origin

of axons terminating within the CNS. Brain Res., 58: 470-477.

Leoffler, 1958. Referred to by C.N. Woolsey, 1960, in: Neural Mechanisms of the Auditory and Vestibular Systems. G. Rasmussen and W. Windle, eds., Charles C. Thomas, Springfield, Ill., pp. 165-180.

Lin, C., M.M. Merzenich, M. Sur, and J.H. Kass. 1978. Connections of areas 3b and 1 of the parietal somatosensory strip with the ventroposterior nucleus in the owl monkey (Aotus Trivirgatus). Submitted.

Locke, S. 1961. The projection of the magnocellular medial geniculate body. J. Comp. Neur., 116: 179-194.

Lorente de No, R. 1933. Anatomy of the eighth nerve. The central projection of the nerve endings of the internal ear. Laryngoscope, 43: 1-38.

Lorente de No, R. 1933a. Studies of the structure of the cerebral cortex. J. Psychol. Neurol., 45: 381.

Lorente de No, R. 1934. Studies of the structure of the cerebral cortex. II. Continuation of the study of the ammonic system. J. Psychol. Neurol., 46: 113.

Massopust, Jr., L.C. and J.M. Ordy. 1962. Auditory organization of the inferior colliculi in the cat. Exp. Neurol., 66: 465-477.

Mehler, W.R., M.E. Feferman and W.J.H. Nauta. 1960. Ascending axon degeneration following anterolateral cordotomy. An experimental study in the monkey. Brain, 83: 718-750.

Merzenich, M.M. and J.F. Brugge. 1973. Representation of the cochlear partition on the superior temporal plane of the macaque monkey. Brain Res., 50: 275-296.

Merzenich, M.M. and S.A. Colwell. 1975. Spatially ordered convergent projection from the auditory thalamus to and from AI in the cat. J. Acoust. Soc. Amer., 57: S55.

Merzenich, M.M., S.A. Colwell and R.A. Andersen. 1979. Thalamocortical projection to AI in the cat. In preparation.

Merzenich, M.M., J.H. Kaas, and G.L. Roth. 1976. Auditory cortex in the grey squirrel: tonotopic organization and architectonic fields. J. Comp. Neur., 166: 387-402.

Merzenich, M.M., P.L. Knight and G.L. Roth. 1975. Representation of cochlea within primary auditory cortex in the cat. J. Neurophysiol., 38: 231-249.

Merzenich, M.M. and M.D. Reid. 1974. Representation of the cochlea within the inferior colliculus of the cat. Brain Res., 77: 397-415.

Merzenich, M.M., G.L. Roth, R.A. Andersen, P.L. Knight, and S.A. Colwell. 1977. Some basic features of organization of the central auditory system. In: Psychophysics and Physiology of Hearing, E.F. Evans and J.P. Wilson, eds., Academic Press, London.

Mettler, F.A. 1932. Connections of the auditory cortex in the cat. J. Comp. Neur., 55: 139-183, 1932.

Middlebrooks, J.C., R.W. Dykes, and M.M. Merzenich. 1978. Binaural response-specific bands within AI in the cat: specialization within isofrequency contours. Society for Neuroscience Abstracts, 4: 8.

Moore, R.Y. and J.M. Goldberg. 1963. Ascending projections of the inferior colliculus in the cat. J. Comp. Neur., 121: 109-136.

Morest, D.K. 1964. The neuronal architecture of the medial geniculate body of the cat. J. Anat., 98: 611-630.

Morest, D.K. 1964a. The laminar structure of the inferior colliculus of the cat. Anat. Rec., 148: 314.

Morest, D.K. 1964b. The probable significance of synaptic and dendritic patterns of the thalamic and midbrain auditory system. Anat. Rec., 148:

390-391.

Morest, D.K. 1965. The laminar structure of the medial geniculate body body of the cat. J. Anat., 99: 143-160.

Morest, D.K. 1966. The cortical structure of the inferior quadrigeminal lamina of the cat. Anat. Rec., 154: 389-390.

Morest, D.K. 1966a. The non-cortical neuronal architecture of the inferior colliculus of the cat. Anat. Rec., 154: 477.

Morest, D.K. 1975. Synaptic relationships of Golgi type II cells in the medial geniculate body of the cat. J. Comp. Neur., 162: 157-194.

Neff, W.D., J.F. Fisher, I.T. Diamond and M. Yela. 1956. Role of auditory cortex in a discrimination requiring localization of sound in space. J. Neurophysiol., 16: 475-489.

Niimo, K. and F. Naito. 1974. Cortical projections of the medial geniculate body in the cat. Exp. Brain Res., 19: 326-342.

Nurikashvili, S.P. 1976. Facts and reflections on thalamocortical reverberation of impulses. Neuroscience and Beh. Physiol., 7: 77-81.

Ogren, M. and A. Hendrickson. 1976. Pathways between striate cortex and subcortical regions in Macaca mulatta and Saimiri sciureus: Evidence for a reciprocal pulvinar connection. Exp. Neurol., 53: 780-800.

Oonishi, S. and Y. Katsuki. 1965. Functional organization and integrative mechanism of the auditory cortex of the cat. Jap. J. Physiol., 15: 342-365.

Osen, K.K. 1972. Projection of the cochlear nuclei on the inferior colliculus in the cat. J. Comp. Neur., 144: 355-372.

Perl, E.R. and D.G. Whitlock. 1961. Somatic stimuli exciting spinothalamic projection to thalamic neurons in cat and monkey. Exp. Neurol., 3: 256-296.

Phillips, D.P. and D.R.F. Irvine. 1976. Acoustic input to neurons in pulvinar-posterior complex of cat thalamus. Proc. Australian Physiol. Pharmacol. Soc., 7: 126P.

Poggio, G.F. and V.B. Mountcastle. 1960. A study of the functional contributions of the lemniscal and spinothalamic systems to somatic sensibility. Bull. Johns Hopkins Hosp., 106: 266-316.

Pontes, C., F.F. Reis, and A. Sousa-Pinto. 1975. The auditory cortical projections onto the medial geniculate body in the cat. An experimental anatomical study with silver and autoradiographic methods. Brain Res., 91: 43-63.

Ralston, H.J. III and P.V. Sharpe. 1973. The identification of thalamo-cortical relay cells in the adult cat by means of retrograde axonal transport of horseradish peroxidase. Brain Res., 62: 273-278.

Ramon y Cajal, S. 1903. Las fibras nerviosas de origen cerebral del tuberculo cuadrigemino anterior y del talamo optico. Trab. Lab. Inv. Biol., 2: 5-20.

Ramon y Cajal, S. 1955. Histológie du Systeme Nerveux de L'home et des Vertebres. (Reprinted from the original 1909-1911 ed.) Consejo Superior de Investigaciones Cientificas, Madrid.

Ramon y Cajal, S. 1966. Studies on the Diencephalon. Compiled and translated by E. Ramon-Moliner. Charles C. Thomas, Springfield, Ill.

Rasmussen, G.L. 1946. The olivary peduncle and other fiber projections of the superior complex. J. Comp. Neur., 84: 141-219.

Rasmussen, G.L. 1960. Efferent fibers of the cochlear nerve and cochlear nucleus. In: Neural Mechanisms of Auditory and Vestibular Systems. G.L. Rasmussen and W.F. Windle, eds., C.C. Thomas, Springfield, Ill., pp. 105-115.

Rasmussen, G.L. 1964. Anatomic relationships of the ascending and descending auditory systems. In: Neurological Aspects of Auditory and Vestibular Disorders. W.S. Field and B.R. Alford, eds., C.C. Thomas, Springfield, Ill., pp. 5-19.

Reale, R.A. and T.J. Imig. 1977. An orderly frequency representation in the posterior ectosylvian sulcus of the cat. Society for Neuroscience Abstracts, 3: 10.

Rioch, D. 1929. Studies on the diencephalon of carnivora: I: The nuclear configuration of the thalamus, epithalamus, and hypothalamus of the dog and cat. J. Comp. Neur., 49: 1-119.

Robards, M.J., D.W. Watkins and R.B. Masterton. An anatomical study of some somesthetic afferents to the intercollicular terminal zone of the midbrain of the opossum. J. Comp. Neur., 170: 499-524.

Rockel, A.J. and E.G. Jones. 1973. The neuronal organization of the inferior colliculus of the adult cat. I. The central nucleus. J. Comp. Neur., 147: 11-60.

Rockel, A.J. and E.G. Jones. 1973a. The neuronal organization of the inferior colliculus of the adult cat. II. The pericentral nucleus. J. Comp. Neur., 149: 301-334.

Rockel, A.J. and E.G. Jones. 1973b. Observations on the fine structure of the central nucleus of the inferior colliculus of the cat. J. Comp. Neur., 147: 61-92.

Rose, J.E. 1949. The cellular structure of the auditory region of the cat. J. Comp. Neur., 91: 409-440.

Rose, J.E. and R. Galambos. 1952. Microelectrode studies on medial geniculate body of cat. I. Thalamic region activated by click stimuli. J. Neurophysiol., 15: 343-357.

Rose, J.E., R. Galambos and J. Hughes. 1960. Organization of frequency sensitive neurons in the cochlear nuclear complex of the cat. In: Neural Mechanisms of the Auditory and Vestibular Systems. G. Rasmussen and W. Windle, eds., Charles C. Thomas, Springfield, Ill., pp. 116-136.

Rose, J.E., D.O. Greenwood, J.M. Goldberg and J.E. Hind. 1963. Some discharge characteristics of single neurons in the inferior colliculus of the cat. I. Tonotopic organization, relation of spike-counts to tone intensity, and firing patterns of single elements. J. Neurophysiol., 26: 294-320.

Rose, J.E., N.B. Gross, C.D. Geisler and J.E. Hind. 1966. Some neural mechanisms in the inferior colliculus of the cat which may be relevant to localization of a sound source. J. Neurophysiol., 29: 288-314.

Rose, J.E. and C.N. Woolsey. 1949. The relations of the thalamic connections, cellular structure and evocable electrical activity in the auditory region of the cat. J. Comp. Neur., 91: 441-466.

Rose, J.E. and C.N. Woolsey. 1958. Cortical connections and functional organization of the thalamic auditory system of the cat. In: Biological and Biochemical Bases of Behavior. H.F. Harlow and C.N. Woolsey, eds., University of Wisconsin Press, Madison, pp. 127-150.

Roth, G.L. 1977. Some Features of the Anatomical and Physiological Organization of the Central Nucleus of the Inferior Colliculus: Implications for its Role in the Processing of Auditory Information. Thesis. University of California, San Francisco.

Roth, G.L., L.M. Aitkin, R.A. Andersen and M.M. Merzenich. 1978. Some features of the spatial organization of the central nucleus of the inferior colliculus of the cat. J. Comp. Neur., 182: 661-680.

Rowe, M.J. and B. Sessle. 1968. Somatic afferent input to posterior thalamic neurons and their axon projection to cerebral cortex in cat. J. Physiol., (Lond.), 196: 19-35.

Ryugo, D.K. and Killacky, H.P. 1974. Differential telencephalic projections of the medial and ventral divisions of the medial geniculate body of the rat. Brain Res., 82: 173-177.

Sindberg, R.M. and R.F. Thompson. 1962. Auditory response fields in ventral temporal and insular cortex of cat. J. Neurophysiol., 25: 21-28.

Sousa-Pinto, A. 1973. Cortical projections of the medial geniculate body in the cat. Adv. Anat. Embry. Cell Biol., 48: 1-42.

Sperry, R.W., N. Miner, R.E. Myers. 1955. Visual pattern perception following subpial slicing and tantalum wire implantations in the visual cortex. J. Comp. Physiol. Psychol., 48: 50-58.

Thompson, R.F. and R.M. Sindberg. 1960. Auditory response fields in association and motor cortex of cat. J. Neurophysiol., 23: 87-105.

Tigges, J., M. Tigges and A.A. Perachio. 1977. Complementary laminar terminations of afferents to Area 17 originating in Area 18 and in the lateral geniculate nucleus in squirrel monkey. J. Comp. Neur., 176: 87-100.

Trojanowski, J.Q. and S. Jacobson. 1975. A combined horseradish peroxidase-autoradiographic investigation of reciprocal connections between superior temporal gyrus and pulvinar in squirrel monkey. Brain Res., 85: 347-353.

Tunturi, A.R. 1952. A difference in the representation of auditory signals for the left and right ears in the isofrequency contours of the right

middle ectosylvian cortex of the dog. Amer. J. Physiol., 168: 712-727.

Tunturi, A.R. 1945. Further afferent connections of the acoustic cortex of the dog. Amer. J. Physiol., 144: 389-394.

Tunturi, A.A. 1950. Physiological determination of the boundary of the acoustic area in the cerebral cortex of the dog. Amer. J. Physiol. 160: 395-401.

Tunturi, A.R. 1950a. Physiological determination of the arrangement of the afferent connections to the middle ectosylvian area in the dog. Amer. J. Physiol., 162: 489-502.

Van Noort, J. 1969. The Structure and Connections of the Inferior Colliculus. van Gorcum, Assen.

Waller, W.H. 1940. Thalamic degeneration induced by temporal lesions in the cat. J. of Anat., 74: 528-536.

White, E.L. and R.A. DeAmicis. 1977. Afferent and efferent projections of the region in mouse Sml cortex which contains the posteromedial barrel subfield. J. Comp. Neur., 175: 455-482.

Wilson, M.E. and B.G. Cragg. 1969. Projection from the medial geniculate body to the cerebral cortex of the cat. Brain Res., 13: 462-475.

Winer, J.A., I.T. Diamond and D. Raczkowski. 1977. Subdivisions of the auditory cortex of the cat: the retrograde transport of horseradish peroxidase to the medial geniculate body and posterior thalamic nuclei. J. Comp. Neur., 176: 387-418.

Wong-Riley, M.T.T. 1976. Endogenous peroxidatic activity in brain stem neurons as demonstrated by their staining with diaminobenzidine in normal squirrel monkeys. Brain Res., 108: 257-277.

Woollard, H.H. and A. Harpman. 1939. The cortical projection of the medial geniculate body. J. of Neur. and Psychiat., 2: 35-44.

Woolsey, C.N. 1960. Organization of cortical auditory system: a review and a synthesis. In: Neural Mechanisms of the Auditory and Vestibular Systems. G. Rasmussen and W. Windle, eds., Charles C. Thomas, Springfield, Ill., pp. 165-180.

Woolsey, C.N. and D. Fairman. 1946. Contralateral, ipsilateral and bilateral representation of cutaneous receptors in somatic areas I and II of the cerebral cortex of pig, sheep and other mammals. Surgery, 19: 684-702.

Woolsey, C.N. and E.M. Walzl. 1942. Topical projections of nerve fibers from local regions of the cochlea to the cerebral cortex of the cat. Bull. Johns Hopkins Hosp., 71: 315-344.